

TX1803-TB-C, Hurricane Harvey Post Storm Topography/Bathymetry Project Final Report of Survey

Produced for the National Oceanic and Atmospheric Administration, National Geodetic Survey

Contract: EA-133C-14-CQ-0008

Task Order: TX1803-TB-C, Hurricane Harvey Post Storm Topography/Bathymetry Lidar Project

December 31, 2019

Produced by:

Dewberry

1000 North Ashley Drive, Suite 801

Tampa, FL 33602

813.225.1325

Table of Contents

Executive Summary	4
The Project Team.....	4
Project Area	4
Date of Survey.....	5
Coordinate Reference System	5
Lidar Vertical Accuracy	5
Project Deliverables	6
Overview of Classification	6
Lidar Acquisition Report	7
Lidar Acquisition Details.....	7
Lidar System Parameters	8
Acquisition Status Report and Flightlines	9
Acquisition Static Control	9
Airborne GPS Kinematic	10
Generation and Calibration of Laser Points (raw data)	10
Boresight and Relative Accuracy	11
Final Calibration Verification.....	13
Refraction Correction	14
Lidar Processing & Qualitative Assessment	14
Initial Processing	14
Final Swath Vertical Accuracy Assessment.....	14
Inter-Swath (Between Swath) Relative Accuracy	15
Intra-Swath (Within a Single Swath) Relative Accuracy	16
Horizontal Alignment	16
Point Density and Spatial Distribution	17
Data Classification and Editing	19
Breakline Creation and QA/QC.....	19
GeoCue and Terrascan Processing.....	20
Submerged Objects	24
Temporal Changes	24
Flightline Ridges	26
Lidar Qualitative Assessment.....	27
Visual Review	27
Create Void Polygons	27
Formatting	27
Derivative Lidar Products	28

Confidence Layer	28
Lidar Positional Accuracy	28
Background.....	28
Survey Vertical Accuracy Checkpoints	29
Vertical Accuracy Test Procedures	34
NVA	34
Bathymetric Vertical Accuracy	34
VVA	34
Vertical Accuracy Results	35
Horizontal Accuracy Test Procedures	37
Horizontal Accuracy Results	38
DEM Processing & Qualitative Assessment.....	38
Final Void Polygons.....	39
DEM Generation.....	39
DEM Qualitative Review	39
DEM Quantitative Assessment.....	40
DEM Checklist	42
Metadata	42

Attachments

Appendix A: Checkpoint Survey Report
Appendix B: Ground Control Point Survey Report
Appendix C: Complete List of Lidar Delivered Tiles
Appendix D: GPS Processing Reports

Executive Summary

Dewberry was tasked with developing a consistent and accurate topographic and bathymetric (topobathymetric) elevation dataset acquired with high-accuracy light detection and ranging (lidar) technology for the National Oceanic and Atmospheric Administration (NOAA) Hurricane Harvey post-storm Texas project area.

The lidar data were processed and classified according to NOAA's Shoreline Mapping SOW (Version 14A) and the project instructions for this specific task order. Topobathymetric Digital Elevation Models (DEMs) were produced for the project area. Lidar data were formatted into tiles, each covering an area of 1,000 m × 1,000 m. A total of 3,813 lidar tiles were produced for the project, encompassing a total area of approximately 942 square miles.

THE PROJECT TEAM

Dewberry served as the prime contractor for the project. In addition to project management, Dewberry was responsible for all lidar classification and production, including ancillary datasets and quality assurance.

Dewberry's Gary Simpson completed the ground survey activities for this project. His team acquired survey checkpoints for use in independent vertical accuracy testing of the lidar and lidar-derived elevation model. He also verified the GPS base station coordinates used during lidar data acquisition to ensure that the base station coordinates were accurate. The checkpoint survey report is included as Appendix A.

Leading Edge Geomatics, LLC (LEG) completed lidar data acquisition and data calibration for the project area.

PROJECT AREA

The project area addressed by this report covers the Gulf Coast of Texas ranging from the Bolivar Peninsula to Corpus Christi, including Galveston, Freeport, Matagorda Bay and Aransas National Wildlife Refuge (figure 1). The total size of the project is approximately 942 square miles.

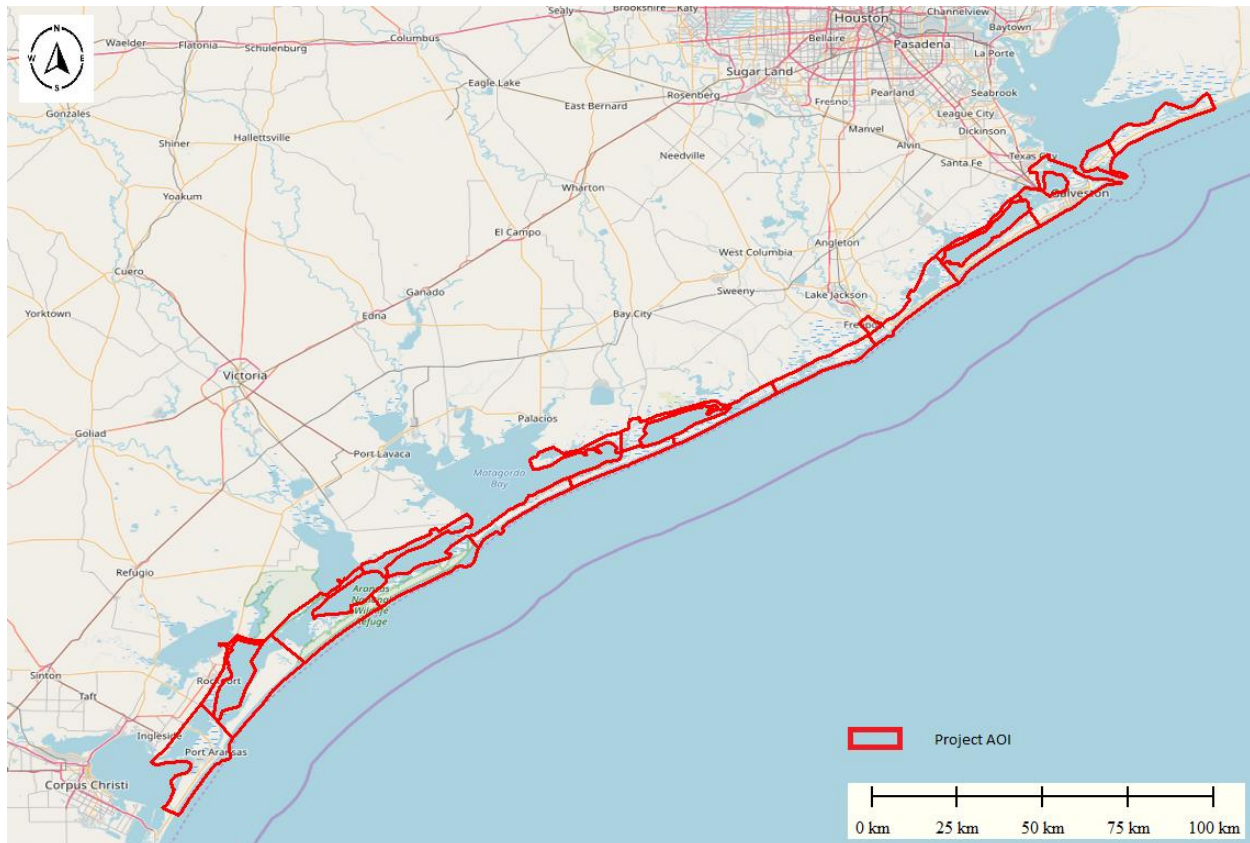


Figure 1 – Area of Interest for the TX1803-TB-C Topobathymetric Lidar Project.

DATE OF SURVEY

The lidar aerial acquisition was conducted from October 22, 2018 through May 31, 2019.

COORDINATE REFERENCE SYSTEM

Data produced for the project were delivered in the following reference system:

- **Horizontal Datum:** North American Datum of 1983 with the 2011 Adjustment (NAD83(2011))
- **Vertical Datum:** North American Datum of 1983 with the 2011 Adjustment (NAD83(2011), epoch 2010), ellipsoid heights
- **Coordinate System:** UTM Zones 14 and 15
- **Units:** Horizontal units are in meters; vertical units are in meters
- **Geoid Model:** Geoid 12B was used to convert ellipsoid heights to orthometric heights

LIDAR VERTICAL ACCURACY

The tested $RMSE_z$ of the classified lidar data for checkpoints in non-vegetated terrain is 7.1 cm compared with the 10 cm specification. The non-vegetated vertical accuracy (NVA) of the classified lidar data computed using $RMSE_z \times 1.9600$ was equal to 13.8 cm, compared with the 19.6 cm specification.

The tested vegetated vertical accuracy (VVA) of the classified lidar data computed using the 95th percentile was 26.4 cm, compared with the 30 cm specification.

The tested submerged bathymetry vertical accuracy (SMB) of the classified lidar data computed

using the 95th percentile was is 29.2 cm, compared with the 35.3 cm specification.

Additional accuracy information and statistics for the classified lidar, raw swaths and topobathymetric DEMs are found in the subsequent sections of this report.

PROJECT DELIVERABLES

The deliverables for the project are listed below:

1. Project Extents including boundary and tile grid (shapefiles)
2. Refraction extents delineating topographic and bathymetric domains (GDB feature class)
3. Final classified lidar tiles (LAS)
4. Tiled topobathymetric DEMs with voids enforced (IMG)
5. Void layer (shapefile)
6. Tiled standard deviation confidence rasters (IMG)
7. Temporal polygons (shapefile)
8. Survey data
9. Metadata (XML)
10. Final Project report

OVERVIEW OF CLASSIFICATION

The raw lidar from the bathymetric and topographic sensors were kept in the classes that were outputted by the Leica processing software. This aided in the classification of the ground and bathymetric bottom. The raw swaths delivered to NOAA were preserved in the classification schema listed below.

Lidar Classification – Raw Sensor Data	
Class	Description
1	Unclassified
2	Ground
3	Low Vegetation
4	Medium Vegetation
5	High Vegetation
7	Low Noise
18	Noise
20	Water Surface IR
40	Bathymetric Point
41	Water Surface Green
42	Derived Water Surface
43	Submerged Object
64	Shallow Bathymetric Point
65	Turbid Water Enhancement 1
66	Deep Bathymetric Point
67	Turbid Water Enhancement 2
101	Unclassified (water)
102	Ground (water)
103	Low Vegetation (water)
104	Medium Vegetation (water)
105	High Vegetation (water)
107	Low Noise (water)
118	Noise (water)

Table 1 – Lidar classification schema of raw lidar data.

Once the raw topographic and bathymetric sensor data had been tiled out, routines were run to reclassify the data into the classification schema below. This classification schema was used during manual editing and was also the schema used for the final LAS delivered to NOAA, as required by the project's scope of work.

Lidar Classification – Manual Editing and Final Deliverables	
Class	Description
1	Unclassified (includes buildings and vegetation)
2	Ground
7	Noise (low or high)
40	Bathymetric Point
41	Water Surface
42	Derived Water Surface (synthetic water surface used in computing refraction at water surface)
43	Submerged Object (not otherwise specified)
45	No Bottom Found
46	Temporal Change (from varying lifts; not utilized in bathymetric or ground point classes)

Table 2 – Final lidar classification schema.

Lidar Acquisition Report

Dewberry elected to subcontract the lidar acquisition and calibration activities to LEG. Dewberry received multiple calibrated swath deliveries from LEG. The last delivery of data was on July 12, 2019.

LIDAR ACQUISITION DETAILS

LEG planned 1,240 passes for the project area as a series of parallel flight lines with 25 cross flightlines quality control. Before the first flightline of each mission was collected, an “S-Turn” was performed to preempt inertial measurement unit (IMU) drift. In order to reduce potential errors in the data attributable to flight planning, LEG followed FEMA’s *Guidelines and Specifications for Flood Hazard Mapping Partners, Appendix A: Guidance for Aerial Mapping and Survey*. The guidances includes the following minimum criteria:

- A digital flight line layout using Leica MissionPro flight design software for direct integration into the aircraft flight navigation system;
- Planned flight lines, flight line numbers, and coverage area;
- Lidar coverage extended by a predetermined margin beyond all project borders to ensure necessary over-edge coverage appropriate for specific task order deliverables;
- Investigation of local restrictions related to air space and any controlled areas so that required permissions can be obtained in a timely manner with respect to project schedule; and
- Filed flight plans as required by local Air Traffic Control (ATC) prior to each mission.

LEG monitored weather and atmospheric conditions and conducted lidar missions only when no conditions existed below the sensor that would affect the collection of data. Good lidar collection conditions include no rain, fog, smoke, mist, or low clouds. LEG also performed in-situ measurements to gauge expected water quality conditions throughout the project area. Lidar systems are active sensors that do not require light. Thus, missions may be conducted during night hours when weather restrictions do not prevent collection. LEG accessed reliable weather

sites and indicators (webcams) to establish the highest probability for successful data acquisition.

Within 72-hours prior to the planned day(s) of acquisition, LEG closely monitored the weather, checking all sources for forecasts at least twice daily. As soon as weather conditions were conducive to acquisition, the aircraft mobilized to the project site to begin data collection. Once on site, the acquisition team and project leads worked together for weather analysis. LEG was on site for 20 days before the first mission was completed due to changes in weather.

LEG lidar sensors are calibrated at a designated site located over Fredericton, NB, Canada. They were also periodically calibrated over a local site in Galveston, TX, USA.

LIDAR SYSTEM PARAMETERS

LEG operated a Piper Navajo (Tail #GKCN) outfitted with a Leica Chiroptera II topobathy lidar system. Table 3 lists Leading Edge Geomatic's system parameters for lidar acquisition on this project.

Item	Parameter	Parameter
System	Chiroptera II Bathymetric	Chiroptera II Topographic
Gyro Stabilization Mount	Yes-Leica PAV100	Yes-Leica PAV100
Altitude (m. AGL)	400	400
Approx. Flight Speed (kts)	120	120
Scanner Pulse Rate (KhZ)	35	200
Scan Frequency (RPM)	2239	5862
Pulse Duration of the Scanner (nanoseconds)	0.5	5
Pulse Width of the Scanner (m)	0.15	0.5
Swath Width (m)	291	291
Central Wavelength of the Sensor Laser (nanometers)	515	1064
Will the Sensor Operate with Multiple Pulses in The Air? (yes/no)	No	No
Laser Beam Divergence (milliradians)	4.5	0.5
Nominal Swath Width on the Ground (m)	291	291
Swath Overlap (%)	55	55
Total Sensor Scan Angle (degree)	40	40
Computed Along Track Spacing (m)	0.82	0.31
Computed Cross Track Spacing (m)	0.82	0.31
Nominal Pulse Spacing (single swath), (m)	0.82	0.31
Nominal Pulse Density (single swath) (ppsm), (m)	1.48	10.21
Aggregate NPS (m) (if ANPS was designed to be met through single coverage, ANPS and NPS will be equal)	0.59	0.22
Aggregate NPD (m) (if ANPD was designed to be met through single coverage, ANPD and NPD will be equal)	2.9	20.4
Maximum Number of Returns per Pulse	unlimited	unlimited

Table 3 – LEG's lidar system parameters.

ACQUISITION STATUS REPORT AND FLIGHTLINES

Upon notification to proceed, the flight crew loaded the flight plans and validated the flight parameters. The acquisition manager contacted air traffic control and coordinated flight pattern requirements. Lidar acquisition began immediately upon notification that control base stations were in place. During flight operations, the flight crew monitored weather and atmospheric conditions. Lidar missions were flown only when no condition existed below the sensor that would affect the collection of data. The pilot constantly monitored the aircraft course, position, pitch, roll and yaw of the aircraft. The sensor operator monitored the lidar sensor, the position dilution of precision (PDOP), and performed the first quality control review during acquisition. The flight crew reviewed weather and cloud locations. Any flight lines impacted by unfavorable conditions were marked as invalid and re-flown.

The figure below shows an example of a trajectory from mission 301A flown on October 28, 2018. This trajectory contains a set of parallel lines as well as a cross flightline.

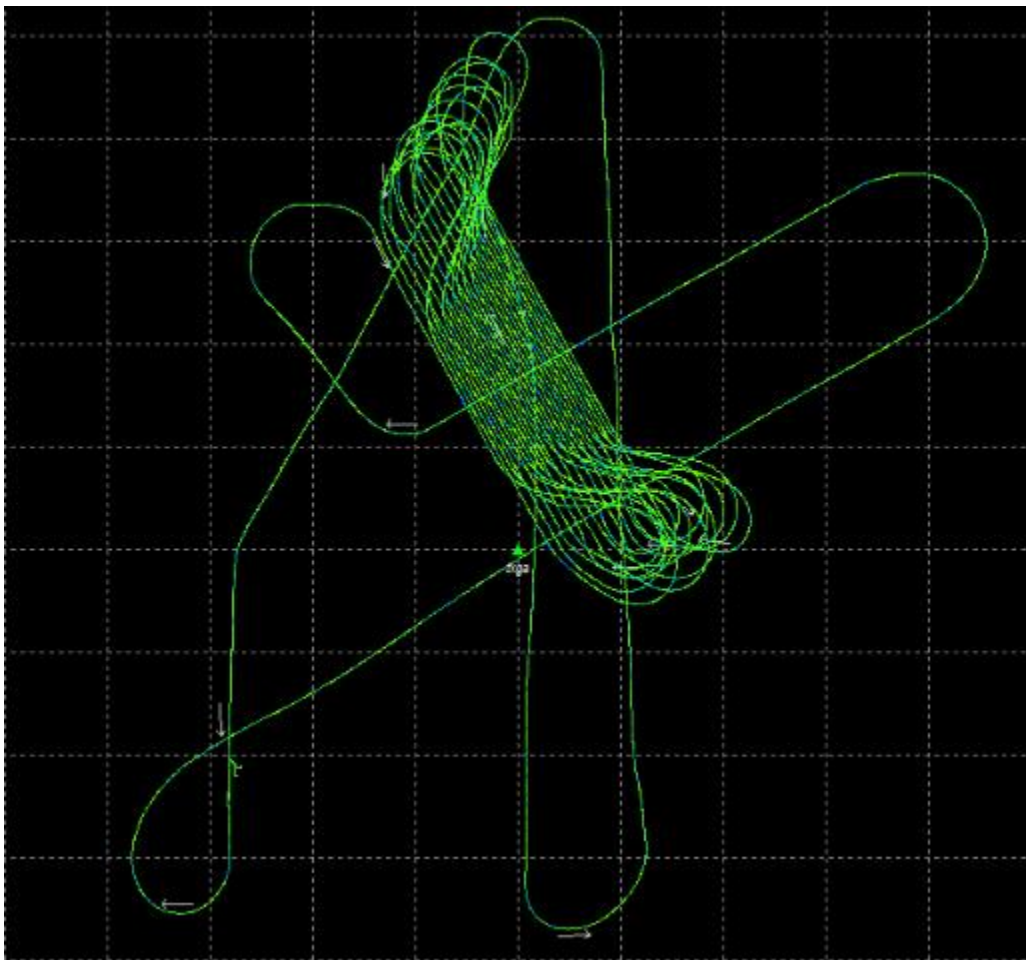


Figure 2 – 301A Trajectory as flown by Leading Edge Geomatics

ACQUISITION STATIC CONTROL

LEG deployed static GPS base stations during the acquisition of the TX1803-TB-C Topobathymetric Lidar Project to complete coverage not achievable through active networks. Considerations were made for location access and clear visibility of the horizon. Additionally, these static sessions were recorded at 1 Hz samples for the highest quality post-processed

solution. The sessions were then incorporated during the kinematic post-processing of aircraft position. Base stations were either set on existing control monuments or newly- established benchmarks. The coordinates of these base stations are provided in the table below. CORS and SmartNet stations were also used for completion of this project and are included in the list below.

Name	NAD83(2011) UTM Zones 14 and 15		Ellipsoid Ht (NAD83(2011), m)
	Easting X (m)	Northing Y (m)	
CORS			
TXGA	672120.828	3245615.349	-9.363
TXLM	696378.631	3253143.847	-16.172
TXAG	735274.784	3228594.49	-14.684
DW11	734121.677	3211875.132	-18.713
TXPO	309926.999	3080913.792	-19.433
TXCC	346405.148	3069461.641	-9.085
SmartNet			
TXHD	634734.766	3271222.188	-12.219
LEG			
HLDY	301376.895	3115682.127	-22.791
SEAD	262652.566	3140099.995	-25.767
PALA	231634.84	3180655.784	-22.953
WADS	775933.26	3187258.999	-25.067
SEAD2	262566.947	3140099.845	-25.938
WADS2	779824.281	3185092.937	-23.375
HLDY2	301376.537	3115680.001	-22.783

Table 4 – Base stations used to control lidar acquisition for the NOAA_TX-1803 project.

AIRBORNE GPS KINEMATIC

Airborne GPS data was processed using Inertial Explorer as part of the Waypoint software suite. Flights were flown with a minimum of 6 satellites in view (13° above the horizon) and with a PDOP of better than 4. Distances from base station to aircraft were kept to a maximum of 30 km.

The GPS average residuals for all flights were 3 cm or better, with no residuals greater than 10 cm recorded.

GPS processing reports for each mission are included in Appendix A.

GENERATION AND CALIBRATION OF LASER POINTS (RAW DATA)

The initial step of calibration is to verify availability and status of all needed GPS and laser data against field notes and compile any data if not complete. The Texas Department of Transportation provided data at a 1 second sampling rate to LEG.

Subsequently, the mission points are output using Leica's LiDAR Survey Studio (LSS). The data is reviewed for any errors. Calibration values are determined within LSS using built-in algorithms, then exported for further checks.

Data processing and refraction are all performed in LSS and output to LAS format. Data is reviewed for completeness, acceptable density, and to make sure all data is captured without errors or corrupted values. In addition, all GPS, aircraft trajectory, mission information and ground control files are reviewed and logged into a database.

On a project level, a supplementary coverage check is carried out to ensure no data voids unreported by field operations are present. Checks are also performed to determine the quality of bathymetric returns.



Figure 3 – Sample lidar swath output showing complete coverage of selected area.

BORESIGHT AND RELATIVE ACCURACY

The initial points for each mission calibration are inspected for flight line errors, flight line overlap, slivers or gaps in the data, point data minimums, or issues with the lidar unit or GPS. Roll, pitch and yaw are optimized during the calibration process until the relative accuracy is met.

Relative accuracy and internal quality are checked using at least 3 regularly spaced QC blocks in which points from all lines are loaded and inspected. Vertical differences between ground surfaces of each line are displayed. Color scale is adjusted so that errors greater than the specifications are flagged. Cross sections are visually inspected across each block to validate point-to-point, flight line-to-flight line, and mission-to-mission agreement.

For this project, the specifications used are as follows: Relative accuracy ≤ 6 cm maximum differences within individual swaths and ≤ 8 cm RMSD_z between adjacent and overlapping swaths.

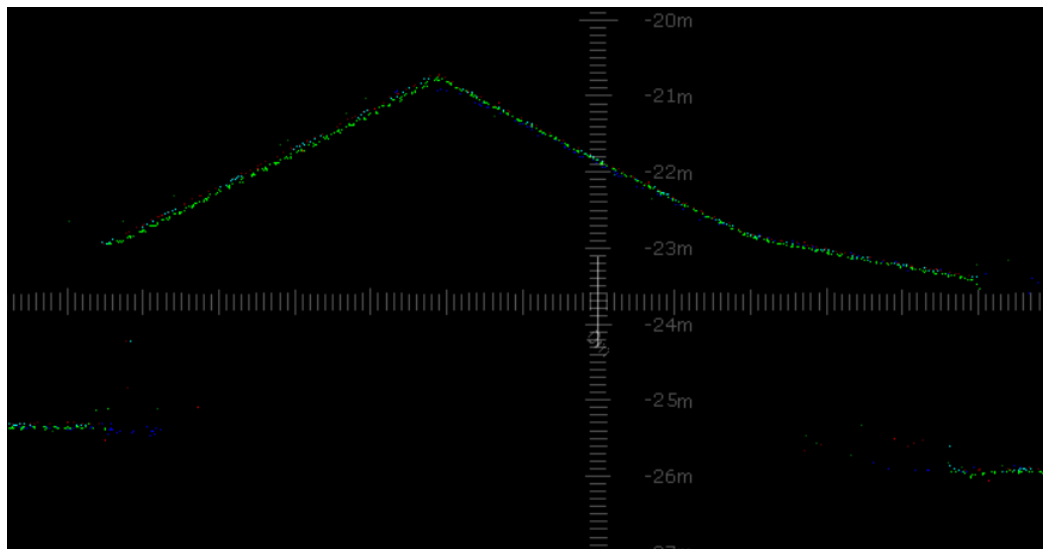


Figure 4 – Profile view showing correct roll and pitch adjustments.

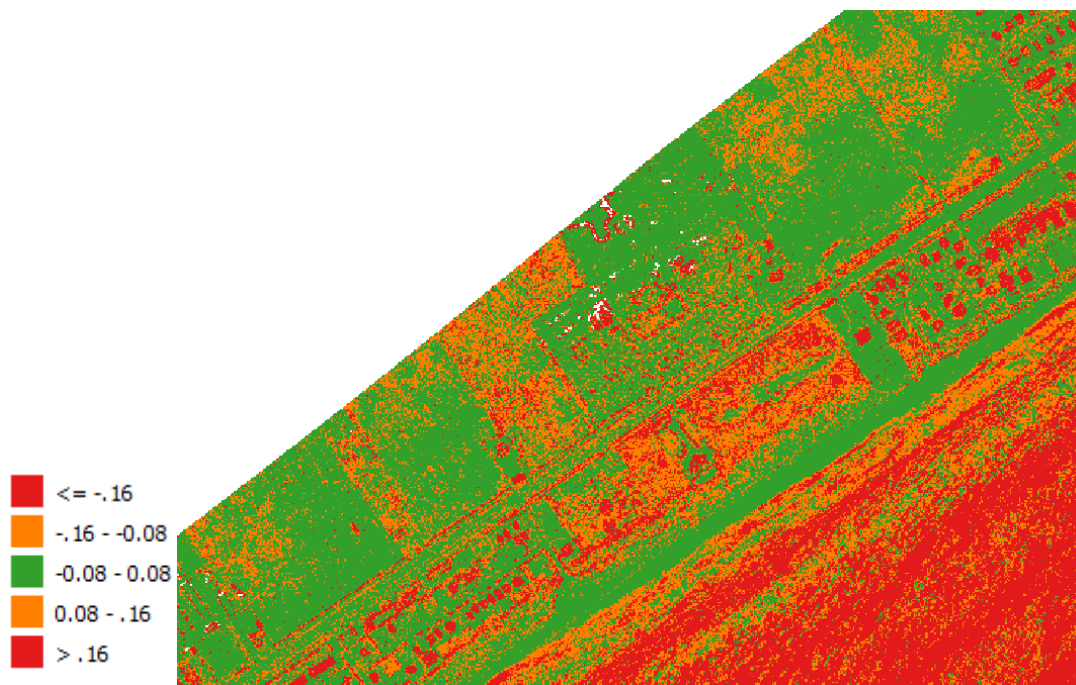


Figure 5 – QC block colored by vertical difference to ensure accuracy at swath edges and throughout.

FINAL CALIBRATION VERIFICATION

Dewberry conducted the survey for 25 ground control points (GCPs) which were used to test the accuracy of the calibrated swath data. These 25 GCPs were available to use as control in case the swath data exhibited any biases which would need to be adjusted or removed. The coordinates of all GCPs are provided in table 3 and the accuracy results from testing the calibrated swath data against the GCPs is provided in table 5; a 6cm bias adjustment was applied to the data.

Point ID	NAD83(2011) UTM Zone 18N		Ellipsoid Ht (NAD83(2011), m)
	Easting X (m)	Northing Y (m)	
GCP-1	680032.651	3062261.214	-24.565
GCP-10	210062.983	3177259.634	-24.085
GCP-11	315388.241	3242969.274	-24.115
GCP-12	329224.924	3249691.342	-22.762
GCP-13	326814.533	3243701.035	-25.140
GCP-14	687572.411	3094697.385	-23.866
GCP-15	241887.793	3184781.651	-25.362
GCP-16	261101.011	3195923.566	-25.247
GCP-17	293250.844	3217901.405	-25.205
GCP-18	357002.035	3268435.361	-25.892
GCP-19	315235.921	3251146.069	-25.343
GCP-2	686821.386	3074184.479	-24.333
GCP-20	311162.097	3233850.889	-25.103
GCP-21	309602.892	3241612.382	-24.314
GCP-22	697839.951	3113236.456	-24.906
GCP-23	682793.180	3088105.687	-24.927
GCP-24	282416.393	3209745.474	-25.231
GCP-25	302090.470	3225775.470	-23.888
GCP-26	745921.275	3145063.541	-22.846
GCP-3	691076.157	3080163.536	-24.337
GCP-4	676927.210	3080359.159	-19.861
GCP-5	341213.284	3259491.459	-24.442
GCP-6	271459.834	3204361.123	-26.107
GCP-7	752568.424	3148957.833	-24.462
GCP-8	208760.392	3167046.086	-23.360
GCP-9	693153.277	3105580.326	-25.330

Table 5 – NOAA_TX-1803 surveyed ground control points (GCPs).

This project must meet Non-vegetated Vertical Accuracy (NVA) ≤ 19.6 cm at the 95% confidence level based on $RMSE_z \leq 10$ cm x 1.9600.

100 % of Totals	# of Points	RMSE _z (m) Spec=0.100 m	NVA (RMSE _z x 1.9600) Spec=0.196 m	Mean (m)	Median (m)	Skew	Std Dev (m)	Min (m)	Max (m)	Kurtosis
GCP	25	0.086	0.168	0.058	0.052	0.573	0.064	-0.068	0.216	0.663

Table 6 - Ground control points (GCPs) vertical accuracy results

REFRACTION CORRECTION

Bathymetric data must have a refraction correction applied, which corrects the horizontal and vertical (depth) positions of each data point by accounting for the change in direction and speed of light as it enters and travels through water. The refraction correction was performed by LEG using AHAB's Lidar Survey Studio (LSS) application.

Lidar Processing & Qualitative Assessment

INITIAL PROCESSING

Dewberry performs several validations on the dataset prior to starting full-scale production on the project. These validations include vertical accuracy of the swath data, inter-swath (between swath) relative accuracy validation, intra-swath (within a single swath) relative accuracy validation, verification of horizontal alignment between swaths, and confirmation of point density and spatial distribution. This initial assessment allows Dewberry to determine if the data are suitable for full-scale production. Addressing issues at this stage allows the data to be corrected while imposing the least disruption possible on the overall production workflow and overall schedule.

The refraction correction was performed by LEG as part of the swath data processing and calibration. After Dewberry received refracted swath data, the initial validation of these calibrated swath revealed systematic outliers in the data's vertical accuracy. It was determined that the calibrated swaths required a -6 cm bias adjustment, which was performed by Dewberry.

Final Swath Vertical Accuracy Assessment

Dewberry tested the vertical accuracy of the non-vegetated terrain swath data prior to additional processing. Dewberry tested the vertical accuracy of the swath data using seventy two non-vegetated (open terrain and urban) independent survey check points. The vertical accuracy is tested by comparing survey checkpoints in non-vegetated terrain to a triangulated irregular network (TIN) that is created from the raw swath points. Only checkpoints in non-vegetated terrain can be tested against raw swath data because the data has not undergone classification techniques to remove vegetation, buildings, and other artifacts from the ground surface.

Checkpoints are always compared to interpolated surfaces from the lidar point cloud because it is unlikely that a survey checkpoint will be located at the location of a discrete lidar point. Dewberry typically uses Terrascan software to test the swath lidar vertical accuracy and the classified lidar vertical accuracy, and Esri ArcMap to test the DEM vertical accuracy so that different software programs are used to validate the vertical accuracy for each project.

Project specifications require a NVA of 19.6 cm based on the RMSE_z (10 cm x 1.9600). The dataset for the TX1803-TB-C Topobathymetric Lidar Project satisfies this criteria. This raw lidar swath data was tested to meet ASPRS Positional Accuracy Standards for Digital Geospatial Data (2014) for a 10 cm RMSE_z vertical accuracy class. Actual NVA accuracy was found to be RMSE_z=

7.3 cm, equating to ± 14.4 cm at 95% confidence level. The table below shows all calculated statistics for the raw swath data.

100 % of Totals	# of Points	RMSEz (m) Spec=0.100 m	NVA (RMSEz x 1.9600) Spec=0.196 m	Mean (m)	Media n (m)	Skew	Std Dev (m)	Kurtosis	Min (m)	Max (m)
NVA	72	0.073	0.144	0.017	0.017	-0.154	0.072	0.593	-0.189	0.175

Table 7 – NVA at 95% confidence level for raw swaths.

Inter-Swath (Between Swath) Relative Accuracy

Dewberry verified inter-swath or between swath relative accuracy of the dataset by creating Delta-Z (DZ) orthos. According to the SOW, USGS Lidar Base Specifications v1.4, and ASPRS Positional Accuracy Standards for Digital Geospatial Data, 10 cm Vertical Accuracy Class or QL2 data must meet inter-swath relative accuracy of 8 cm RMSD_z or less with maximum differences less than 16 cm. These measurements are to be taken in non-vegetated, flat open terrain using single or only returns from all classes.

Measurements are calculated in the DZ orthos on 1-meter pixels. Areas in the dataset where overlapping flight lines are within 8 cm of each other within each pixel are colored green, areas in the dataset where overlapping flight lines have elevation differences in each pixel between 8 cm to 16 cm are colored yellow and areas in the dataset where overlapping flight lines have elevation differences in each pixel greater than 16 cm are colored red. Flat, open areas are expected to be green in the DZ orthos. Areas of vegetation and steep slopes (slopes with 16 cm or more of valid elevation change across 1 linear meter) are expected to appear yellow or red in the DZ orthos. If the project area is heavily vegetated, Dewberry may also create DZ orthos from the initial ground classification only, while keeping all other parameters consistent. This allows Dewberry to review the ground classification relative accuracy beneath vegetation and to ensure flight line ridges or other issues do not exist in the final classified data.

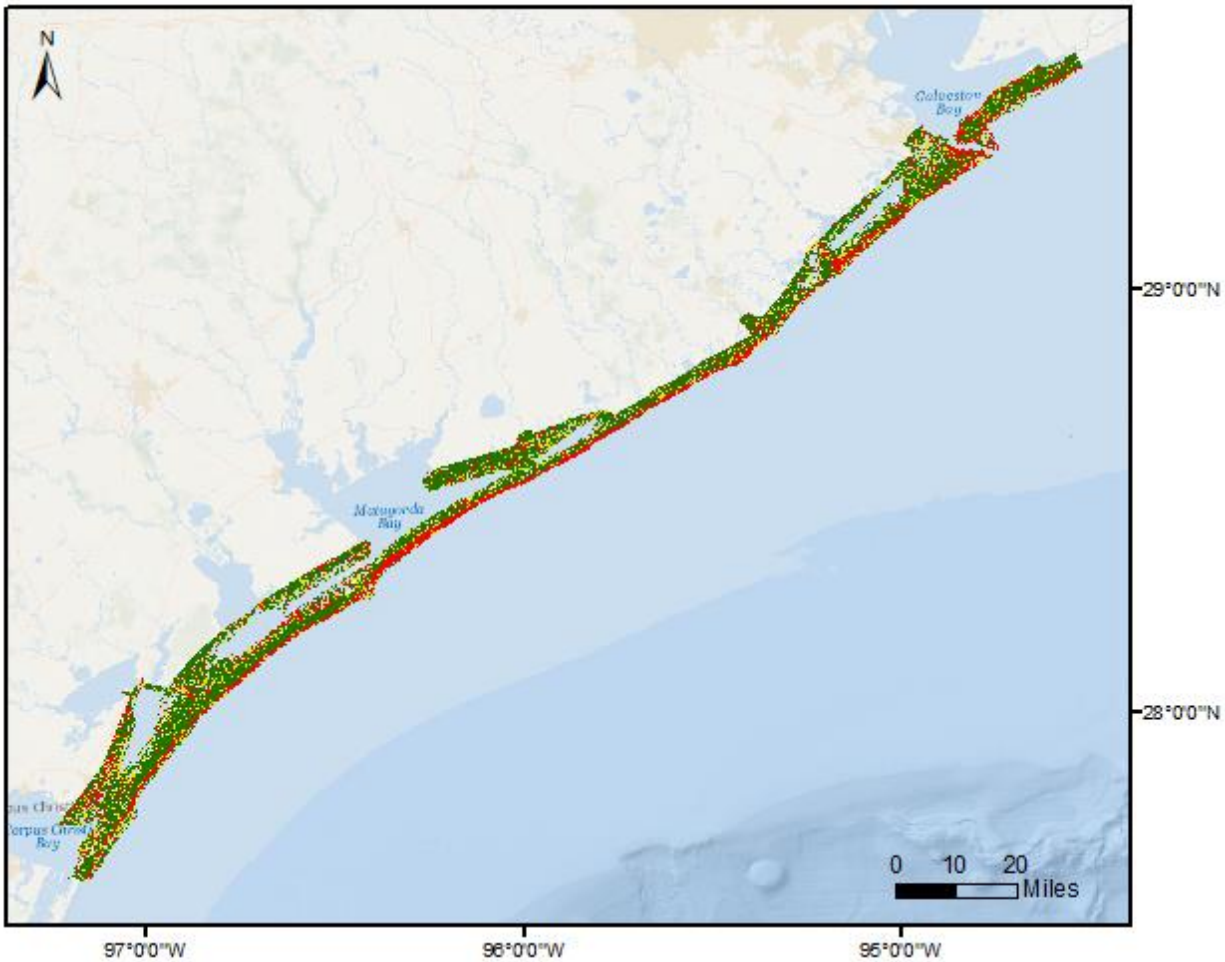


Figure 6 – DZ orthos of 1-meter pixels showing areas where overlapping flight lines are within 8 cm of each other (green), areas where flight lines are between 8 to 16 cm (yellow), and areas greater than 16 cm (red).

Bathymetric areas may be yellow or red due to varying elevations of returns within the water column. Large or continuous sections of yellow or red pixels following flight line patterns and not the terrain, vegetation, or bathymetric areas can indicate the data was not calibrated correctly or that there were issues during acquisition that could affect the usability of the data. This project meets inter-swath relative accuracy specifications.

Intra-Swath (Within a Single Swath) Relative Accuracy

Dewberry verifies the intra-swath (within swath) relative accuracy by using Esri and GeoCue software to generate Z-range rasters that colorize the precision of the laser point density within each swath. Visual inspections are performed using these z-range rasters. Areas that are not aligned with project specifications are flagged and investigated. According to the SOW, USGS Lidar Base Specifications v1.4, and ASPRS Positional Accuracy Standards for Digital Geospatial Data, 10 cm Vertical Accuracy Class or QL2 data must meet intra-swath relative accuracy of 6 cm maximum difference or less.

Horizontal Alignment

Dewberry visually inspects the data to ensure horizontal alignment between adjacent or overlapping flight lines. This inspection targets areas of flat, planar, and reliable surfaces

including rooftops, impervious surface lots, etc. to inspect for horizontal shifts or misalignments between swaths on roof tops and other elevated planar surfaces are highlighted and investigated.

The image below shows an example of the horizontal alignment between swaths for the TX1803-TB-C Topobathymetric Lidar Project. No horizontal alignment issues were identified.

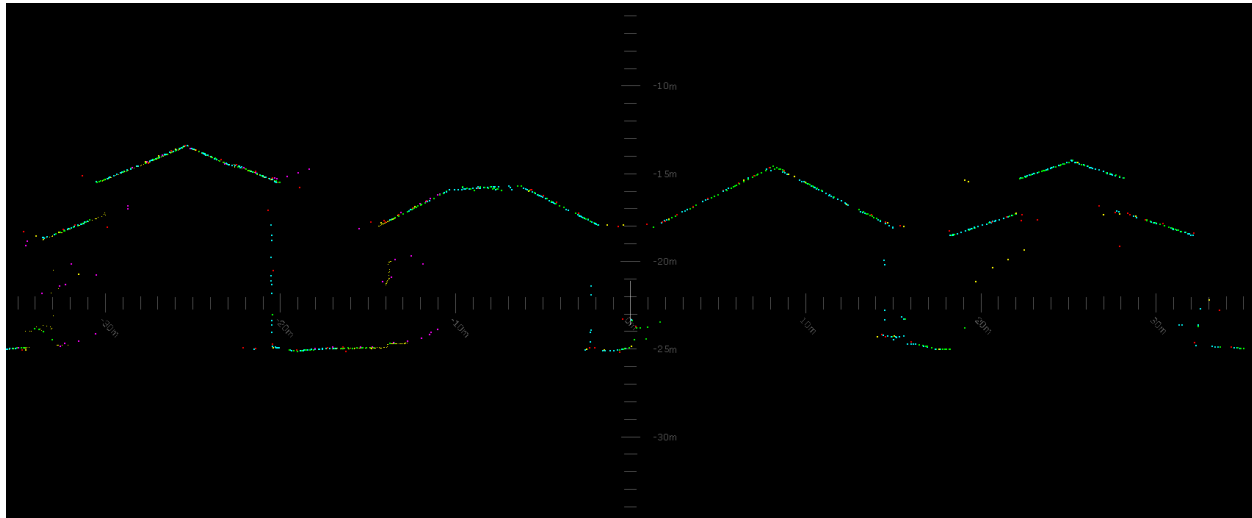


Figure 7 – Horizontal Alignment. Multiple flight lines differentiated by color (Green/Teal/Red/Yellow/Pink) are shown in this profile. There is no visible offset between these flight lines. No horizontal alignment issues were identified.

Point Density and Spatial Distribution

For topographic areas, the required Aggregate Nominal Point Spacing (ANPS) for this project is no greater than 0.71 meters, which equates to an Aggregate Nominal Point Density (ANPD) of 2 points per square meter or greater. For bathymetric areas, the required Aggregate Nominal Point Spacing (ANPS) for this project is no greater than 1.41 meters, which equates to an Aggregate Nominal Point Density (ANPD) of 0.5 points per square meter or greater.

Density calculations were performed using first return data only located in the geometrically usable center portion (typically ~90%) of each swath. The project area was determined to have a combined topobathymetric ANPS of 0.22 meters or an ANPD of 21.18 points per square meter which satisfies the project requirements. A visual review of a 1-square meter density grid (figure below) shows that there are some 1-meter cells that do not contain 2 points per square meter (red areas) due to the irregular spacing of lidar point cloud data. Most 1-square meter cells contain at least 2 points per square meter (green areas) and when density is viewed/analyzed by representative 1-square kilometer areas (to account for the irregular spacing of lidar point clouds), density passes with no issues.

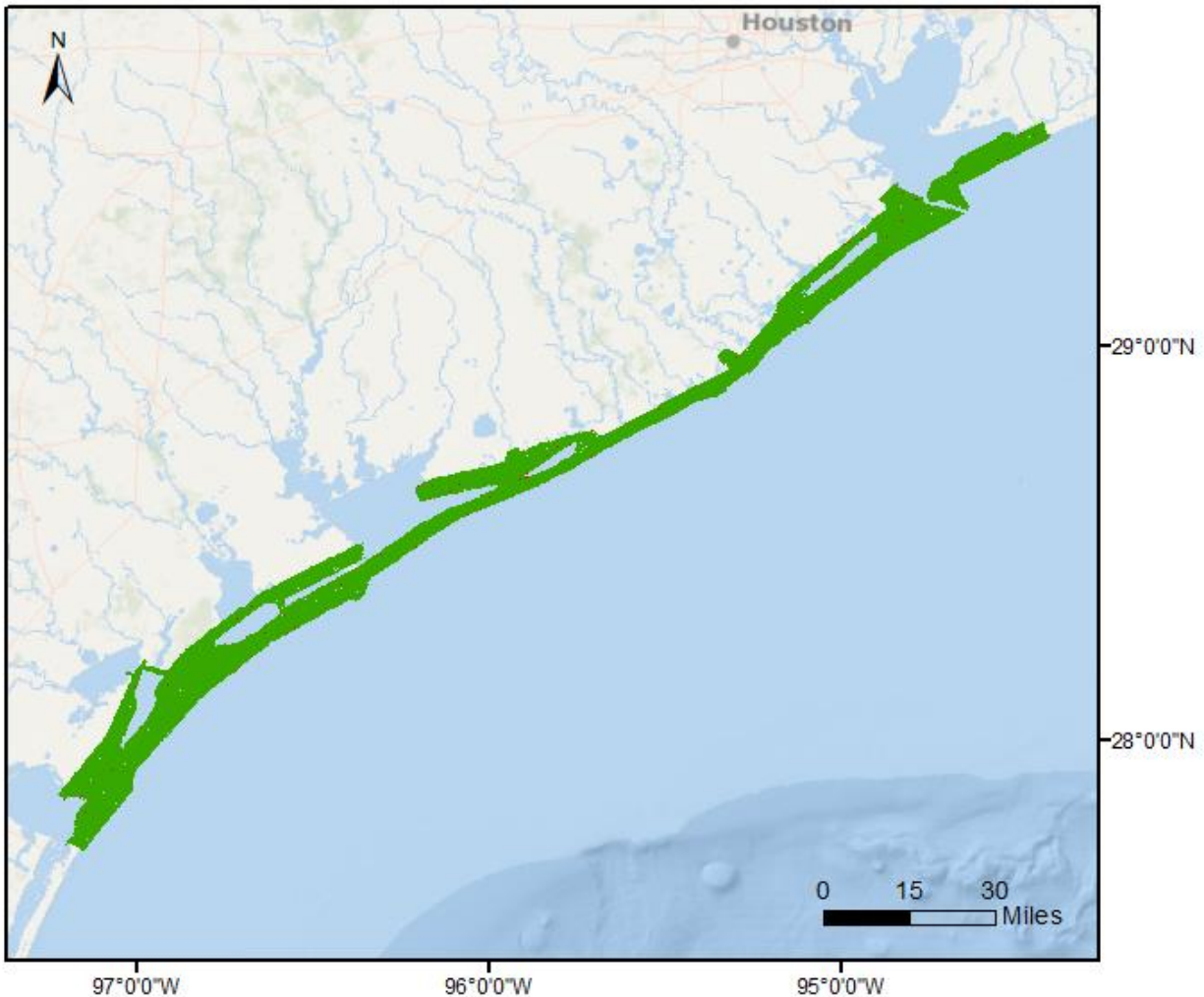


Figure 8 – One square meter density grid of the project AOI. There are some 1-meter cells that do not contain 2 points per square meter (red areas) due to the irregular spacing of lidar point cloud data. Most 1-square meter cells contain at least 2 points per square meter (green areas), showing there are no systematic density issues. When density is viewed/analyzed by representative 1-square kilometer areas, density passes with no issues.

The spatial distribution of points must be uniform and free of clustering. This specification is tested by creating a grid with cell sizes equal to the design 2 x NPS. ArcGIS tools are then used to calculate the number of first return points of each swath within each grid cell. At least 90% of the cells must contain 1 lidar point, excluding acceptable void areas such as low NIR reflectivity features, i.e. some asphalt and roof composition materials. This project passes spatial distribution requirements, as shown in the image below.

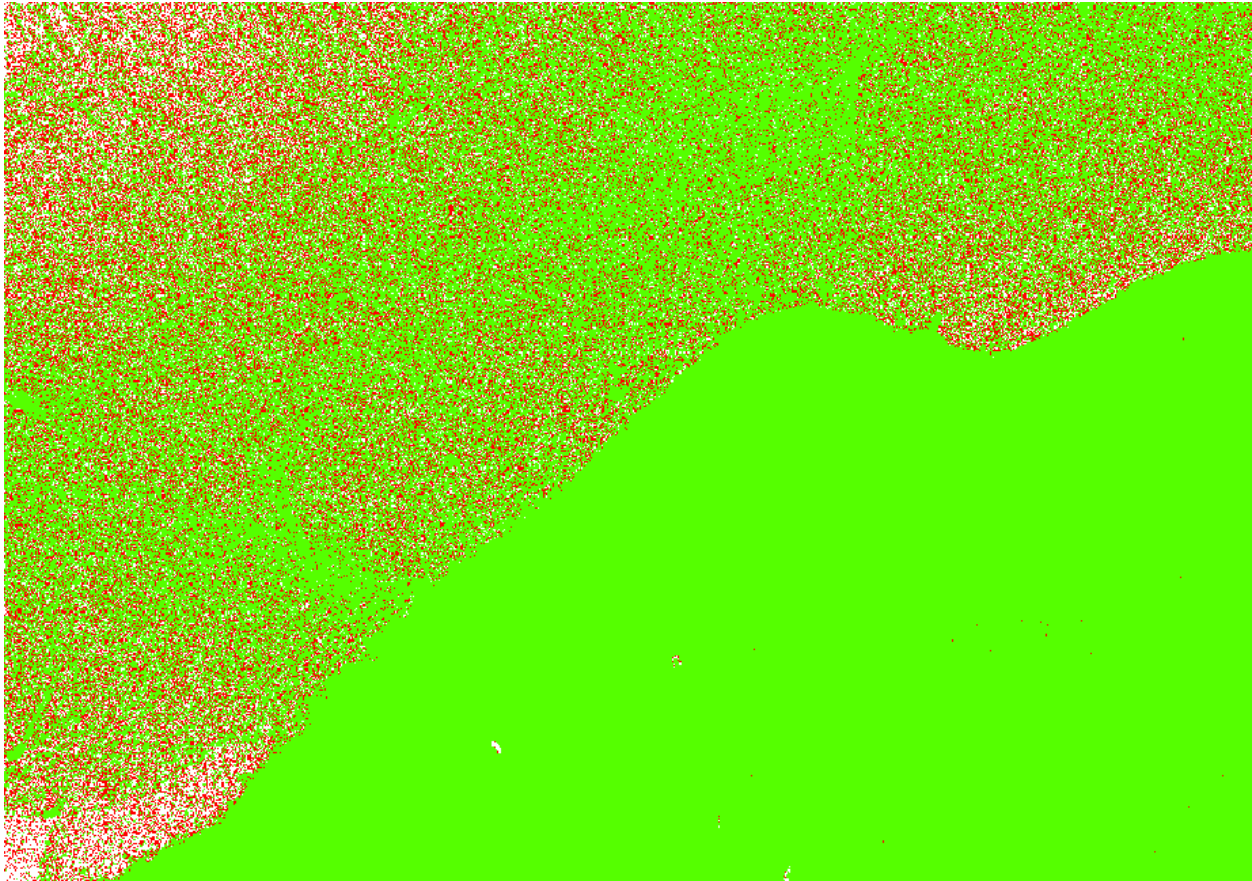


Figure 9 – Spatial Distribution. All cells containing at least one lidar point are colored green. Cells that do not contain a lidar point are colored red. 98.7% of cells contain at least one lidar point.

DATA CLASSIFICATION AND EDITING

Once the calibration, absolute swath vertical accuracy and relative accuracy of the data was confirmed, Dewberry utilized a variety of software suites for data processing. Data processing included breakline creation to define the land/water interface, automated and manual editing of the lidar tiles, quality assurance and quality control (QA/QC), and final formatting of the LAS files.

Breakline Creation and QA/QC

Refraction extents representing the boundary between refracted (bathymetric) and non-refracted (topographic) points must be created so that bathymetric bottom and ground points can be classified properly in the lidar. The processing software for the Leica Chiroptera II system does a basic classification on the lidar, differentiating between land and bathymetric areas. The points designated as bathymetry are then refracted. These refracted points were aggregated into polygons using LAsTools and ArcGIS. As the refraction extents are created from the lidar data, they inherit the horizontal accuracy of the source lidar.

The final refraction extent delineation was used in the lidar classification of ground and bathymetric points.

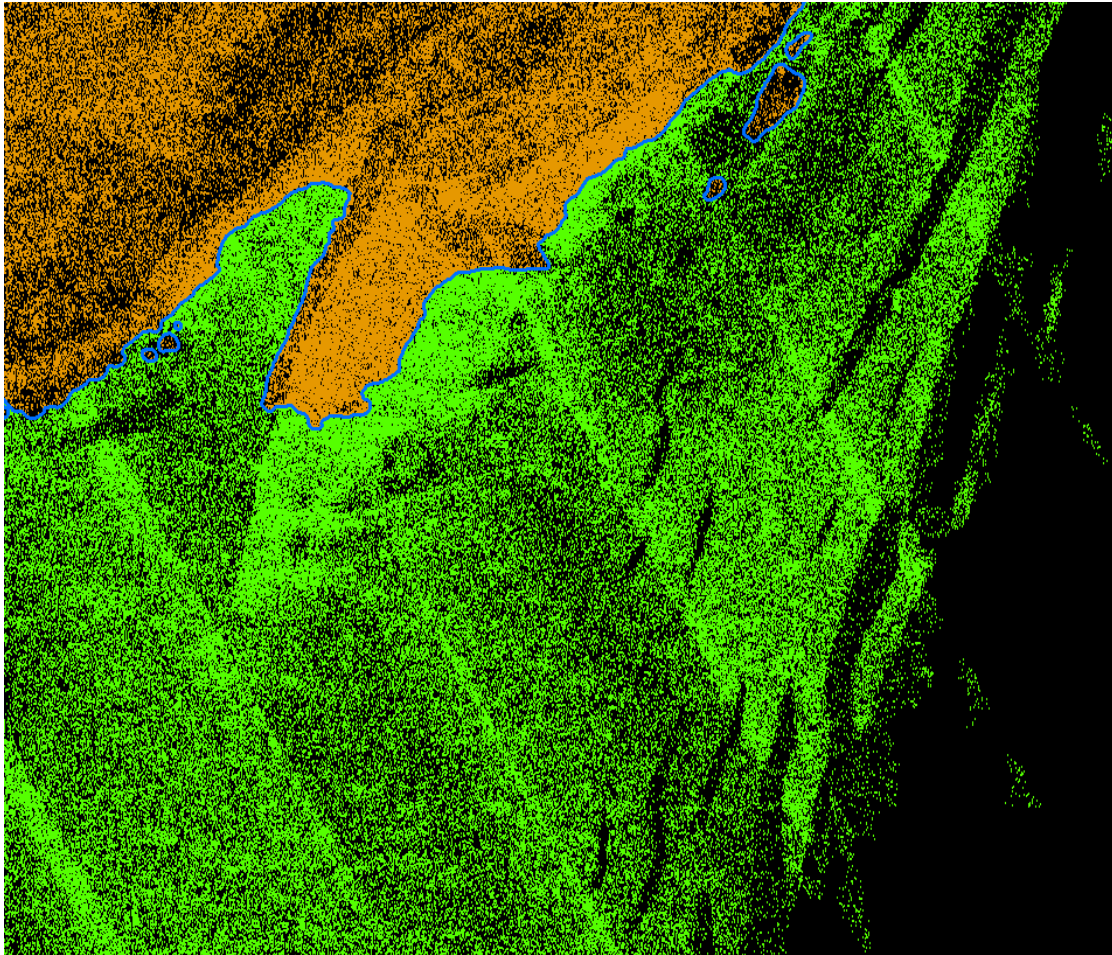


Figure 10 – Tile 2018_331600e_3250240n_las. The refraction extent is shown outlined in blue. The lidar point cloud shows topographic points in orange and bathymetric points in green.

GeoCue and Terrascan Processing

Next is the setup of the GeoCue project, which is done by importing a project-defined tile boundary index encompassing the entire project area. The acquired 3D laser point clouds, in LAS binary format, were imported into the GeoCue project and tiled according to the project tile grid. Once tiled, the laser points were classified using a proprietary routine in TerraScan to create the initial automated ground and bathy bottom classifications, using the final project classification schema.

This routine classifies any obvious outliers in the dataset to class 7. Points along flight line edges that are geometrically unusable are identified as withheld and classified to a separate class so that they will not be used in the initial ground algorithm. After points that could negatively affect the ground are removed from class 1, the ground layer is extracted from this remaining point cloud. The ground extraction process encompassed in this routine takes place by building an iterative surface model.

This surface model is generated using three main parameters: building size, iteration angle and iteration distance. The initial model is based on low points being selected by a "roaming window" with the assumption that these are the ground points. The size of this roaming window is determined by the building size parameter. The low points are triangulated and the remaining points are evaluated and subsequently added to the model if they meet the iteration angle and

distance constraints. This process is repeated until no additional points are added within iterations. A second critical parameter is the maximum terrain angle constraint, which determines the maximum terrain angle allowed within the classification model.

The final breaklines defining the refraction extents are then used to classify “ground” points within the water breaklines as bathymetric bottom. The breaklines are also used as part of the classification routines to ensure water surface and water column points are classified correctly.

Each tile was then imported into Terrascan and a surface model was created to examine the ground (class 2) and bathy bottom (class 40) classification. Dewberry analysts employ 3D visualization techniques to view the point cloud at multiple angles and in profile to ensure that non-ground points are removed from the ground classification and that class 40 accurately represents submerged topography. Dewberry analysts visually reviewed the surface models and corrected errors in the ground classification such as vegetation, buildings, and bridges that were present following the initial processing conducted by Dewberry. Common errors in the bathymetric classification that were corrected by Dewberry include some of the issues outlined below.

Special attention was given along shorelines or the land/water interface as no hard edges or seams should exist between ground and bathy bottom.

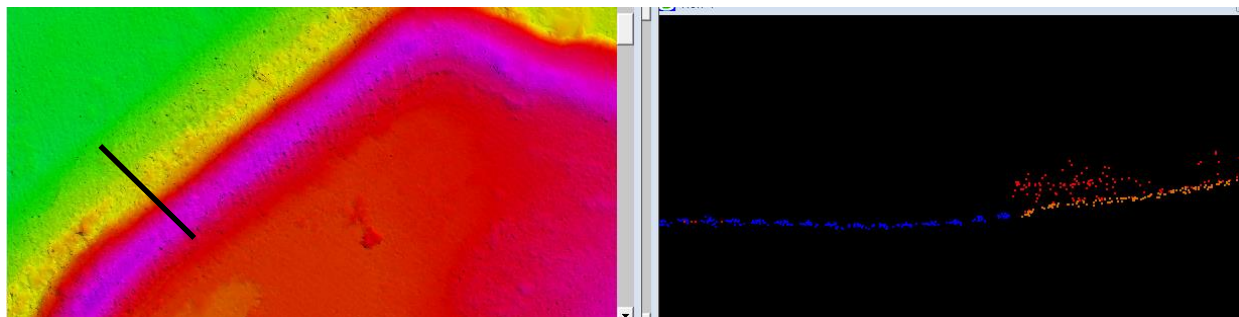


Figure 11 – The land water interface should be seamless with no hard edges or seamlines. The topobathy surface model is shown on the left with a profile location overlaid. The profile is shown in the right image where bathy bottom points are blue, ground points are orange, and unclassified points are red.

Areas of rapids or swift moving water may also need to be removed from the bathy bottom class as these may be surface or water column points and not bathy bottom points due to the water movement and stirring of sediment (increased turbidity). When possible, color orthos were used to help determine water clarity and likelihood of full penetration to the submerged bottom. Generally, editors looked for consistency in data, especially continuous topography (connecting the dots method to ensure channel geometry is reasonable).

Special attention was given in deeper areas where there may not be any true bathy bottom points, but the automated algorithm classified lower water column points as bathy bottom. When evaluating points to determine if they are low water column points or true bathy bottom, the following rules were used as guidelines to maintain accuracy and consistency:

1. Gradient consistency—if the points are part of consistent gradients or consistent channel geometry, they are more likely to be bathy bottom rather than low water column noise. Conversely, points that would cause abrupt changes or inconsistency in the overall gradient or channel geometry are less likely to be bathy bottom points, especially if the

abrupt change would result in shallower (higher) bathy bottom points above lower bathy bottom points with a high confidence.

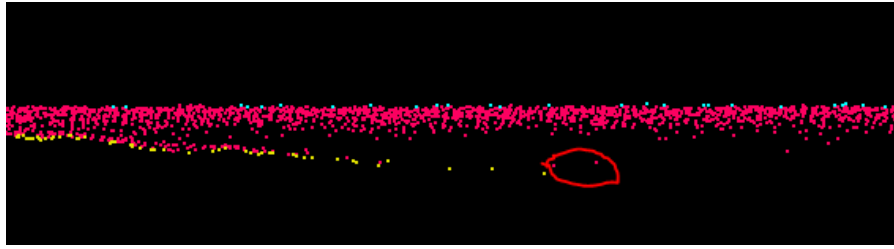


Figure 12 – Bathy Bottom points (yellow) are shown with water column (pink) and water surface points (turquoise) in this profile. The two water column points circled in red would cause inconsistent and upward changes in the topobathy model if these points were classified to bathy bottom. These points should remain classified as water column.

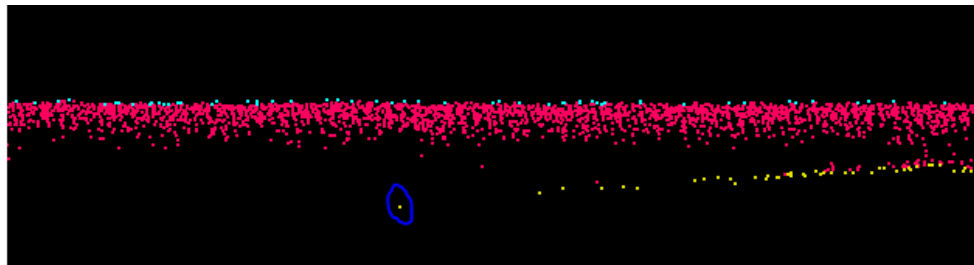


Figure 13 – Bathy Bottom points (yellow) are shown with water column (pink) and water surface points (turquoise) in this profile. The bathy bottom point circled in blue is isolated, but maintains a consistent gradient with other bathy bottom points to the right. This point should remain classified as bathy bottom.

2. Manmade object consistency—manmade objects, such as marinas and artificial or modified channels, are more likely to have been created consistently and at similar depths when multiple channels or inlets are in close proximity to each other. In these locations, if one channel appears much shallower than other manmade channels, the points classified as bathy bottom are more likely to be low water column points.

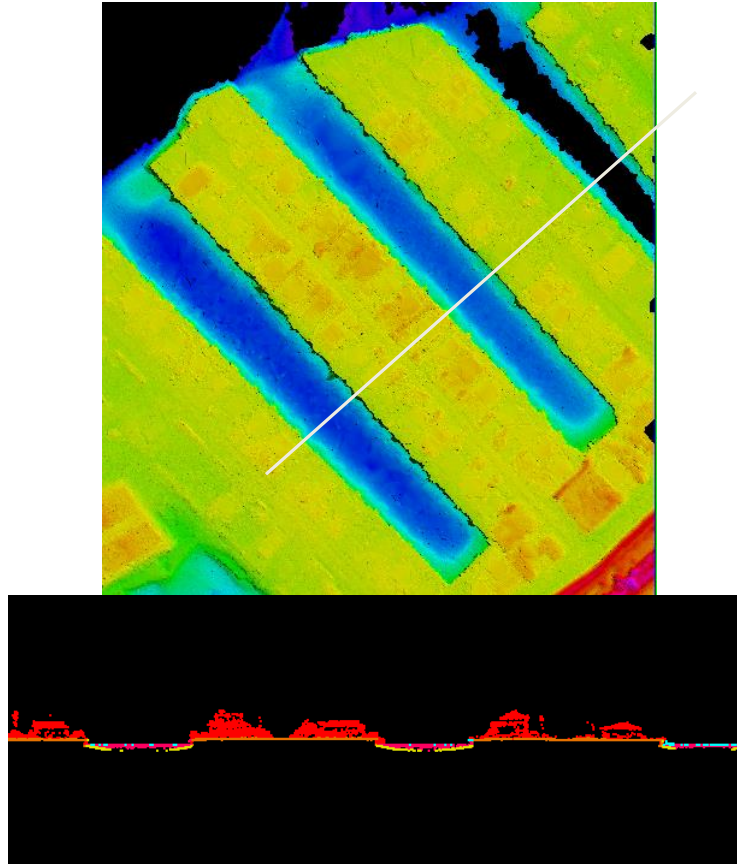


Figure 14 – The topobathy surface model is shown on the top with a profile location overlaid. The profile is shown in the bottom image where bathy bottom points are yellow, ground points are orange, water column points are pink, water surface points are turquoise, and unclassified points are red. These three marina inlets are man-made and likely at very similar depths, as shown in the overview profile. In locations similar to this, points significantly deeper (lower) or shallower (higher) are likely not legitimate bathy bottom, but are more likely to be noise or water column, respectively.

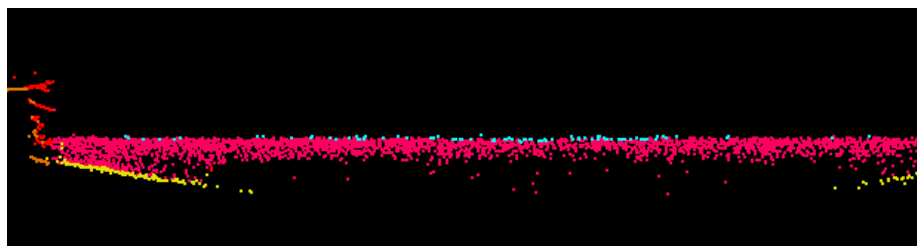


Figure 15 – This profile is a close-up of one of the marina inlets shown in the previous figure. Bathy bottom points are yellow, ground points are orange, water column points are pink, water surface points are turquoise, and unclassified points are red. These marina inlets are man-made and likely at very similar depths. The low water column points are not classified as possible bathy bottom because that classification would cause this inlet to be much shallower than its neighboring inlets in close proximity.

3. Small gap verification—if bathy bottom was obtained for the vast majority of a channel, but small random gaps or voids in the bathy bottom exist after the initial grounding where it is unclear if existing points are bathy bottom or low water column, these small gaps should usually be filled by classifying the points in question to bathy bottom. It is unlikely

such small portions of the channel are that much deeper where no bathy bottom was obtained when the lidar penetrated to the bathy bottom in the rest of the channel. However, if the gaps/voids are larger or consistently form over specific areas or locations, then these areas are more likely to represent deeper areas where the lidar may not have penetrated to the submerged bottom.

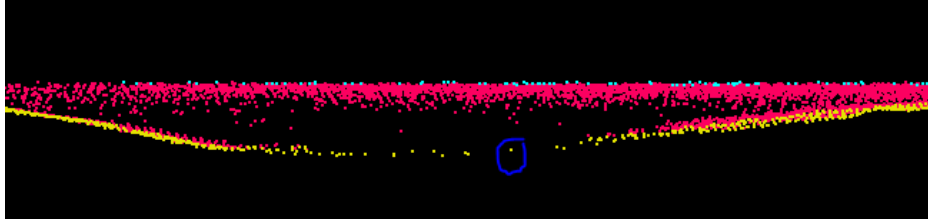


Figure 16 – Bathy Bottom points (yellow) are shown with water column (pink) and water surface points (turquoise) in this profile. The bathy bottom point circled in blue was classified as bathy noise by the initial grounding macro, resulting in a small void. This point was re-classified as bathy bottom to the fill the small gap because this point is at the same depth as surrounding points, maintains a consistent gradient, and is more likely to be submerged bottom rather than low water column noise. Based on the surrounding data, this point most likely represents bathy bottom.

After manual classification, the LAS tiles were peer reviewed and then underwent a final QA/QC. After the final QA/QC and corrections, all headers, appropriate point data records, and variable length records, including spatial reference information, were updated in GeoCue software and then verified using proprietary Dewberry tools.

Submerged Objects

When objects were encountered that were blatantly foreign to the natural bathymetric surface, these features were considered submerged objects and classified as class 43-submerged object.

Temporal Changes

Data acquisition for the project area was collected over a wide time period (October 2018 thru May 2019). Due to varying environmental conditions at the time of different acquisitions, there may be temporal changes within and between flightlines where missions from different acquisitions are merged together. Areas of temporal changes were identified during the manual editing and review of the lidar data. An additional classification, class 46-temporal, was added to the final classification schema to accommodate these temporal differences within the data.

When temporal changes were discovered in the dataset, the following priorities were maintained:

1. Use most recent flight lines to model bathy bottom data.
2. Use older flight lines if it will provide full coverage, will prevent ridges/abrupt changes in the data, or represents better water clarity (i.e. bathy returns) than more recent data.
3. If ridge/abrupt change is unavoidable or boundaries for #1 or #2 are not definable, then use more recent data to full extent and fill in with older/earlier collect where necessary.

Class 46 was used when data was edited to classify out the incorrect ground/bathy surface (to class 46), and classify in the correct ground/bathy surface from class 1/45.

Dewberry identified areas in the bathymetric bottom where multiple ground surfaces were identified between lidar swaths. An example is shown in the figure below.

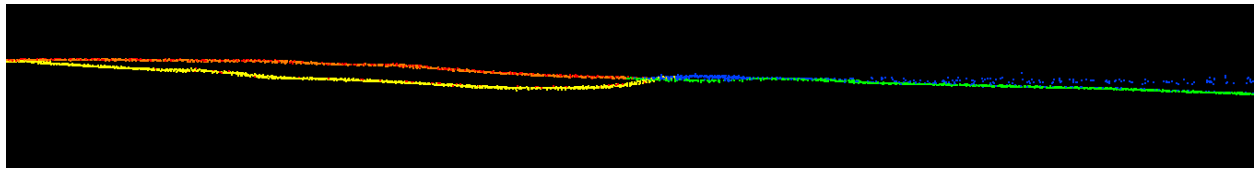


Figure 17 – Points colored by class showing the elevation differences along the identified ground surface. Orange represents topography, yellow represents the temporal class (i.e. less-recent ground), green represents bathymetry, blue is water column, and red is unclassified. Care was taken to use the most recent data to represent the topobathy surface. In this example, the orange line represents the most current ground while yellow represents a ground surface captured from different day's flight; the green bathymetric surface was not affected in this example.

Dewberry also identified areas where tidal fluctuations caused temporal changes in the dataset. Polygons were placed around areas where dramatic tidal fluctuations affected bathymetric coverage. In areas of tidal change between flights, editing was performed in an effort to maintain as much consistency as possible in the bathy bottom. The goal was to minimize abrupt changes but also use the most recently-acquired lidar data. However, there are areas in the dataset where abrupt termination of bathymetric coverage is present due to these tidal variations. The figure below illustrates this. *Note:* the temporal polygons shapefile represent temporal changes influenced by tidal fluctuations whereas class 46 represents temporal changes that resulted in multiple ground surfaces due to overlapping flightlines from different collection periods.

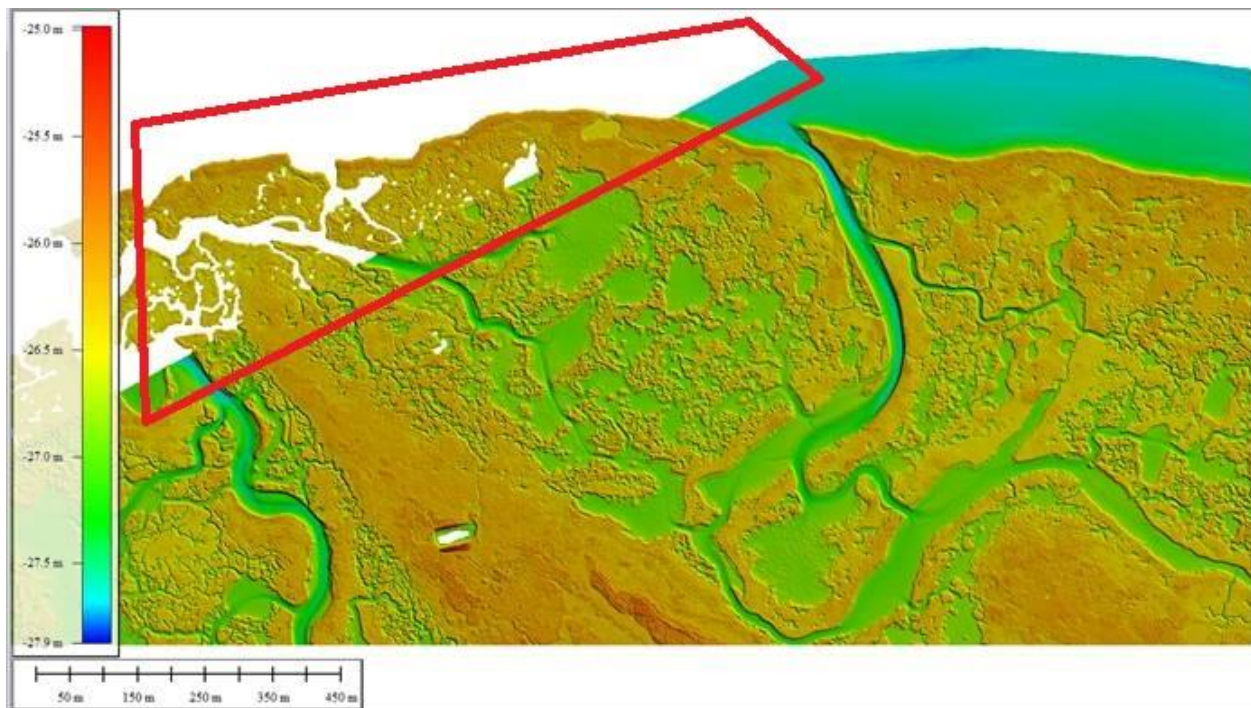


Figure 18 – Temporal changes caused by dramatic tidal fluctuations which affected bathymetric coverage. This caused abrupt temporal changes in the dataset, as identified here by the red polygon. The bathymetric coverage terminates on a linear diagonal consistent with the flightline edge. Instances where tidal fluctuations impacted bathymetric returns were identified in a temporal polygon shapefile. *Note:* the temporal polygons shapefile represent temporal changes influenced by tidal fluctuations whereas class 46-temporal represented temporal changes that resulted in multiple ground surfaces due to overlapping flightlines from different collection periods.

The temporal change polygon shapefile and class 46-temporal data were provided to NOAA with each delivery block as needed.

Flightline Ridges

The flat geographic characteristics of the AOI along the eastern coastline of Texas offered unique challenges post-acquisition during flightline calibration. Flightline ridges occasionally appear in the final digital elevation model in the flat bathymetric surfaces in back bay areas. Every attempt was made to eliminate or minimize these data artifacts. Although these ridges are fully within the projects specifications (≤ 10 cm), they are visible in the final digital elevation model. The figure below illustrates an example of one of these data artifacts.

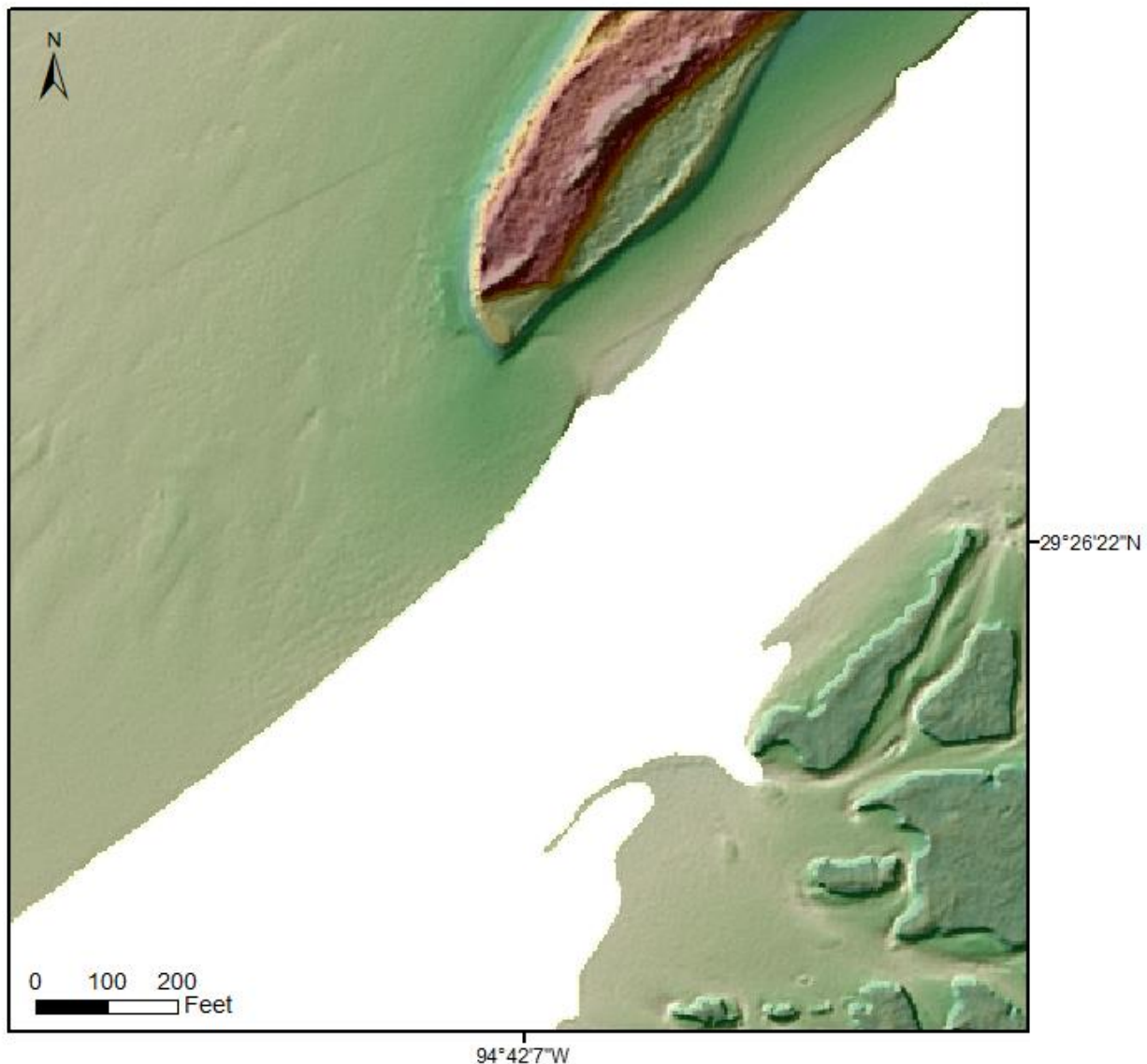


Figure 19 – Flightline ridges similar to the one circled in red occasionally appear in the back bay bathymetric areas throughout the AOI. Although every attempt was made to eliminate or minimize these data artifacts, some still appear in the final digital elevation model.

Since different software and different view settings are used to view geospatial data, these flightline ridges may appear more or less pronounced to different users.

LIDAR QUALITATIVE ASSESSMENT

Dewberry's qualitative assessment utilizes a combination of statistical analysis and interpretative methodology to assess the quality of the data for topobathymetric DEMs. This includes creating pseudo image products such as lidar orthos produced from the intensity returns, TINs, DEMs, void polygons and 3-dimensional models as well as reviewing the actual point cloud data.

Visual Review

During QA/QC, reviewers check for consistent and correct classification. This process looks for anomalies in the data, areas where man-made structures or vegetation points may not have been classified properly to produce a bare-earth model, areas where bathymetry was not classified correctly to produce an accurate submerged topography model, and other classification errors. Reviewers verified that all guidelines outlined in the Data Classification and Editing section were adhered to.

Create Void Polygons

Void polygons were created as part of QA/QC. The void polygons identify areas of sparse to no bathymetric bottom points. The void polygons were loaded when reviewing the data to ensure correct and full classification of bathy bottom. All void areas 9 sq m or larger in the bathymetry domain were delineated with a void polygon.

The void polygon layer was generated using LAStools and ArcGIS to eliminate interpolation across areas greater than 9 square meters in the bathy class (40) for the final elevation raster. A DEM was created using LAStools' 'las2dem' utility, which created and rasterized a TIN from the LAS data. A user-defined threshold specifying the maximum allowable edge length during triangulation was set to 4 m, restricting rasterization in areas of sparse data. Once the constrained DEM was created, ArcGIS was used to vectorize the void (NoData) areas. The resulting polygons were then used to constrain interpolation in the final elevation raster.

Formatting

After the final QA/QC is performed and all corrections have been applied to the dataset, all lidar files are updated to the final format requirements and the final formatting, header information, point data records, and variable length records are verified using proprietary Dewberry tools. The table below lists some of the main lidar header fields that are updated and verified.

Classified Lidar Formatting		
Parameter	Requirement	Pass/Fail
LAS Version	1.4	Pass
Point Data Format	6	Pass
Coordinate Reference System	NAD83 (2011) UTM Zone 14/15, meters and Ellipsoid, meters in WKT Format	Pass
Global Encoder Bit	17	Pass
Time Stamp	Adjusted GPS Time (unique timestamps)	Pass
System ID	NIIRS10 for GeoCue software	Pass
Multiple Returns	The sensor shall be able to collect multiple returns per pulse and the return numbers are recorded	Pass
Intensity	16 bit intensity values are recorded for each pulse	Pass

Classified Lidar Formatting		
Parameter	Requirement	Pass/Fail
Classification	Required Classes include: Class 0: Created, Never Classified Class 1: Unclassified Class 2: Ground Class 7: Noise Class 40: Bathymetric Bottom (submerged topography) Class 41: Water Surface Class 42: Derived Water Surface Class 43: Submerged Object Class 45: No Bottom Found Class 46: Temporal Bathy Bottom	Pass
Overlap and Withheld Points	Points trimmed from overlap edges are flagged as withheld	Pass
Scan Angle	Recorded for each pulse	Pass
XYZ Coordinates	Unique Easting, Northing, and Elevation coordinates are recorded for each pulse	Pass

Table 8 – LAS formatting of final deliverables

Derivative Lidar Products

NOAA required a derivative lidar product to be created, which is described below.

CONFIDENCE LAYER

A confidence layer that reports the standard deviation of all ground and submerged topography points within each 1 meter grid cell has been created for the entire project area. Each 1-meter grid cell has an associated standard deviation value, in meters. The confidence layer extents are the same as the extents for the final topobathymetric DEMs so that the pixels align. The confidence layer shows the standard deviations of topobathymetric points on a cell-by-cell basis. However, changing the symbology of the confidence layer will allow ranges or bins to be set so that the layer can be grouped by threshold and analyzed over large areas.

Lidar Positional Accuracy

BACKGROUND

Dewberry quantitatively tested the dataset by testing the vertical accuracy of the lidar. The vertical accuracy is tested by comparing the discreet measurement of the survey checkpoints to that of the interpolated value within the three closest lidar points that constitute the vertices of a three-dimensional triangular face of the TIN. Therefore, the end result is that only a small sample of the lidar data is actually tested. However there is an increased level of confidence with lidar data due to the relative accuracy. This relative accuracy, in turn, is based on how well one lidar point "fits" in comparison to the next contiguous lidar measurement and is verified as part of the initial processing. If the relative accuracy of a dataset is within specifications and the dataset passes vertical accuracy requirements at the location of survey checkpoints, the vertical accuracy results can be applied to the whole dataset with high confidence due to the passing relative accuracy. Dewberry typically uses Terrascan software to test the initial swath accuracy and the classified lidar vertical accuracy, and Esri ArcMap to test the DEM vertical accuracy so that different software programs are used to validate the vertical accuracy for each project.

Dewberry also tests the horizontal accuracy of lidar datasets when checkpoints are photo-identifiable in the intensity imagery. Photo-identifiable checkpoints in intensity imagery typically include checkpoints located at the ends of paint stripes on concrete or asphalt surfaces or checkpoints located at 90 degree corners of different reflectivity, e.g. a sidewalk corner adjoining a grass surface. The XY coordinates of checkpoints, as defined in the intensity imagery, are compared to surveyed XY coordinates for each photo-identifiable checkpoint. These differences are used to compute the test horizontal accuracy of the lidar. As not all projects contain photo-identifiable checkpoints, the horizontal accuracy of the lidar cannot always be tested.

SURVEY VERTICAL ACCURACY CHECKPOINTS

For the vertical accuracy assessment, 148 check points were surveyed for the project and are located within bare earth/open terrain, grass/weeds/crops, forested/fully grown, and submerged topography land cover categories. The survey report, including a complete list of surveyed checkpoints, is attached as Appendix A.

Every effort was made to ensure checkpoints were evenly distributed throughout the project area. However, the lack of municipal development surrounding Matagorda Bay hindered accessibility to this area. Figure 20 depicts the distribution of survey checkpoints and illustrates the gap in checkpoint coverage at the northern end of the UTM14 boundary due to inaccessibility.

The figure below shows the location of the QA/QC checkpoints used to test the positional accuracy of the dataset.

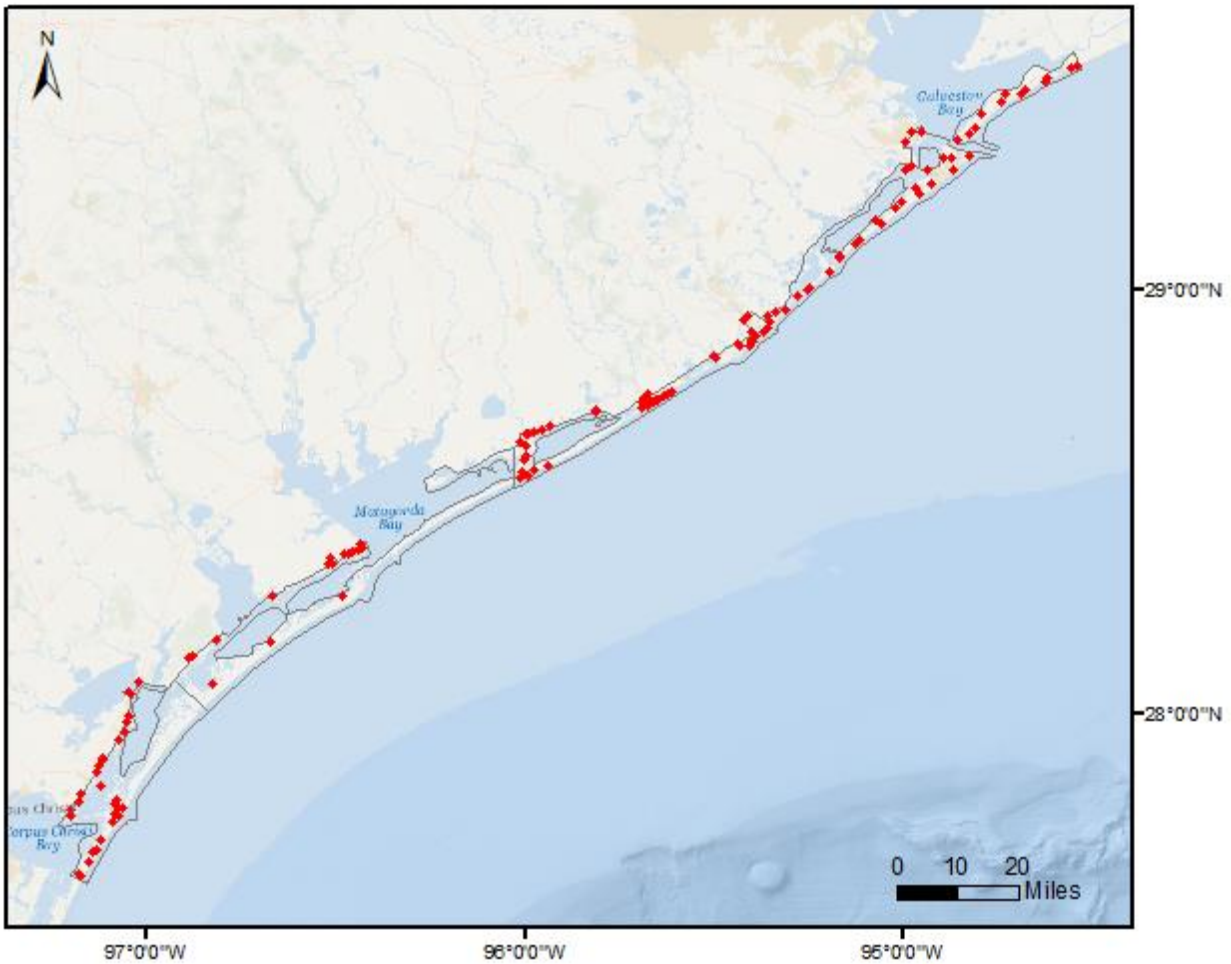


Figure 20 – Location of QA/QC Checkpoints

Fourteen checkpoints were removed from the vertical accuracy testing for the classified lidar due to environmental factors including temporal changes, changes in land cover, out of bounds, or lack of coverage. The coordinates of these checkpoints are provided in the table below and profiles showing the checkpoints are provided in the figures below.

Point ID	NAD83(2011) UTM Zone 18N		NAVD88 (Geoid 12B)		DeltaZ	AbsDeltaZ	Notes
	Easting X (m)	Northing Y (m)	Z-Survey (m)	Z-LiDAR (m)			
NVA-68	336508.111	3256700.765	-24.563	-24.790	-0.227	0.227	Truck in driveway
VVA-10	712716.585	3124813.468	-24.729	outside	0.485	0.485	outside boundary
VVA-25	229371.022	3183842.073	-26.325	-25.840	N/A	N/A	submerged
VVA-9	711107.429	3122616.285	-25.284	outside	0.676	0.676	outside boundary
SMB-16	300930.501	3225657.057	-27.116	-26.440	N/A	N/A	no bathy coverage

TX1803-TB-C, Hurricane Harvey Post Storm Topography/Bathymetry Project Report of Survey
December 31, 2019

SMB-10	242203.918	3185197.538	-26.592	outside	N/A	N/A	no bathy coverage
SMB-17	313382.739	3235081.321	-26.995	outside	N/A	N/A	no bathy coverage
SMB-18	317392.337	3252674.983	-27.657	outside	N/A	N/A	no bathy coverage
SMB-19	327418.716	3246480.684	-27.568	-27.200	0.368	0.368	no bathy coverage
SMB-20	329204.601	3252427.169	-27.398	outside	N/A	N/A	no bathy coverage
SMB-22	354358.144	3264976.596	-27.636	-26.650	0.986	0.986	temporal
SMB-5	693982.587	3111398.277	-27.447	outside	N/A	N/A	no bathy coverage
SMB-8	210496.628	3173968.397	-26.827	outside	N/A	N/A	no bathy coverage
SMB-9	229632.187	3183388.961	-26.965	outside	N/A	N/A	no bathy coverage

Table 9 – Checkpoints removed from vertical accuracy testing.

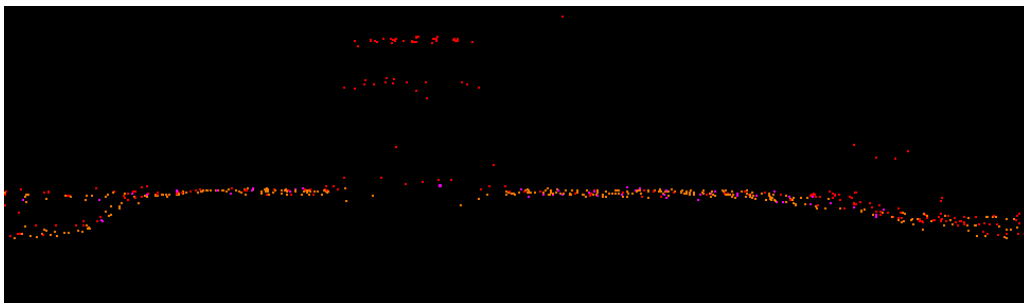


Figure 21 – NVA-68 is located under a vehicle. This checkpoint was removed from all vertical accuracy calculations.



Figure 22 – VVA-9 (left) and VVA-10 (right). These checkpoints were outside of the lidar swath coverage for the AOI. Accuracy could not be assessed. These checkpoints were removed from all vertical accuracy calculations.

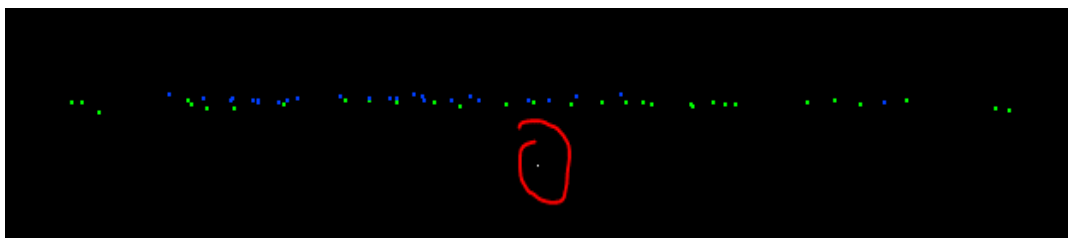
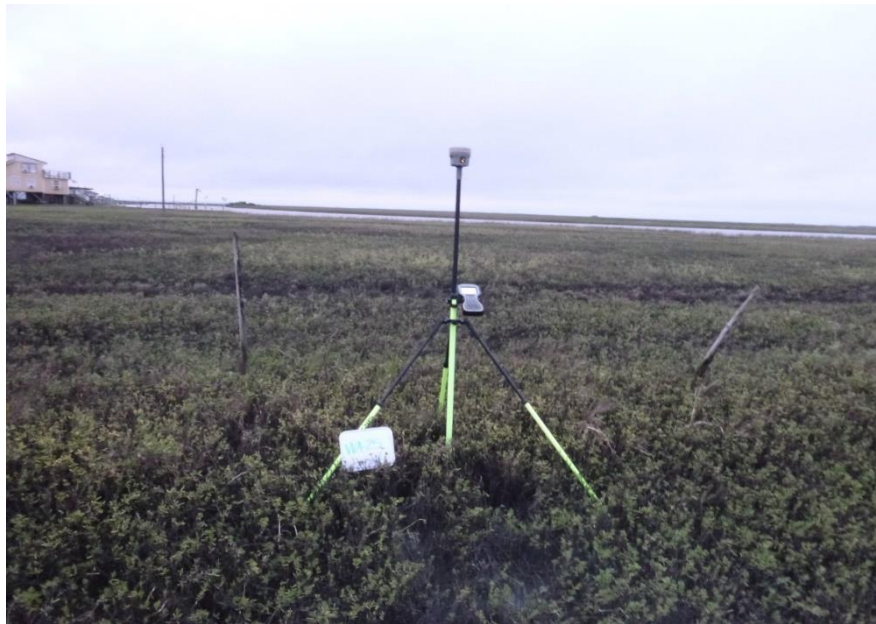


Figure 23 – VVA-25 is circled in red. This checkpoint was submerged during the time of lidar data acquisition. Accuracy could not be assessed. This checkpoint was removed from all vertical accuracy calculations.

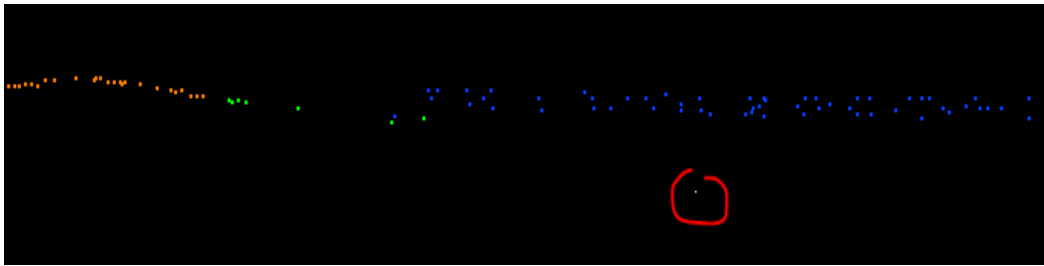
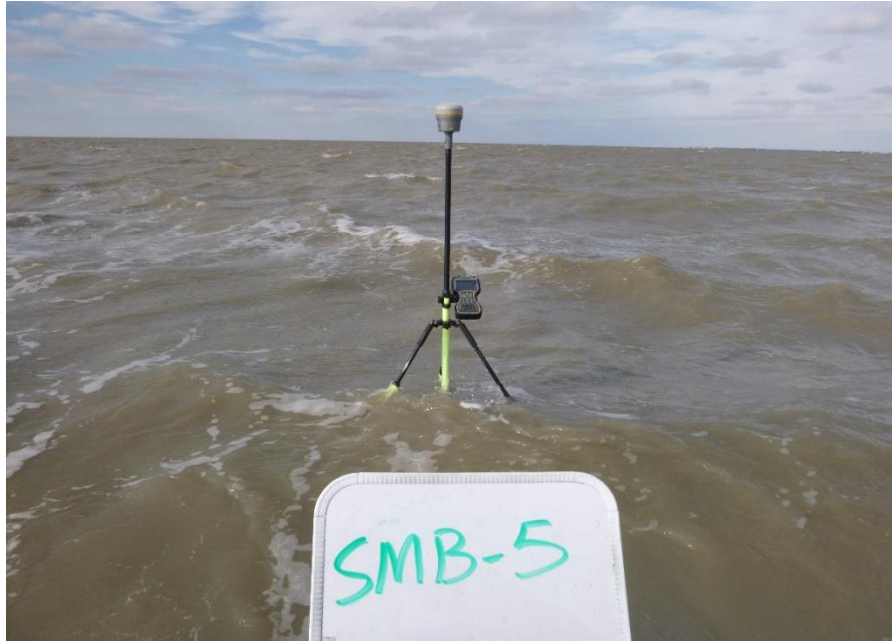


Figure 24 – SMB checkpoints 5, 8, 9, 10, 16, 17, 18, 19, and 20 were all in areas where the lidar sensor was unable to penetrate fully to the submerged ground. An example, SMB-5, is circled in red. Accuracy could not be assessed. These checkpoint was removed from all vertical accuracy calculations.



Figure 25 – SMB- 22 circled in red. This checkpoint was affected by temporal between the date of survey and data acquisition. Accuracy could not be assessed. This checkpoint was removed from all vertical accuracy calculations.

VERTICAL ACCURACY TEST PROCEDURES

NVA is determined with checkpoints located only in non-vegetated terrain, including open terrain (grass, dirt, sand, and/or rocks) and urban areas, where there is a very high probability that the lidar sensor will have detected the bare-earth ground surface and where random errors are expected to follow a normal error distribution. The NVA determines how well the calibrated lidar sensor performed. With a normal error distribution, the vertical accuracy at the 95% confidence level is computed as the vertical root mean square error ($RMSE_z$) of the checkpoints $\times 1.9600$. For the TX1803-TB-C Topobathymetric Lidar Project, vertical accuracy must be 19.6 cm or less based on an $RMSE_z$ of 10 cm $\times 1.9600$.

Bathymetric Vertical Accuracy is determined with check points located only in submerged topography. With a normal error distribution, the vertical accuracy at the 95% confidence level is computed as the vertical root mean square error ($RMSE_z$) of the checkpoints $\times 1.9600$. For the TX1803-TB-C Topobathymetric Lidar Project, bathymetric vertical accuracy must be 35.3 cm or less based on an $RMSE_z$ of 18 cm $\times 1.9600$.

VVA is determined with all checkpoints in vegetated land cover categories, including tall grass, weeds, crops, brush and low trees, and fully forested areas, where there is a possibility that the lidar sensor and post-processing may yield elevation errors that do not follow a normal error distribution. VVA at the 95% confidence level equals the 95th percentile error for all checkpoints in all vegetated land cover categories combined. The TX1803-TB-C Topobathymetric Lidar Project VVA standard is 30 cm based on the 95th percentile. The VVA is accompanied by a listing

of the 5% outliers that are larger than the 95th percentile used to compute the VVA; these are always the largest outliers that may depart from a normal error distribution. Here, Accuracy_z differs from VVA because Accuracy_z assumes elevation errors follow a normal error distribution where RMSE procedures are valid, whereas VVA assumes lidar errors may not follow a normal error distribution in vegetated categories, making the RMSE process invalid.

The relevant testing criteria are summarized in table 10.

Quantitative Criteria	Measure of Acceptability
Non-Vegetated Vertical Accuracy (NVA) in open terrain and urban land cover categories using RMSE _z x 1.9600	19.6 cm (based on RMSE _z (10 cm) * 1.9600)
Bathymetric Vertical Accuracy in submerged topography using RMSE _z x 1.9600	35.3 cm (based on RMSE _z (30 cm) * 1.9600)
Vegetated Vertical Accuracy (VVA) in all vegetated land cover categories combined at the 95% confidence level	30.0 cm (based on combined 95 th percentile)

Table 10 – Acceptance criteria.

The primary QA/QC vertical accuracy testing steps used by Dewberry are summarized as follows:

1. Dewberry's team surveyed QA/QC vertical checkpoints in accordance with the project's specifications.
2. Next, Dewberry interpolated the topobathy lidar DEM to provide the z-value for every checkpoint.
3. Dewberry then computed the associated z-value differences between the interpolated z-value from the lidar data and the ground truth survey checkpoints and computed NVA, VVA, bathymetric vertical accuracy and other statistics.
4. The data were analyzed by Dewberry to assess the accuracy of the data. The review process examined the various accuracy parameters as defined by the scope of work. The overall descriptive statistics of each dataset were computed to assess any trends or anomalies. This report provides tables, graphs and figures to summarize and illustrate data quality.

VERTICAL ACCURACY RESULTS

The table below summarizes the tested vertical accuracy resulting from a comparison of the surveyed checkpoints to the elevation values present within the fully classified lidar LAS files.

Land Cover Category	# of Points	NVA (RMSE _z x 1.9600) Spec=0.196 m	VVA (95th Percentile) Spec=0.300 m	Bathymetric Vertical Accuracy (RMSE _z x 1.9600) Spec=0.353 m
NVA	72	0.138		
VVA	50		0.264	
Bathymetric Vertical Accuracy	12			0.292

Table 11 – Tested vertical accuracy of the classified lidar by land cover category.

The topographic portion of this lidar dataset was tested to meet ASPRS Positional Accuracy Standards for Digital Geospatial Data (2014) for a 10 cm RMSE_z Vertical Accuracy Class. Actual NVA accuracy was found to be RMSE_z = 7.1 cm, equating to ± 13.8 cm at 95% confidence level. Actual VVA accuracy was found to be ± 26.4 cm at the 95th percentile. The bathymetric portion

of this lidar dataset was tested to meet the vertical RMSE_z of QL2_b specified in the Draft National Coastal Mapping Strategy 1.0 Document where vertical accuracy coefficients *a* and *b* are defined as 0.30 and 0.0130, respectively. Using the formula $\sqrt{(a^2 + (b \times d)^2)}$ where *a* equals constant depth errors, *b* equals depth dependent errors, and *d* equals depth, the bathymetric portion of this lidar dataset was tested to meet 30 cm RMSE_z based on the depths of the surveyed submerged topography checkpoints. Actual bathymetric vertical accuracy was found to be RMSE_z = 14.9 cm, equating to ± 29.2 cm at 95% confidence level.

Overall descriptive statistics for each land cover category are provided in table 12. Table 13 lists the VVA 5% outliers that are larger than the 95th percentile.

Land Cover Category	# of Points	RMSE _z (m) Spec=0.100 m NVA/ 0.180 m Submerged Topography	Mean (m)	Median (m)	Skew	Std Dev (m)	Kurtosis	Min (m)	Max (m)
NVA	72	0.071	0.006	0.004	-0.021	0.071	0.593	-0.189	0.165
VVA	50	N/A	0.105	0.086	0.136	0.100	1.021	-0.160	0.379
Submerged Topography	12	0.149	0.132	0.118	1.518	0.073	4.131	0.017	0.320

Table 12 – Vertical accuracy descriptive statistics by land cover category.

Point ID	NAD83(2011) UTM Zone 18N		NAVD88 (Geoid 12B)		DeltaZ	AbsDeltaZ
	Easting X (m)	Northing Y (m)	Z-Survey (m)	Z-LiDAR (m)		
VVA-27	242846.129	3186973.387	-25.849	-25.470	0.379	0.379
VVA-31	261155.838	3196167.500	-25.667	-25.390	0.277	0.277
VVA-34	270062.614	3206383.668	-26.090	-25.790	0.300	0.300

Table 13 – VVA 5% outliers.

The figure below shows a histogram of the elevation discrepancies between the QA/QC checkpoints and elevations interpolated from the lidar TIN. The frequency shows the number of discrepancies within each band of elevation differences. Although the discrepancies vary between a low of -0.189 meters and a high of +0.379 meters, the histogram shows that the majority of the discrepancies are skewed on the positive side. The majority of points are within the range of -0.05 meters to +0.05 meters.

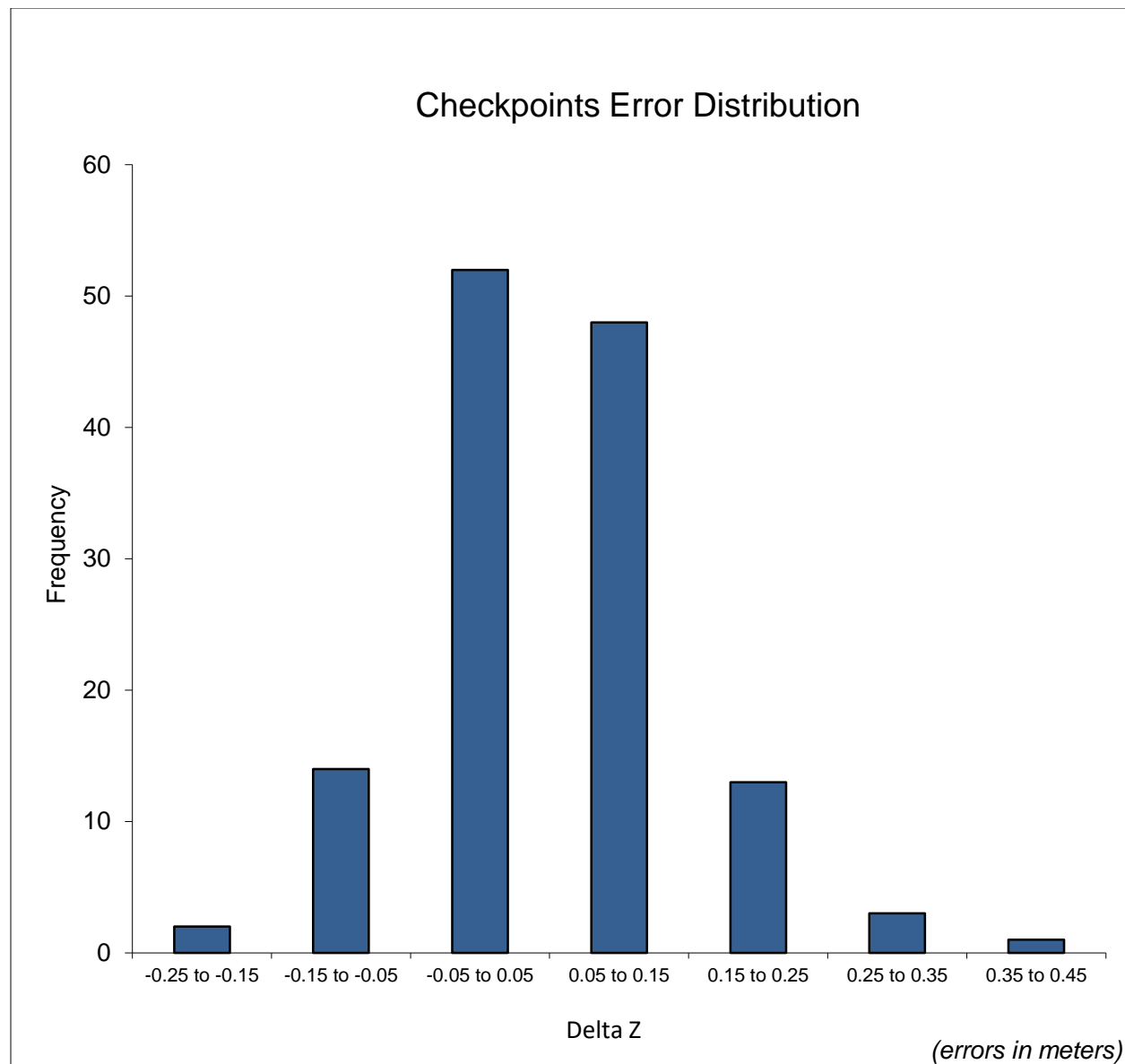


Figure 26 – Histogram of elevation discrepancies. Error (Delta Z) is illustrated in 0.10 meter bins.

Based on the vertical accuracy testing conducted by Dewberry, the lidar dataset for the NOAA TX1803-TB-C Topobathymetric Lidar Project satisfies the project's pre-defined vertical accuracy criteria.

HORIZONTAL ACCURACY TEST PROCEDURES

Horizontal accuracy testing requires well-defined checkpoints that can be identified in the dataset. Elevation datasets, including lidar datasets, do not always contain well-defined checkpoints suitable for horizontal accuracy assessment. However, the ASPRS Positional Accuracy Standards for Digital Geospatial Data (2014) recommends at least half of the NVA vertical check points should be located at the ends of paint stripes or other point features visible on the lidar intensity image, allowing them to double as horizontal check points.

Dewberry reviews all NVA checkpoints to determine which, if any, of these checkpoints are located on photo-identifiable features in the intensity imagery. This subset of checkpoints are then used for horizontal accuracy testing.

The primary QA/QC horizontal accuracy testing steps used by Dewberry are summarized as follows:

1. Dewberry's team surveyed QA/QC vertical checkpoints in accordance with the project's specifications and tried to locate half of the NVA checkpoints on features photo-identifiable in the intensity imagery.
2. Next, Dewberry identified the well-defined features in the intensity imagery.
3. Dewberry then computed the associated xy-value differences between the coordinates of the well-defined feature in the lidar intensity imagery and the ground truth survey checkpoints.
4. The data were analyzed by Dewberry to assess the accuracy of the data. Horizontal accuracy was assessed using NSSDA methodology where horizontal accuracy is calculated at the 95% confidence level. This report provides the results of the horizontal accuracy testing.

HORIZONTAL ACCURACY RESULTS

Seven checkpoints were determined to be photo-identifiable in the intensity imagery and were used to test the horizontal accuracy of the lidar dataset. As only seven checkpoints were photo-identifiable, the results reported herein are not statistically significant enough to report as a final tested value, but the results of the testing are shown in the table below.

Using NSSDA methodology (endorsed by the ASPRS Positional Accuracy Standards for Digital Geospatial Data (2014)), horizontal accuracy at the 95% confidence level (called $ACCURACY_r$) is computed by the formula $RMSE_r \times 1.7308$ or $RMSE_{xy} \times 2.448$.

No horizontal accuracy requirements or thresholds were provided for this project. However, lidar datasets are generally calibrated by methods designed to ensure a horizontal accuracy of 1 m or less at the 95% confidence level.

# of Points	RMSE _x (m)	RMSE _y (m)	RMSE _r (m)	ACCURACY _r (RMSE _r x 1.7308) Target = 1.000 m
7	0.294	0.218	0.366	0.633

Table 14 – Tested horizontal accuracy at the 95% confidence level.

This data set was produced to meet ASPRS Positional Accuracy Standards for Digital Geospatial Data (2014) for a 41 cm RMSE_x/RMSE_y Horizontal Accuracy Class which equates to Positional Horizontal Accuracy = ± 1 meter at a 95% confidence level. Seven checkpoints were photo-identifiable but do not produce a statistically significant tested horizontal accuracy value. Using this small sample set of photo-identifiable checkpoints, positional accuracy of this dataset was found to be RMSE_x = 29.4 cm and RMSE_y = 21.8 cm which equates to ± 63.3 cm at 95% confidence level.

DEM Processing & Qualitative Assessment

The final topobathy DEMs are IMG format with 1 meter pixel cell size, tiled, and named according to project specifications. Void polygons were enforced in the DEMs so that bathymetric areas where no bathymetry was collected are NoData in the DEMs.

FINAL VOID POLYGONS

Final void polygons were created after all lidar edits and corrections were made. The void polygon layer was generated using LAStools 'las2dem' utility and ArcGIS to eliminate interpolation across areas greater than 9 sq m in the bathy class (40) in the final elevation raster. A user-defined threshold specifying the maximum allowable edge length during triangulation was set to 4 m, restricting rasterization in areas of sparse data. Once the constrained DEM was created, ArcGIS was used to vectorize the void (NoData) areas.

Once the final void polygons were created, they were used as a constraint to enforce voids (NoData) during the topobathymetric DEM creation.

DEM GENERATION

Digital elevation models were created using only ground (class 2) and submerged topography (class 40) lidar point data. A TIN was generated from these data and rasterized at a 1 m spatial resolution using LAStools 'blast2dem' utility. Void polygons (discussed previously) were used to eliminate large areas of interpolation in the DEM ($\geq 9 \text{ m}^2$). The DEM was clipped to the tile grid to create individual tiled DEMs that were named according to project specifications.

DEM QUALITATIVE REVIEW

Dewberry performed a comprehensive qualitative assessment of the topobathy DEM deliverables to ensure that all tiled DEM products were delivered with the proper extents and formatting, and contained the proper referencing information. This process was performed in ArcGIS with the use of a proprietary toolset.

The final topobathy DEMs were then reviewed in Global Mapper at a 1:3000 scale. A review with the void polygons visible and another review without the void polygons visible was performed in order to ensure voids were enforced properly and there were no issues along the boundaries of the void layer. Special attention was given along the land/water interface to ensure there were no hard edges along the interface. Any remaining lidar issues and DEM artifacts were flagged by the reviewer and corrected by the editing team as necessary.

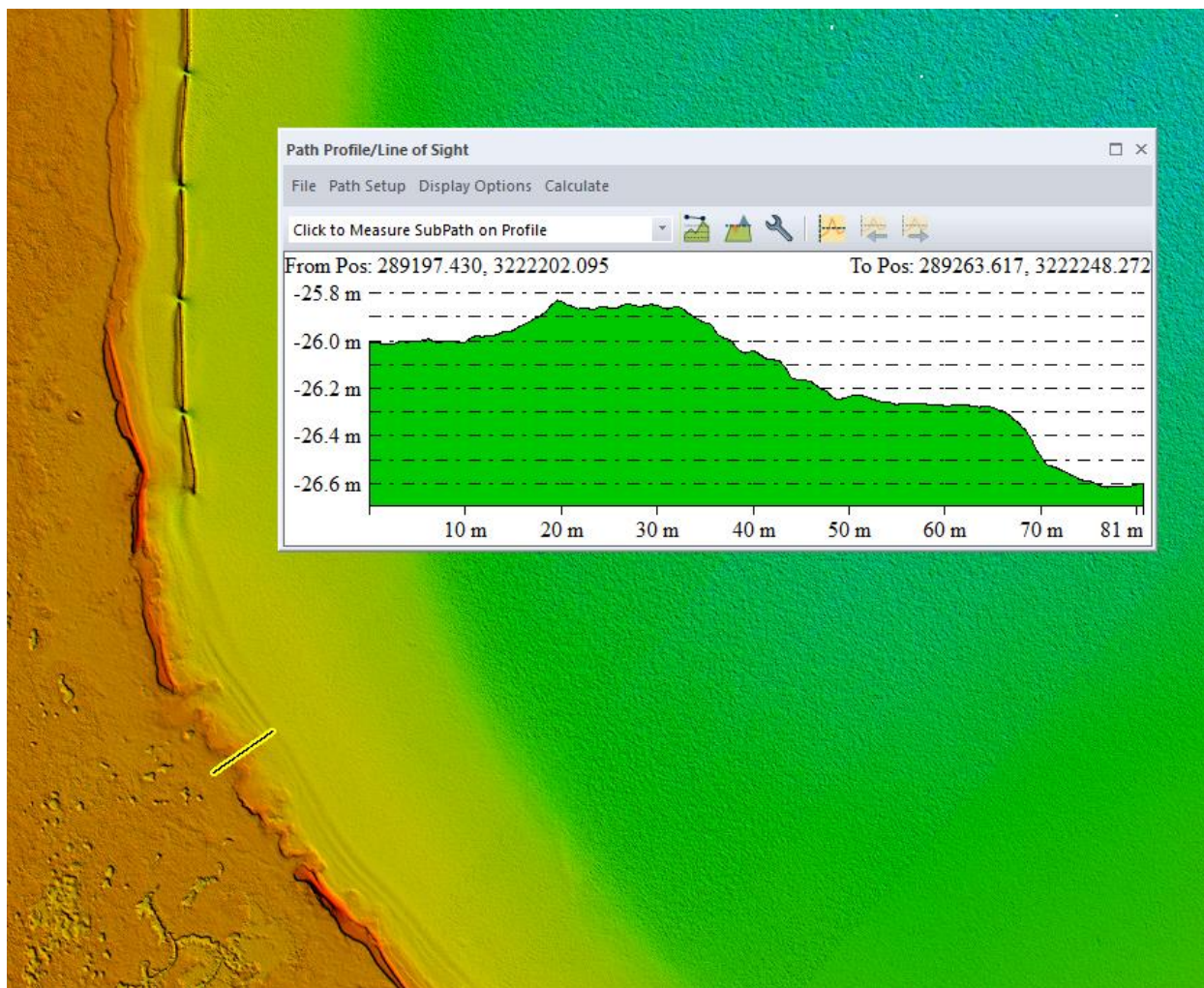


Figure 27 – DEM tile 2018_288600e_3223240n_dem. An example of the land-water interface is shown. No hard edges along the interface were identified during DEM QA/QC.

DEM QUANTITATIVE ASSESSMENT

The same 134 checkpoints that were used to test the vertical accuracy of the lidar were used to validate the vertical accuracy of the final DEM products. Accuracy results may vary between the source lidar and final DEM deliverable. DEMs are created by averaging several lidar points within each pixel which may result in slightly different elevation values at each survey checkpoint when compared to the source LAS, which does not average lidar points together but may interpolate (linearly) between two or three points to derive an elevation value. The vertical accuracy of the DEM is tested by extracting the elevation of the pixel that contains the x/y coordinates of the checkpoint and comparing these DEM elevations to the surveyed elevations. Dewberry typically uses Terrascan software to test the lidar vertical accuracy and the classified lidar vertical accuracy, and Esri ArcMap to test the DEM vertical accuracy so that different software programs are used to validate the vertical accuracy for each project.

The survey checkpoints used to test this topobathymetric dataset are listed in the survey report included as Appendix A.

The table below summarizes the tested vertical accuracy results from a comparison of the surveyed checkpoints to the elevation values in the final DEM dataset.

Land Cover Category	# of Points	NVA (RMSE _z x 1.9600) Spec=0.196 m	VVA (95th Percentile) Spec=0.300 m	Bathymetric Vertical Accuracy (RMSE _z x 1.9600) Spec=0.353 m
NVA	72	0.166		
VVA	50		0.299	
Bathymetric Vertical Accuracy	12			0.349

Table 15 – Tested vertical accuracy of the DEM by land cover category.

The topographic portion of this DEM dataset was tested to meet ASPRS Positional Accuracy Standards for Digital Geospatial Data (2014) for a 10 cm RMSE_z Vertical Accuracy Class. Actual NVA accuracy was found to be RMSE_z = 8.5 cm, equating to ± 16.6 cm at 95% confidence level. Actual VVA accuracy was found to be ± 29.9 cm at the 95th percentile. The bathymetric portion of this DEM dataset was tested to meet the vertical RMSE_z of QL2_b specified in the Draft National Coastal Mapping Strategy 1.0 Document where vertical accuracy coefficients *a* and *b* are defined as 0.30 and 0.0130, respectively. Using the formula $\sqrt{(a^2 + (b \times d)^2)}$ where *a* equals constant depth errors, *b* equals depth dependent errors, and *d* equals depth, the bathymetric portion of this DEM dataset was tested to meet 30 cm RMSE_z based on the depths of the surveyed submerged topography checkpoints. Actual bathymetric vertical accuracy was found to be RMSE_z = 17.8 cm, equating to ± 34.9 cm at 95% confidence level.

Overall descriptive statistics for each land cover category are provided in table 16. Table 17 lists the VVA 5% outliers that are larger than the 95th percentile.

100 % of Totals	# of Points	RMSE _z (m) Spec=0.100 m NVA/ 0.180 m Submerged Topography	Mean (m)	Median (m)	Skew	Std Dev (m)	Kurtosis	Min (m)	Max (m)
NVA	72	0.085	0.022	0.019	-0.106	0.082	0.862	-0.228	0.257
VVA	50	N/A	0.135	0.111	0.041	0.104	0.146	-0.117	0.387
Submerged Topography	12	0.178	0.166	0.141	1.080	0.069	0.354	0.103	0.313

Table 16 – DEM vertical accuracy descriptive statistics by land cover category.

Point ID	NAD83(2011) UTM Zone 18N		NAVD88 (Geoid 12B)		DeltaZ	AbsDeltaZ
	Easting X (m)	Northing Y (m)	Z-Survey (m)	Z-LiDAR (m)		
VVA-27	242846.129	3186973.387	0.563	0.950	0.387	0.38743
VVA-28	245682.393	3185955.636	1.342	1.643	0.301	0.301333
VVA-3	689270.418	3079559.005	0.954	1.255	0.301	0.30117

Table 17 – VVA 5% outliers.

Based on the vertical accuracy testing conducted by Dewberry, the DEM dataset for the NOAA TX1803-TB-C Topobathymetric Lidar Project satisfies the project's pre-defined vertical accuracy criteria.

DEM CHECKLIST

The following table represents a portion of the high-level steps in Dewberry's DEM Production and QA/QC checklist that were performed for this project.

Pass/Fail	Validation Step
Pass	Final void polygons are created
Pass	LASTools utilities and void polygons are used to create the final topobathymetric model using project specifications for grid type, formatting, and cell size
Pass	Manually review topobathymetric DEMs to check for issues
Pass	Special attention should be paid along the land/water interface
Pass	DEMs should be seamless across tile boundaries
Pass	Bridges should NOT be present in final topobathy DEMs.
Pass	All qualitative issues present in the DEMs as a result of lidar processing and editing issues must be marked for corrections in the lidar. These DEMs will need to be recreated after the lidar has been corrected.
Pass	Calculate DEM Vertical Accuracy including NVA, VVA, Bathymetric Vertical Accuracy and other statistics
Pass	Split the DEMs into tiles according to the project tiling scheme
Pass	Verify all properties of the tiled DEMs, including coordinate reference system information, cell size, cell extents, and that compression has not been applied to the tiled DEMs
Pass	Load all tiled DEMs into Global Mapper to verify complete coverage to the (buffered) project boundary and that no tiles are corrupt.

Table 18 – Subset of the high-level steps from Dewberry's bare earth DEM Production and QA/QC checklist performed for this project.

Metadata

Project level metadata files were delivered in XML format for all project deliverables including lidar, DEMs, refraction extent breaklines, and void polygons. All metadata files are FGDC-compliant and were verified to be error-free according to the USGS MetaParser.

Appendix A

Checkpoint Survey Report

Appendix B

Ground Control Point Survey Report

Appendix C

Complete List of Lidar Delivered Tiles

TX1803-TB-C, Hurricane Harvey Post Storm Topography/Bathymetry Project Report of Survey
December 31, 2019

2018_731900e_3126880n_las	2018_722900e_3128880n_las	2018_693900e_3110880n_las
2018_700900e_3091880n_las	2018_767900e_3152880n_las	2018_775900e_3171880n_las
2018_749900e_3133880n_las	2018_784900e_3165880n_las	2018_709900e_3118880n_las
2018_746900e_3145880n_las	2018_725900e_3132880n_las	2018_786900e_3172880n_las
2018_692900e_3110880n_las	2018_704900e_3096880n_las	2018_703900e_3116880n_las
2018_716900e_3125880n_las	2018_772900e_3166880n_las	2018_691900e_3108880n_las
2018_716900e_3111880n_las	2018_751900e_3142880n_las	2018_770900e_3158880n_las
2018_723900e_3116880n_las	2018_777900e_3158880n_las	2018_769900e_3169880n_las
2018_692900e_3091880n_las	2018_696900e_3113880n_las	2018_683900e_3082880n_las
2018_698900e_3101880n_las	2018_709900e_3121880n_las	2018_713900e_3125880n_las
2018_736900e_3131880n_las	2018_773900e_3170880n_las	2018_750900e_3147880n_las
2018_713900e_3107880n_las	2018_777900e_3166880n_las	2018_756900e_3140880n_las
2018_747900e_3140880n_las	2018_699900e_3094880n_las	2018_781900e_3169880n_las
2018_738900e_3131880n_las	2018_720900e_3117880n_las	2018_735900e_3127880n_las
2018_744900e_3134880n_las	2018_685900e_3088880n_las	2018_698900e_3114880n_las
2018_767900e_3155880n_las	2018_772900e_3169880n_las	2018_692900e_3094880n_las
2018_772900e_3158880n_las	2018_693900e_3089880n_las	2018_681900e_3082880n_las
2018_717900e_3128880n_las	2018_680900e_3069880n_las	2018_733900e_3126880n_las
2018_680900e_3077880n_las	2018_721900e_3119880n_las	2018_705900e_3107880n_las
2018_718900e_3111880n_las	2018_745900e_3143880n_las	2018_716900e_3120880n_las
2018_705900e_3112880n_las	2018_737900e_3131880n_las	2018_721900e_3116880n_las
2018_700900e_3099880n_las	2018_691900e_3091880n_las	2018_711900e_3119880n_las
2018_750900e_3141880n_las	2018_746900e_3143880n_las	2018_712900e_3118880n_las
2018_687900e_3080880n_las	2018_708900e_3114880n_las	2018_776900e_3158880n_las
2018_683900e_3090880n_las	2018_701900e_3112880n_las	2018_788900e_3170880n_las
2018_757900e_3140880n_las	2018_691900e_3107880n_las	2018_768900e_3152880n_las
2018_677900e_3083880n_las	2018_710900e_3118880n_las	2018_687900e_3086880n_las
2018_730900e_3121880n_las	2018_706900e_3114880n_las	2018_742900e_3136880n_las
2018_702900e_3112880n_las	2018_787900e_3168880n_las	2018_697900e_3088880n_las
2018_704900e_3110880n_las	2018_742900e_3133880n_las	2018_676900e_3063880n_las
2018_783900e_3161880n_las	2018_682900e_3065880n_las	2018_686900e_3092880n_las
2018_738900e_3130880n_las	2018_701900e_3093880n_las	2018_785900e_3173880n_las
2018_785900e_3161880n_las	2018_683900e_3068880n_las	2018_755900e_3147880n_las
2018_786900e_3166880n_las	2018_684900e_3085880n_las	2018_744900e_3130880n_las
2018_715900e_3112880n_las	2018_780900e_3163880n_las	2018_763900e_3146880n_las
2018_688900e_3086880n_las	2018_754900e_3146880n_las	2018_782900e_3170880n_las
2018_712900e_3116880n_las	2018_686900e_3073880n_las	2018_690900e_3107880n_las
2018_693900e_3111880n_las	2018_736900e_3137880n_las	2018_733900e_3132880n_las
2018_732900e_3133880n_las	2018_678900e_3073880n_las	2018_748900e_3145880n_las
2018_780900e_3167880n_las	2018_749900e_3137880n_las	2018_721900e_3128880n_las
2018_679900e_3067880n_las	2018_672900e_3076880n_las	2018_735900e_3131880n_las
2018_758900e_3142880n_las	2018_710900e_3113880n_las	2018_739900e_3135880n_las
2018_743900e_3141880n_las	2018_698900e_3094880n_las	2018_695900e_3092880n_las

TX1803-TB-C, Hurricane Harvey Post Storm Topography/Bathymetry Project Report of Survey
December 31, 2019

2018_684900e_3089880n_las	2018_697900e_3091880n_las	2018_743900e_3130880n_las
2018_759900e_3148880n_las	2018_687900e_3097880n_las	2018_731900e_3122880n_las
2018_706900e_3119880n_las	2018_764900e_3148880n_las	2018_733900e_3127880n_las
2018_711900e_3124880n_las	2018_756900e_3139880n_las	2018_745900e_3139880n_las
2018_704900e_3097880n_las	2018_716900e_3110880n_las	2018_695900e_3097880n_las
2018_732900e_3132880n_las	2018_684900e_3066880n_las	2018_781900e_3160880n_las
2018_728900e_3136880n_las	2018_679900e_3072880n_las	2018_782900e_3160880n_las
2018_744900e_3144880n_las	2018_743900e_3140880n_las	2018_701900e_3097880n_las
2018_705900e_3106880n_las	2018_721900e_3115880n_las	2018_702900e_3095880n_las
2018_735900e_3130880n_las	2018_724900e_3117880n_las	2018_780900e_3160880n_las
2018_771900e_3167880n_las	2018_709900e_3104880n_las	2018_706900e_3102880n_las
2018_706900e_3116880n_las	2018_678900e_3068880n_las	2018_693900e_3080880n_las
2018_746900e_3146880n_las	2018_766900e_3148880n_las	2018_735900e_3136880n_las
2018_723900e_3123880n_las	2018_784900e_3169880n_las	2018_693900e_3081880n_las
2018_699900e_3108880n_las	2018_754900e_3135880n_las	2018_737900e_3134880n_las
2018_721900e_3117880n_las	2018_686900e_3083880n_las	2018_760900e_3147880n_las
2018_726900e_3121880n_las	2018_763900e_3147880n_las	2018_703900e_3115880n_las
2018_682900e_3084880n_las	2018_713900e_3112880n_las	2018_790900e_3169880n_las
2018_784900e_3167880n_las	2018_697900e_3113880n_las	2018_788900e_3162880n_las
2018_704900e_3105880n_las	2018_720900e_3127880n_las	2018_690900e_3093880n_las
2018_688900e_3097880n_las	2018_783900e_3163880n_las	2018_781900e_3168880n_las
2018_726900e_3132880n_las	2018_709900e_3115880n_las	2018_736900e_3129880n_las
2018_679900e_3085880n_las	2018_711900e_3108880n_las	2018_753900e_3141880n_las
2018_720900e_3113880n_las	2018_686900e_3090880n_las	2018_693900e_3083880n_las
2018_705900e_3113880n_las	2018_713900e_3110880n_las	2018_727900e_3122880n_las
2018_680900e_3068880n_las	2018_719900e_3118880n_las	2018_680900e_3075880n_las
2018_768900e_3156880n_las	2018_705900e_3100880n_las	2018_783900e_3172880n_las
2018_684900e_3082880n_las	2018_748900e_3133880n_las	2018_685900e_3071880n_las
2018_744900e_3143880n_las	2018_785900e_3171880n_las	2018_732900e_3126880n_las
2018_726900e_3120880n_las	2018_788900e_3165880n_las	2018_773900e_3157880n_las
2018_695900e_3085880n_las	2018_705900e_3099880n_las	2018_793900e_3166880n_las
2018_677900e_3064880n_las	2018_747900e_3136880n_las	2018_680900e_3074880n_las
2018_780900e_3161880n_las	2018_698900e_3103880n_las	2018_727900e_3123880n_las
2018_682900e_3091880n_las	2018_775900e_3167880n_las	2018_736900e_3134880n_las
2018_680900e_3076880n_las	2018_685900e_3079880n_las	2018_689900e_3086880n_las
2018_718900e_3114880n_las	2018_754900e_3138880n_las	2018_679900e_3064880n_las
2018_763900e_3149880n_las	2018_783900e_3173880n_las	2018_784900e_3173880n_las
2018_765900e_3151880n_las	2018_732900e_3123880n_las	2018_721900e_3127880n_las
2018_678900e_3067880n_las	2018_730900e_3123880n_las	2018_679900e_3075880n_las
2018_715900e_3118880n_las	2018_690900e_3074880n_las	2018_683900e_3083880n_las
2018_694900e_3089880n_las	2018_790900e_3164880n_las	2018_687900e_3071880n_las
2018_714900e_3110880n_las	2018_751900e_3140880n_las	2018_775900e_3165880n_las
2018_728900e_3125880n_las	2018_782900e_3171880n_las	2018_693900e_3088880n_las

TX1803-TB-C, Hurricane Harvey Post Storm Topography/Bathymetry Project Report of Survey
December 31, 2019

2018_774900e_3167880n_las	2018_757900e_3142880n_las	2018_691900e_3092880n_las
2018_781900e_3171880n_las	2018_684900e_3075880n_las	2018_739900e_3141880n_las
2018_745900e_3142880n_las	2018_742900e_3137880n_las	2018_793900e_3167880n_las
2018_777900e_3161880n_las	2018_727900e_3134880n_las	2018_692900e_3093880n_las
2018_754900e_3151880n_las	2018_680900e_3066880n_las	2018_738900e_3139880n_las
2018_677900e_3065880n_las	2018_711900e_3116880n_las	2018_680900e_3088880n_las
2018_685900e_3094880n_las	2018_697900e_3114880n_las	2018_681900e_3072880n_las
2018_791900e_3170880n_las	2018_735900e_3140880n_las	2018_729900e_3134880n_las
2018_723900e_3119880n_las	2018_685900e_3085880n_las	2018_699900e_3105880n_las
2018_753900e_3151880n_las	2018_691900e_3104880n_las	2018_689900e_3079880n_las
2018_686900e_3087880n_las	2018_699900e_3112880n_las	2018_734900e_3133880n_las
2018_738900e_3129880n_las	2018_710900e_3119880n_las	2018_727900e_3125880n_las
2018_677900e_3080880n_las	2018_688900e_3089880n_las	2018_782900e_3169880n_las
2018_703900e_3098880n_las	2018_730900e_3138880n_las	2018_703900e_3095880n_las
2018_708900e_3121880n_las	2018_710900e_3110880n_las	2018_706900e_3105880n_las
2018_683900e_3081880n_las	2018_734900e_3135880n_las	2018_687900e_3076880n_las
2018_748900e_3140880n_las	2018_740900e_3130880n_las	2018_725900e_3122880n_las
2018_722900e_3120880n_las	2018_697900e_3112880n_las	2018_745900e_3140880n_las
2018_745900e_3133880n_las	2018_700900e_3100880n_las	2018_791900e_3174880n_las
2018_706900e_3107880n_las	2018_712900e_3115880n_las	2018_770900e_3151880n_las
2018_699900e_3102880n_las	2018_771900e_3170880n_las	2018_787900e_3167880n_las
2018_756900e_3137880n_las	2018_714900e_3119880n_las	2018_719900e_3128880n_las
2018_719900e_3127880n_las	2018_720900e_3120880n_las	2018_696900e_3089880n_las
2018_786900e_3168880n_las	2018_704900e_3102880n_las	2018_690900e_3105880n_las
2018_682900e_3069880n_las	2018_683900e_3086880n_las	2018_774900e_3156880n_las
2018_753900e_3142880n_las	2018_691900e_3087880n_las	2018_736900e_3142880n_las
2018_739900e_3133880n_las	2018_684900e_3083880n_las	2018_789900e_3172880n_las
2018_751900e_3148880n_las	2018_683900e_3073880n_las	2018_709900e_3105880n_las
2018_703900e_3105880n_las	2018_705900e_3108880n_las	2018_699900e_3093880n_las
2018_692900e_3104880n_las	2018_755900e_3138880n_las	2018_733900e_3133880n_las
2018_699900e_3107880n_las	2018_751900e_3143880n_las	2018_791900e_3169880n_las
2018_730900e_3133880n_las	2018_767900e_3148880n_las	2018_788900e_3174880n_las
2018_688900e_3076880n_las	2018_769900e_3168880n_las	2018_690900e_3108880n_las
2018_733900e_3136880n_las	2018_685900e_3069880n_las	2018_716900e_3114880n_las
2018_718900e_3118880n_las	2018_762900e_3146880n_las	2018_685900e_3076880n_las
2018_729900e_3125880n_las	2018_678900e_3069880n_las	2018_776900e_3167880n_las
2018_697900e_3095880n_las	2018_681900e_3074880n_las	2018_694900e_3110880n_las
2018_711900e_3111880n_las	2018_790900e_3167880n_las	2018_740900e_3141880n_las
2018_694900e_3112880n_las	2018_736900e_3136880n_las	2018_724900e_3116880n_las
2018_679900e_3080880n_las	2018_713900e_3124880n_las	2018_747900e_3147880n_las
2018_688900e_3102880n_las	2018_680900e_3087880n_las	2018_790900e_3171880n_las
2018_692900e_3088880n_las	2018_739900e_3142880n_las	2018_711900e_3121880n_las
2018_702900e_3097880n_las	2018_693900e_3112880n_las	2018_729900e_3137880n_las

TX1803-TB-C, Hurricane Harvey Post Storm Topography/Bathymetry Project Report of Survey
December 31, 2019

2018_752900e_3149880n_las	2018_709900e_3122880n_las	2018_676900e_3080880n_las
2018_749900e_3145880n_las	2018_732900e_3131880n_las	2018_681900e_3084880n_las
2018_719900e_3129880n_las	2018_736900e_3138880n_las	2018_693900e_3102880n_las
2018_740900e_3136880n_las	2018_719900e_3114880n_las	2018_730900e_3136880n_las
2018_689900e_3088880n_las	2018_772900e_3159880n_las	2018_779900e_3162880n_las
2018_778900e_3159880n_las	2018_773900e_3166880n_las	2018_749900e_3136880n_las
2018_744900e_3141880n_las	2018_744900e_3131880n_las	2018_707900e_3105880n_las
2018_691900e_3086880n_las	2018_747900e_3142880n_las	2018_711900e_3105880n_las
2018_731900e_3123880n_las	2018_750900e_3135880n_las	2018_696900e_3099880n_las
2018_687900e_3093880n_las	2018_732900e_3125880n_las	2018_786900e_3173880n_las
2018_695900e_3086880n_las	2018_746900e_3140880n_las	2018_779900e_3160880n_las
2018_728900e_3134880n_las	2018_746900e_3135880n_las	2018_757900e_3147880n_las
2018_752900e_3141880n_las	2018_784900e_3163880n_las	2018_790900e_3165880n_las
2018_684900e_3086880n_las	2018_690900e_3111880n_las	2018_694900e_3111880n_las
2018_716900e_3127880n_las	2018_692900e_3080880n_las	2018_712900e_3107880n_las
2018_689900e_3078880n_las	2018_722900e_3131880n_las	2018_719900e_3115880n_las
2018_706900e_3115880n_las	2018_773900e_3156880n_las	2018_769900e_3150880n_las
2018_681900e_3087880n_las	2018_679900e_3065880n_las	2018_683900e_3087880n_las
2018_730900e_3128880n_las	2018_740900e_3131880n_las	2018_718900e_3117880n_las
2018_690900e_3075880n_las	2018_791900e_3168880n_las	2018_786900e_3169880n_las
2018_707900e_3116880n_las	2018_692900e_3106880n_las	2018_792900e_3176880n_las
2018_682900e_3077880n_las	2018_691900e_3078880n_las	2018_696900e_3098880n_las
2018_771900e_3165880n_las	2018_680900e_3064880n_las	2018_733900e_3131880n_las
2018_695900e_3087880n_las	2018_758900e_3143880n_las	2018_691900e_3098880n_las
2018_725900e_3135880n_las	2018_729900e_3133880n_las	2018_679900e_3068880n_las
2018_731900e_3130880n_las	2018_689900e_3089880n_las	2018_693900e_3095880n_las
2018_691900e_3096880n_las	2018_692900e_3085880n_las	2018_764900e_3146880n_las
2018_689900e_3103880n_las	2018_686900e_3078880n_las	2018_740900e_3132880n_las
2018_758900e_3145880n_las	2018_693900e_3113880n_las	2018_688900e_3095880n_las
2018_676900e_3082880n_las	2018_692900e_3098880n_las	2018_785900e_3174880n_las
2018_712900e_3124880n_las	2018_760900e_3143880n_las	2018_710900e_3116880n_las
2018_746900e_3138880n_las	2018_681900e_3075880n_las	2018_679900e_3073880n_las
2018_718900e_3116880n_las	2018_675900e_3081880n_las	2018_738900e_3143880n_las
2018_678900e_3072880n_las	2018_720900e_3114880n_las	2018_759900e_3147880n_las
2018_741900e_3144880n_las	2018_749900e_3149880n_las	2018_685900e_3073880n_las
2018_685900e_3074880n_las	2018_680900e_3085880n_las	2018_730900e_3134880n_las
2018_689900e_3102880n_las	2018_695900e_3089880n_las	2018_717900e_3111880n_las
2018_775900e_3168880n_las	2018_701900e_3098880n_las	2018_688900e_3103880n_las
2018_693900e_3107880n_las	2018_757900e_3148880n_las	2018_739900e_3130880n_las
2018_791900e_3172880n_las	2018_786900e_3163880n_las	2018_686900e_3069880n_las
2018_695900e_3088880n_las	2018_702900e_3109880n_las	2018_759900e_3145880n_las
2018_689900e_3101880n_las	2018_701900e_3103880n_las	2018_685900e_3090880n_las
2018_712900e_3122880n_las	2018_737900e_3129880n_las	2018_736900e_3127880n_las

TX1803-TB-C, Hurricane Harvey Post Storm Topography/Bathymetry Project Report of Survey
December 31, 2019

2018_788900e_3173880n_las	2018_759900e_3149880n_las	2018_718900e_3119880n_las
2018_687900e_3094880n_las	2018_777900e_3170880n_las	2018_792900e_3164880n_las
2018_726900e_3118880n_las	2018_757900e_3146880n_las	2018_770900e_3157880n_las
2018_744900e_3146880n_las	2018_692900e_3092880n_las	2018_745900e_3134880n_las
2018_784900e_3160880n_las	2018_737900e_3130880n_las	2018_751900e_3141880n_las
2018_689900e_3080880n_las	2018_690900e_3102880n_las	2018_698900e_3113880n_las
2018_764900e_3153880n_las	2018_719900e_3112880n_las	2018_718900e_3128880n_las
2018_728900e_3135880n_las	2018_713900e_3109880n_las	2018_679900e_3074880n_las
2018_712900e_3117880n_las	2018_676900e_3064880n_las	2018_703900e_3104880n_las
2018_717900e_3120880n_las	2018_784900e_3170880n_las	2018_690900e_3082880n_las
2018_696900e_3095880n_las	2018_749900e_3140880n_las	2018_701900e_3110880n_las
2018_741900e_3140880n_las	2018_691900e_3110880n_las	2018_732900e_3124880n_las
2018_698900e_3093880n_las	2018_731900e_3128880n_las	2018_787900e_3173880n_las
2018_769900e_3154880n_las	2018_717900e_3116880n_las	2018_749900e_3141880n_las
2018_705900e_3103880n_las	2018_722900e_3116880n_las	2018_715900e_3111880n_las
2018_681900e_3064880n_las	2018_682900e_3074880n_las	2018_692900e_3083880n_las
2018_762900e_3151880n_las	2018_691900e_3082880n_las	2018_694900e_3083880n_las
2018_710900e_3117880n_las	2018_713900e_3116880n_las	2018_727900e_3133880n_las
2018_689900e_3100880n_las	2018_736900e_3130880n_las	2018_678900e_3080880n_las
2018_787900e_3169880n_las	2018_765900e_3150880n_las	2018_739900e_3140880n_las
2018_732900e_3138880n_las	2018_678900e_3065880n_las	2018_761900e_3150880n_las
2018_744900e_3132880n_las	2018_712900e_3110880n_las	2018_792900e_3167880n_las
2018_696900e_3086880n_las	2018_724900e_3133880n_las	2018_737900e_3141880n_las
2018_788900e_3163880n_las	2018_697900e_3093880n_las	2018_681900e_3073880n_las
2018_701900e_3107880n_las	2018_690900e_3095880n_las	2018_709900e_3111880n_las
2018_747900e_3141880n_las	2018_755900e_3144880n_las	2018_682900e_3067880n_las
2018_792900e_3170880n_las	2018_693900e_3103880n_las	2018_715900e_3115880n_las
2018_755900e_3140880n_las	2018_759900e_3143880n_las	2018_739900e_3127880n_las
2018_680900e_3070880n_las	2018_697900e_3089880n_las	2018_744900e_3138880n_las
2018_681900e_3062880n_las	2018_727900e_3120880n_las	2018_747900e_3139880n_las
2018_748900e_3144880n_las	2018_693900e_3105880n_las	2018_752900e_3138880n_las
2018_787900e_3165880n_las	2018_688900e_3081880n_las	2018_687900e_3088880n_las
2018_741900e_3136880n_las	2018_695900e_3090880n_las	2018_691900e_3088880n_las
2018_781900e_3162880n_las	2018_782900e_3168880n_las	2018_734900e_3140880n_las
2018_689900e_3097880n_las	2018_766900e_3153880n_las	2018_789900e_3170880n_las
2018_687900e_3099880n_las	2018_693900e_3087880n_las	2018_770900e_3156880n_las
2018_686900e_3091880n_las	2018_735900e_3133880n_las	2018_778900e_3171880n_las
2018_696900e_3087880n_las	2018_785900e_3165880n_las	2018_723900e_3130880n_las
2018_692900e_3097880n_las	2018_784900e_3172880n_las	2018_692900e_3109880n_las
2018_693900e_3086880n_las	2018_681900e_3067880n_las	2018_754900e_3148880n_las
2018_695900e_3094880n_las	2018_750900e_3138880n_las	2018_722900e_3121880n_las
2018_722900e_3129880n_las	2018_677900e_3067880n_las	2018_682900e_3075880n_las
2018_679900e_3079880n_las	2018_773900e_3169880n_las	2018_675900e_3080880n_las

TX1803-TB-C, Hurricane Harvey Post Storm Topography/Bathymetry Project Report of Survey
December 31, 2019

2018_678900e_3082880n_las	2018_735900e_3135880n_las	2018_772900e_3154880n_las
2018_710900e_3111880n_las	2018_674900e_3078880n_las	2018_751900e_3135880n_las
2018_714900e_3125880n_las	2018_693900e_3090880n_las	2018_720900e_3128880n_las
2018_683900e_3089880n_las	2018_752900e_3143880n_las	2018_773900e_3159880n_las
2018_744900e_3145880n_las	2018_774900e_3155880n_las	2018_724900e_3130880n_las
2018_753900e_3149880n_las	2018_700900e_3110880n_las	2018_691900e_3100880n_las
2018_682900e_3068880n_las	2018_726900e_3124880n_las	2018_777900e_3168880n_las
2018_684900e_3072880n_las	2018_725900e_3117880n_las	2018_683900e_3079880n_las
2018_784900e_3168880n_las	2018_762900e_3147880n_las	2018_718900e_3129880n_las
2018_705900e_3111880n_las	2018_700900e_3111880n_las	2018_733900e_3138880n_las
2018_733900e_3128880n_las	2018_682900e_3085880n_las	2018_707900e_3114880n_las
2018_691900e_3112880n_las	2018_689900e_3081880n_las	2018_748900e_3142880n_las
2018_708900e_3101880n_las	2018_742900e_3141880n_las	2018_685900e_3095880n_las
2018_711900e_3106880n_las	2018_748900e_3136880n_las	2018_702900e_3101880n_las
2018_736900e_3141880n_las	2018_763900e_3148880n_las	2018_689900e_3084880n_las
2018_779900e_3166880n_las	2018_746900e_3141880n_las	2018_708900e_3107880n_las
2018_719900e_3116880n_las	2018_791900e_3173880n_las	2018_790900e_3172880n_las
2018_689900e_3096880n_las	2018_707900e_3113880n_las	2018_740900e_3135880n_las
2018_690900e_3096880n_las	2018_763900e_3145880n_las	2018_788900e_3167880n_las
2018_690900e_3089880n_las	2018_742900e_3143880n_las	2018_771900e_3157880n_las
2018_687900e_3098880n_las	2018_780900e_3172880n_las	2018_714900e_3114880n_las
2018_712900e_3111880n_las	2018_745900e_3131880n_las	2018_690900e_3099880n_las
2018_672900e_3077880n_las	2018_691900e_3080880n_las	2018_776900e_3170880n_las
2018_739900e_3137880n_las	2018_680900e_3086880n_las	2018_678900e_3084880n_las
2018_717900e_3114880n_las	2018_684900e_3071880n_las	2018_743900e_3143880n_las
2018_694900e_3087880n_las	2018_736900e_3132880n_las	2018_743900e_3137880n_las
2018_678900e_3081880n_las	2018_709900e_3107880n_las	2018_743900e_3142880n_las
2018_690900e_3101880n_las	2018_717900e_3126880n_las	2018_706900e_3106880n_las
2018_770900e_3167880n_las	2018_696900e_3090880n_las	2018_744900e_3137880n_las
2018_690900e_3091880n_las	2018_699900e_3096880n_las	2018_680900e_3072880n_las
2018_771900e_3154880n_las	2018_700900e_3093880n_las	2018_733900e_3137880n_las
2018_720900e_3131880n_las	2018_678900e_3078880n_las	2018_753900e_3140880n_las
2018_787900e_3172880n_las	2018_688900e_3079880n_las	2018_766900e_3150880n_las
2018_718900e_3124880n_las	2018_698900e_3100880n_las	2018_691900e_3101880n_las
2018_674900e_3075880n_las	2018_734900e_3131880n_las	2018_706900e_3109880n_las
2018_752900e_3139880n_las	2018_684900e_3068880n_las	2018_752900e_3147880n_las
2018_739900e_3134880n_las	2018_717900e_3115880n_las	2018_687900e_3096880n_las
2018_753900e_3145880n_las	2018_747900e_3138880n_las	2018_729900e_3124880n_las
2018_678900e_3083880n_las	2018_746900e_3133880n_las	2018_789900e_3174880n_las
2018_775900e_3166880n_las	2018_683900e_3074880n_las	2018_689900e_3077880n_las
2018_674900e_3077880n_las	2018_716900e_3112880n_las	2018_688900e_3071880n_las
2018_735900e_3138880n_las	2018_689900e_3091880n_las	2018_677900e_3069880n_las
2018_692900e_3081880n_las	2018_696900e_3094880n_las	2018_703900e_3107880n_las

TX1803-TB-C, Hurricane Harvey Post Storm Topography/Bathymetry Project Report of Survey
December 31, 2019

2018_679900e_3071880n_las	2018_702900e_3110880n_las	2018_714900e_3124880n_las
2018_717900e_3110880n_las	2018_703900e_3108880n_las	2018_783900e_3170880n_las
2018_738900e_3140880n_las	2018_762900e_3145880n_las	2018_740900e_3144880n_las
2018_716900e_3117880n_las	2018_786900e_3170880n_las	2018_787900e_3171880n_las
2018_780900e_3168880n_las	2018_685900e_3086880n_las	2018_689900e_3076880n_las
2018_682900e_3066880n_las	2018_717900e_3112880n_las	2018_749900e_3139880n_las
2018_683900e_3088880n_las	2018_749900e_3135880n_las	2018_731900e_3124880n_las
2018_776900e_3171880n_las	2018_703900e_3096880n_las	2018_714900e_3115880n_las
2018_715900e_3109880n_las	2018_786900e_3161880n_las	2018_718900e_3120880n_las
2018_758900e_3149880n_las	2018_708900e_3118880n_las	2018_753900e_3146880n_las
2018_750900e_3145880n_las	2018_731900e_3136880n_las	2018_707900e_3102880n_las
2018_738900e_3133880n_las	2018_719900e_3117880n_las	2018_710900e_3120880n_las
2018_734900e_3129880n_las	2018_715900e_3125880n_las	2018_743900e_3133880n_las
2018_731900e_3132880n_las	2018_767900e_3149880n_las	2018_686900e_3068880n_las
2018_708900e_3112880n_las	2018_716900e_3118880n_las	2018_713900e_3115880n_las
2018_774900e_3157880n_las	2018_715900e_3127880n_las	2018_691900e_3095880n_las
2018_720900e_3126880n_las	2018_690900e_3100880n_las	2018_750900e_3149880n_las
2018_712900e_3114880n_las	2018_781900e_3163880n_las	2018_774900e_3166880n_las
2018_694900e_3114880n_las	2018_768900e_3167880n_las	2018_678900e_3070880n_las
2018_678900e_3064880n_las	2018_685900e_3092880n_las	2018_692900e_3112880n_las
2018_688900e_3098880n_las	2018_710900e_3123880n_las	2018_694900e_3092880n_las
2018_707900e_3109880n_las	2018_738900e_3137880n_las	2018_690900e_3083880n_las
2018_674900e_3080880n_las	2018_687900e_3079880n_las	2018_694900e_3097880n_las
2018_742900e_3135880n_las	2018_689900e_3087880n_las	2018_747900e_3145880n_las
2018_710900e_3122880n_las	2018_699900e_3100880n_las	2018_792900e_3172880n_las
2018_790900e_3170880n_las	2018_701900e_3100880n_las	2018_691900e_3106880n_las
2018_752900e_3144880n_las	2018_778900e_3161880n_las	2018_680900e_3083880n_las
2018_790900e_3166880n_las	2018_701900e_3108880n_las	2018_757900e_3141880n_las
2018_750900e_3148880n_las	2018_685900e_3080880n_las	2018_705900e_3105880n_las
2018_738900e_3134880n_las	2018_737900e_3138880n_las	2018_773900e_3167880n_las
2018_699900e_3104880n_las	2018_748900e_3139880n_las	2018_764900e_3152880n_las
2018_714900e_3121880n_las	2018_785900e_3163880n_las	2018_762900e_3150880n_las
2018_750900e_3136880n_las	2018_692900e_3086880n_las	2018_731900e_3138880n_las
2018_751900e_3137880n_las	2018_714900e_3113880n_las	2018_690900e_3094880n_las
2018_727900e_3132880n_las	2018_687900e_3082880n_las	2018_677900e_3078880n_las
2018_691900e_3111880n_las	2018_702900e_3099880n_las	2018_676900e_3081880n_las
2018_695900e_3093880n_las	2018_714900e_3109880n_las	2018_728900e_3133880n_las
2018_708900e_3109880n_las	2018_690900e_3084880n_las	2018_699900e_3109880n_las
2018_741900e_3145880n_las	2018_683900e_3078880n_las	2018_692900e_3084880n_las
2018_756900e_3143880n_las	2018_717900e_3124880n_las	2018_782900e_3163880n_las
2018_744900e_3133880n_las	2018_752900e_3142880n_las	2018_753900e_3150880n_las
2018_693900e_3114880n_las	2018_747900e_3132880n_las	2018_768900e_3153880n_las
2018_745900e_3137880n_las	2018_704900e_3109880n_las	2018_720900e_3121880n_las

TX1803-TB-C, Hurricane Harvey Post Storm Topography/Bathymetry Project Report of Survey
December 31, 2019

2018_715900e_3124880n_las	2018_754900e_3144880n_las	2018_776900e_3155880n_las
2018_695900e_3091880n_las	2018_731900e_3125880n_las	2018_724900e_3132880n_las
2018_706900e_3117880n_las	2018_716900e_3113880n_las	2018_739900e_3139880n_las
2018_740900e_3128880n_las	2018_697900e_3099880n_las	2018_674900e_3079880n_las
2018_726900e_3122880n_las	2018_713900e_3122880n_las	2018_677900e_3070880n_las
2018_714900e_3120880n_las	2018_695900e_3098880n_las	2018_728900e_3122880n_las
2018_685900e_3091880n_las	2018_739900e_3132880n_las	2018_724900e_3120880n_las
2018_784900e_3162880n_las	2018_742900e_3130880n_las	2018_734900e_3136880n_las
2018_703900e_3109880n_las	2018_721900e_3132880n_las	2018_725900e_3123880n_las
2018_771900e_3169880n_las	2018_777900e_3167880n_las	2018_688900e_3082880n_las
2018_720900e_3118880n_las	2018_781900e_3159880n_las	2018_705900e_3102880n_las
2018_783900e_3168880n_las	2018_740900e_3138880n_las	2018_687900e_3089880n_las
2018_734900e_3125880n_las	2018_730900e_3122880n_las	2018_682900e_3079880n_las
2018_699900e_3111880n_las	2018_735900e_3125880n_las	2018_680900e_3062880n_las
2018_711900e_3120880n_las	2018_727900e_3126880n_las	2018_675900e_3078880n_las
2018_682900e_3082880n_las	2018_694900e_3085880n_las	2018_734900e_3132880n_las
2018_739900e_3143880n_las	2018_683900e_3067880n_las	2018_780900e_3170880n_las
2018_776900e_3161880n_las	2018_683900e_3066880n_las	2018_720900e_3116880n_las
2018_723900e_3132880n_las	2018_702900e_3113880n_las	2018_724900e_3134880n_las
2018_693900e_3091880n_las	2018_747900e_3146880n_las	2018_715900e_3122880n_las
2018_751900e_3144880n_las	2018_694900e_3113880n_las	2018_735900e_3139880n_las
2018_750900e_3144880n_las	2018_738900e_3128880n_las	2018_732900e_3127880n_las
2018_696900e_3096880n_las	2018_722900e_3118880n_las	2018_789900e_3168880n_las
2018_742900e_3132880n_las	2018_785900e_3172880n_las	2018_770900e_3165880n_las
2018_749900e_3147880n_las	2018_690900e_3085880n_las	2018_700900e_3112880n_las
2018_700900e_3104880n_las	2018_693900e_3108880n_las	2018_782900e_3164880n_las
2018_789900e_3171880n_las	2018_697900e_3098880n_las	2018_693900e_3094880n_las
2018_747900e_3133880n_las	2018_685900e_3084880n_las	2018_709900e_3102880n_las
2018_688900e_3084880n_las	2018_700900e_3103880n_las	2018_749900e_3143880n_las
2018_773900e_3168880n_las	2018_674900e_3076880n_las	2018_717900e_3121880n_las
2018_713900e_3111880n_las	2018_751900e_3139880n_las	2018_749900e_3144880n_las
2018_714900e_3122880n_las	2018_774900e_3160880n_las	2018_730900e_3127880n_las
2018_697900e_3092880n_las	2018_772900e_3165880n_las	2018_771900e_3153880n_las
2018_756900e_3138880n_las	2018_738900e_3127880n_las	2018_684900e_3077880n_las
2018_789900e_3175880n_las	2018_790900e_3175880n_las	2018_703900e_3100880n_las
2018_688900e_3080880n_las	2018_790900e_3168880n_las	2018_698900e_3090880n_las
2018_707900e_3118880n_las	2018_686900e_3082880n_las	2018_701900e_3095880n_las
2018_755900e_3146880n_las	2018_705900e_3118880n_las	2018_769900e_3156880n_las
2018_691900e_3089880n_las	2018_732900e_3128880n_las	2018_688900e_3091880n_las
2018_724900e_3123880n_las	2018_750900e_3139880n_las	2018_782900e_3162880n_las
2018_754900e_3140880n_las	2018_731900e_3133880n_las	2018_779900e_3169880n_las
2018_689900e_3105880n_las	2018_778900e_3166880n_las	2018_737900e_3142880n_las
2018_695900e_3095880n_las	2018_712900e_3109880n_las	2018_722900e_3123880n_las

TX1803-TB-C, Hurricane Harvey Post Storm Topography/Bathymetry Project Report of Survey
December 31, 2019

2018_783900e_3171880n_las	2018_714900e_3126880n_las	2018_760900e_3149880n_las
2018_738900e_3142880n_las	2018_779900e_3159880n_las	2018_761900e_3144880n_las
2018_777900e_3157880n_las	2018_679900e_3086880n_las	2018_741900e_3129880n_las
2018_707900e_3119880n_las	2018_695900e_3115880n_las	2018_770900e_3169880n_las
2018_752900e_3145880n_las	2018_740900e_3140880n_las	2018_707900e_3108880n_las
2018_752900e_3137880n_las	2018_729900e_3123880n_las	2018_791900e_3175880n_las
2018_677900e_3066880n_las	2018_725900e_3134880n_las	2018_707900e_3106880n_las
2018_700900e_3105880n_las	2018_683900e_3065880n_las	2018_685900e_3068880n_las
2018_740900e_3133880n_las	2018_681900e_3080880n_las	2018_710900e_3121880n_las
2018_708900e_3120880n_las	2018_707900e_3107880n_las	2018_725900e_3133880n_las
2018_753900e_3138880n_las	2018_679900e_3082880n_las	2018_709900e_3108880n_las
2018_675900e_3076880n_las	2018_772900e_3167880n_las	2018_787900e_3174880n_las
2018_715900e_3117880n_las	2018_690900e_3081880n_las	2018_687900e_3090880n_las
2018_696900e_3093880n_las	2018_688900e_3092880n_las	2018_707900e_3100880n_las
2018_742900e_3131880n_las	2018_702900e_3094880n_las	2018_730900e_3126880n_las
2018_780900e_3171880n_las	2018_679900e_3062880n_las	2018_686900e_3074880n_las
2018_722900e_3130880n_las	2018_709900e_3114880n_las	2018_693900e_3106880n_las
2018_707900e_3103880n_las	2018_699900e_3101880n_las	2018_705900e_3114880n_las
2018_693900e_3078880n_las	2018_688900e_3072880n_las	2018_706900e_3118880n_las
2018_679900e_3066880n_las	2018_791900e_3165880n_las	2018_740900e_3129880n_las
2018_680900e_3084880n_las	2018_788900e_3172880n_las	2018_685900e_3082880n_las
2018_684900e_3074880n_las	2018_687900e_3081880n_las	2018_720900e_3130880n_las
2018_677900e_3068880n_las	2018_770900e_3166880n_las	2018_791900e_3166880n_las
2018_769900e_3155880n_las	2018_706900e_3104880n_las	2018_750900e_3140880n_las
2018_732900e_3137880n_las	2018_718900e_3113880n_las	2018_750900e_3143880n_las
2018_682900e_3071880n_las	2018_700900e_3109880n_las	2018_705900e_3101880n_las
2018_687900e_3072880n_las	2018_721900e_3121880n_las	2018_716900e_3123880n_las
2018_683900e_3069880n_las	2018_745900e_3144880n_las	2018_738900e_3138880n_las
2018_688900e_3073880n_las	2018_722900e_3132880n_las	2018_703900e_3114880n_las
2018_721900e_3131880n_las	2018_785900e_3164880n_las	2018_701900e_3094880n_las
2018_691900e_3090880n_las	2018_713900e_3119880n_las	2018_695900e_3112880n_las
2018_679900e_3083880n_las	2018_767900e_3153880n_las	2018_784900e_3161880n_las
2018_743900e_3139880n_las	2018_749900e_3134880n_las	2018_776900e_3160880n_las
2018_681900e_3089880n_las	2018_789900e_3166880n_las	2018_750900e_3137880n_las
2018_765900e_3152880n_las	2018_717900e_3125880n_las	2018_761900e_3151880n_las
2018_711900e_3110880n_las	2018_775900e_3156880n_las	2018_690900e_3097880n_las
2018_702900e_3096880n_las	2018_698900e_3108880n_las	2018_688900e_3085880n_las
2018_686900e_3085880n_las	2018_741900e_3142880n_las	2018_712900e_3120880n_las
2018_755900e_3143880n_las	2018_698900e_3099880n_las	2018_699900e_3110880n_las
2018_786900e_3165880n_las	2018_683900e_3071880n_las	2018_704900e_3103880n_las
2018_706900e_3113880n_las	2018_698900e_3091880n_las	2018_681900e_3078880n_las
2018_725900e_3131880n_las	2018_692900e_3102880n_las	2018_725900e_3125880n_las
2018_696900e_3091880n_las	2018_736900e_3140880n_las	2018_684900e_3078880n_las

TX1803-TB-C, Hurricane Harvey Post Storm Topography/Bathymetry Project Report of Survey
December 31, 2019

2018_687900e_3075880n_las	2018_683900e_3064880n_las	2018_698900e_3096880n_las
2018_687900e_3078880n_las	2018_678900e_3085880n_las	2018_686900e_3072880n_las
2018_682900e_3088880n_las	2018_741900e_3128880n_las	2018_682900e_3080880n_las
2018_762900e_3152880n_las	2018_776900e_3168880n_las	2018_747900e_3135880n_las
2018_735900e_3128880n_las	2018_754900e_3145880n_las	2018_711900e_3113880n_las
2018_785900e_3170880n_las	2018_776900e_3156880n_las	2018_772900e_3156880n_las
2018_768900e_3165880n_las	2018_689900e_3082880n_las	2018_711900e_3118880n_las
2018_778900e_3157880n_las	2018_699900e_3113880n_las	2018_688900e_3090880n_las
2018_716900e_3116880n_las	2018_745900e_3135880n_las	2018_704900e_3101880n_las
2018_743900e_3132880n_las	2018_777900e_3162880n_las	2018_694900e_3094880n_las
2018_778900e_3158880n_las	2018_782900e_3167880n_las	2018_720900e_3129880n_las
2018_692900e_3078880n_las	2018_683900e_3084880n_las	2018_761900e_3147880n_las
2018_742900e_3140880n_las	2018_682900e_3063880n_las	2018_783900e_3167880n_las
2018_778900e_3170880n_las	2018_716900e_3121880n_las	2018_685900e_3070880n_las
2018_708900e_3110880n_las	2018_719900e_3121880n_las	2018_689900e_3085880n_las
2018_755900e_3139880n_las	2018_767900e_3151880n_las	2018_700900e_3106880n_las
2018_681900e_3083880n_las	2018_759900e_3142880n_las	2018_692900e_3107880n_las
2018_771900e_3164880n_las	2018_728900e_3123880n_las	2018_701900e_3104880n_las
2018_747900e_3137880n_las	2018_741900e_3133880n_las	2018_741900e_3130880n_las
2018_733900e_3139880n_las	2018_715900e_3114880n_las	2018_771900e_3166880n_las
2018_691900e_3102880n_las	2018_766900e_3154880n_las	2018_792900e_3173880n_las
2018_687900e_3073880n_las	2018_779900e_3168880n_las	2018_708900e_3119880n_las
2018_791900e_3164880n_las	2018_780900e_3159880n_las	2018_679900e_3069880n_las
2018_689900e_3074880n_las	2018_793900e_3168880n_las	2018_779900e_3167880n_las
2018_781900e_3166880n_las	2018_777900e_3165880n_las	2018_772900e_3170880n_las
2018_752900e_3150880n_las	2018_716900e_3126880n_las	2018_681900e_3081880n_las
2018_707900e_3115880n_las	2018_686900e_3084880n_las	2018_700900e_3092880n_las
2018_680900e_3078880n_las	2018_743900e_3136880n_las	2018_752900e_3151880n_las
2018_757900e_3145880n_las	2018_723900e_3120880n_las	2018_740900e_3142880n_las
2018_715900e_3113880n_las	2018_686900e_3096880n_las	2018_680900e_3063880n_las
2018_769900e_3165880n_las	2018_717900e_3119880n_las	2018_682900e_3078880n_las
2018_681900e_3088880n_las	2018_728900e_3124880n_las	2018_712900e_3112880n_las
2018_723900e_3117880n_las	2018_679900e_3077880n_las	2018_741900e_3135880n_las
2018_709900e_3117880n_las	2018_685900e_3093880n_las	2018_734900e_3127880n_las
2018_707900e_3104880n_las	2018_751900e_3149880n_las	2018_786900e_3174880n_las
2018_680900e_3061880n_las	2018_778900e_3168880n_las	2018_701900e_3102880n_las
2018_681900e_3063880n_las	2018_682900e_3064880n_las	2018_688900e_3074880n_las
2018_765900e_3153880n_las	2018_736900e_3133880n_las	2018_782900e_3159880n_las
2018_706900e_3100880n_las	2018_769900e_3151880n_las	2018_711900e_3122880n_las
2018_723900e_3131880n_las	2018_699900e_3097880n_las	2018_729900e_3136880n_las
2018_755900e_3137880n_las	2018_790900e_3163880n_las	2018_767900e_3150880n_las
2018_689900e_3075880n_las	2018_781900e_3173880n_las	2018_700900e_3096880n_las
2018_688900e_3075880n_las	2018_758900e_3148880n_las	2018_701900e_3105880n_las

TX1803-TB-C, Hurricane Harvey Post Storm Topography/Bathymetry Project Report of Survey
December 31, 2019

2018_706900e_3101880n_las	2018_753900e_3148880n_las	2018_688900e_3096880n_las
2018_725900e_3130880n_las	2018_691900e_3076880n_las	2018_758900e_3144880n_las
2018_692900e_3099880n_las	2018_710900e_3109880n_las	2018_783900e_3160880n_las
2018_731900e_3135880n_las	2018_686900e_3071880n_las	2018_709900e_3109880n_las
2018_690900e_3087880n_las	2018_709900e_3110880n_las	2018_679900e_3081880n_las
2018_701900e_3106880n_las	2018_741900e_3139880n_las	2018_681900e_3065880n_las
2018_754900e_3150880n_las	2018_700900e_3098880n_las	2018_781900e_3172880n_las
2018_731900e_3137880n_las	2018_694900e_3088880n_las	2018_712900e_3106880n_las
2018_723900e_3129880n_las	2018_704900e_3113880n_las	2018_705900e_3097880n_las
2018_688900e_3100880n_las	2018_746900e_3137880n_las	2018_705900e_3109880n_las
2018_698900e_3104880n_las	2018_711900e_3114880n_las	2018_700900e_3097880n_las
2018_705900e_3104880n_las	2018_703900e_3112880n_las	2018_719900e_3119880n_las
2018_750900e_3146880n_las	2018_766900e_3151880n_las	2018_723900e_3122880n_las
2018_761900e_3148880n_las	2018_726900e_3134880n_las	2018_686900e_3079880n_las
2018_693900e_3104880n_las	2018_760900e_3145880n_las	2018_734900e_3139880n_las
2018_707900e_3111880n_las	2018_773900e_3158880n_las	2018_686900e_3077880n_las
2018_726900e_3136880n_las	2018_686900e_3086880n_las	2018_792900e_3171880n_las
2018_774900e_3171880n_las	2018_734900e_3124880n_las	2018_737900e_3136880n_las
2018_754900e_3149880n_las	2018_749900e_3148880n_las	2018_699900e_3099880n_las
2018_684900e_3087880n_las	2018_692900e_3101880n_las	2018_777900e_3160880n_las
2018_709900e_3119880n_las	2018_692900e_3089880n_las	2018_737900e_3135880n_las
2018_729900e_3121880n_las	2018_774900e_3170880n_las	2018_730900e_3129880n_las
2018_725900e_3119880n_las	2018_693900e_3092880n_las	2018_754900e_3137880n_las
2018_709900e_3106880n_las	2018_770900e_3154880n_las	2018_756900e_3145880n_las
2018_728900e_3121880n_las	2018_792900e_3166880n_las	2018_756900e_3141880n_las
2018_697900e_3101880n_las	2018_721900e_3114880n_las	2018_773900e_3164880n_las
2018_789900e_3163880n_las	2018_781900e_3170880n_las	2018_703900e_3101880n_las
2018_693900e_3109880n_las	2018_748900e_3146880n_las	2018_702900e_3102880n_las
2018_697900e_3096880n_las	2018_727900e_3136880n_las	2018_728900e_3120880n_las
2018_683900e_3080880n_las	2018_766900e_3149880n_las	2018_770900e_3153880n_las
2018_682900e_3073880n_las	2018_735900e_3137880n_las	2018_711900e_3117880n_las
2018_748900e_3137880n_las	2018_690900e_3077880n_las	2018_698900e_3105880n_las
2018_778900e_3162880n_las	2018_737900e_3126880n_las	2018_677900e_3081880n_las
2018_788900e_3166880n_las	2018_731900e_3134880n_las	2018_779900e_3170880n_las
2018_680900e_3073880n_las	2018_751900e_3145880n_las	2018_678900e_3076880n_las
2018_764900e_3149880n_las	2018_687900e_3085880n_las	2018_728900e_3137880n_las
2018_690900e_3080880n_las	2018_687900e_3092880n_las	2018_753900e_3135880n_las
2018_675900e_3075880n_las	2018_787900e_3164880n_las	2018_707900e_3110880n_las
2018_719900e_3120880n_las	2018_693900e_3096880n_las	2018_739900e_3131880n_las
2018_704900e_3111880n_las	2018_699900e_3103880n_las	2018_730900e_3135880n_las
2018_774900e_3159880n_las	2018_725900e_3121880n_las	2018_692900e_3103880n_las
2018_780900e_3162880n_las	2018_692900e_3105880n_las	2018_701900e_3111880n_las
2018_734900e_3126880n_las	2018_723900e_3133880n_las	2018_716900e_3119880n_las

TX1803-TB-C, Hurricane Harvey Post Storm Topography/Bathymetry Project Report of Survey
December 31, 2019

2018_727900e_3124880n_las	2018_755900e_3136880n_las	2018_769900e_3166880n_las
2018_690900e_3103880n_las	2018_704900e_3114880n_las	2018_743900e_3134880n_las
2018_745900e_3136880n_las	2018_788900e_3164880n_las	2018_766900e_3155880n_las
2018_746900e_3136880n_las	2018_721900e_3129880n_las	2018_690900e_3098880n_las
2018_775900e_3158880n_las	2018_713900e_3113880n_las	2018_749900e_3138880n_las
2018_736900e_3126880n_las	2018_737900e_3140880n_las	2018_713900e_3123880n_las
2018_673900e_3076880n_las	2018_775900e_3155880n_las	2018_696900e_3092880n_las
2018_766900e_3152880n_las	2018_759900e_3146880n_las	2018_782900e_3172880n_las
2018_681900e_3070880n_las	2018_754900e_3142880n_las	2018_691900e_3075880n_las
2018_770900e_3155880n_las	2018_686900e_3098880n_las	2018_677900e_3077880n_las
2018_714900e_3123880n_las	2018_702900e_3106880n_las	2018_688900e_3094880n_las
2018_698900e_3102880n_las	2018_684900e_3091880n_las	2018_687900e_3091880n_las
2018_687900e_3070880n_las	2018_708900e_3103880n_las	2018_688900e_3078880n_las
2018_792900e_3165880n_las	2018_688900e_3088880n_las	2018_727900e_3119880n_las
2018_742900e_3145880n_las	2018_740900e_3139880n_las	2018_700900e_3095880n_las
2018_675900e_3063880n_las	2018_684900e_3090880n_las	2018_714900e_3111880n_las
2018_760900e_3150880n_las	2018_684900e_3079880n_las	2018_683900e_3085880n_las
2018_791900e_3171880n_las	2018_724900e_3122880n_las	2018_704900e_3115880n_las
2018_692900e_3087880n_las	2018_702900e_3100880n_las	2018_764900e_3147880n_las
2018_714900e_3117880n_las	2018_747900e_3134880n_las	2018_684900e_3073880n_las
2018_683900e_3076880n_las	2018_702900e_3098880n_las	2018_708900e_3108880n_las
2018_768900e_3150880n_las	2018_774900e_3154880n_las	2018_753900e_3147880n_las
2018_746900e_3142880n_las	2018_771900e_3158880n_las	2018_677900e_3063880n_las
2018_746900e_3132880n_las	2018_697900e_3094880n_las	2018_745900e_3138880n_las
2018_781900e_3161880n_las	2018_722900e_3122880n_las	2018_783900e_3162880n_las
2018_733900e_3135880n_las	2018_689900e_3092880n_las	2018_776900e_3169880n_las
2018_748900e_3134880n_las	2018_691900e_3083880n_las	2018_721900e_3130880n_las
2018_692900e_3082880n_las	2018_760900e_3144880n_las	2018_730900e_3137880n_las
2018_716900e_3128880n_las	2018_772900e_3155880n_las	2018_710900e_3115880n_las
2018_726900e_3133880n_las	2018_730900e_3125880n_las	2018_684900e_3070880n_las
2018_733900e_3130880n_las	2018_711900e_3112880n_las	2018_686900e_3095880n_las
2018_680900e_3082880n_las	2018_681900e_3069880n_las	2018_744900e_3135880n_las
2018_685900e_3067880n_las	2018_704900e_3108880n_las	2018_703900e_3102880n_las
2018_762900e_3149880n_las	2018_700900e_3102880n_las	2018_682900e_3076880n_las
2018_686900e_3070880n_las	2018_706900e_3110880n_las	2018_715900e_3126880n_las
2018_691900e_3084880n_las	2018_765900e_3154880n_las	2018_725900e_3118880n_las
2018_712900e_3119880n_las	2018_678900e_3077880n_las	2018_687900e_3074880n_las
2018_684900e_3080880n_las	2018_721900e_3122880n_las	2018_722900e_3115880n_las
2018_754900e_3139880n_las	2018_708900e_3117880n_las	2018_689900e_3098880n_las
2018_691900e_3105880n_las	2018_792900e_3174880n_las	2018_770900e_3152880n_las
2018_732900e_3129880n_las	2018_686900e_3093880n_las	2018_780900e_3169880n_las
2018_732900e_3130880n_las	2018_778900e_3172880n_las	2018_678900e_3079880n_las
2018_722900e_3119880n_las	2018_772900e_3153880n_las	2018_708900e_3116880n_las

TX1803-TB-C, Hurricane Harvey Post Storm Topography/Bathymetry Project Report of Survey
December 31, 2019

2018_700900e_3107880n_las	2018_678900e_3071880n_las	2018_764900e_3151880n_las
2018_771900e_3168880n_las	2018_690900e_3086880n_las	2018_792900e_3169880n_las
2018_708900e_3106880n_las	2018_788900e_3171880n_las	2018_679900e_3076880n_las
2018_775900e_3161880n_las	2018_677900e_3079880n_las	2018_785900e_3169880n_las
2018_686900e_3080880n_las	2018_703900e_3099880n_las	2018_704900e_3107880n_las
2018_775900e_3160880n_las	2018_769900e_3164880n_las	2018_783900e_3169880n_las
2018_751900e_3146880n_las	2018_680900e_3080880n_las	2018_753900e_3143880n_las
2018_733900e_3124880n_las	2018_699900e_3090880n_las	2018_690900e_3112880n_las
2018_702900e_3104880n_las	2018_698900e_3112880n_las	2018_779900e_3172880n_las
2018_683900e_3092880n_las	2018_694900e_3091880n_las	2018_702900e_3108880n_las
2018_789900e_3165880n_las	2018_701900e_3113880n_las	2018_706900e_3112880n_las
2018_733900e_3125880n_las	2018_741900e_3131880n_las	2018_712900e_3108880n_las
2018_697900e_3097880n_las	2018_714900e_3112880n_las	2018_684900e_3067880n_las
2018_731900e_3129880n_las	2018_697900e_3090880n_las	2018_734900e_3138880n_las
2018_685900e_3087880n_las	2018_699900e_3091880n_las	2018_725900e_3124880n_las
2018_733900e_3134880n_las	2018_725900e_3120880n_las	2018_717900e_3118880n_las
2018_685900e_3089880n_las	2018_744900e_3142880n_las	2018_682900e_3087880n_las
2018_685900e_3078880n_las	2018_753900e_3136880n_las	2018_769900e_3163880n_las
2018_789900e_3173880n_las	2018_702900e_3111880n_las	2018_733900e_3123880n_las
2018_687900e_3084880n_las	2018_700900e_3101880n_las	2018_704900e_3112880n_las
2018_726900e_3131880n_las	2018_683900e_3091880n_las	2018_772900e_3157880n_las
2018_718900e_3112880n_las	2018_710900e_3108880n_las	2018_776900e_3165880n_las
2018_690900e_3078880n_las	2018_707900e_3120880n_las	2018_675900e_3077880n_las
2018_703900e_3110880n_las	2018_748900e_3135880n_las	2018_677900e_3082880n_las
2018_719900e_3125880n_las	2018_710900e_3112880n_las	2018_702900e_3105880n_las
2018_755900e_3142880n_las	2018_777900e_3159880n_las	2018_682900e_3089880n_las
2018_780900e_3158880n_las	2018_789900e_3169880n_las	2018_751900e_3136880n_las
2018_694900e_3090880n_las	2018_689900e_3093880n_las	2018_709900e_3103880n_las
2018_684900e_3093880n_las	2018_771900e_3155880n_las	2018_681900e_3068880n_las
2018_761900e_3145880n_las	2018_703900e_3103880n_las	2018_718900e_3126880n_las
2018_737900e_3128880n_las	2018_785900e_3168880n_las	2018_774900e_3158880n_las
2018_753900e_3144880n_las	2018_710900e_3107880n_las	2018_695900e_3096880n_las
2018_730900e_3124880n_las	2018_689900e_3104880n_las	2018_679900e_3084880n_las
2018_700900e_3108880n_las	2018_729900e_3127880n_las	2018_784900e_3164880n_las
2018_698900e_3095880n_las	2018_735900e_3141880n_las	2018_694900e_3115880n_las
2018_700900e_3113880n_las	2018_729900e_3135880n_las	2018_775900e_3157880n_las
2018_762900e_3148880n_las	2018_686900e_3094880n_las	2018_763900e_3151880n_las
2018_688900e_3087880n_las	2018_710900e_3114880n_las	2018_782900e_3173880n_las
2018_680900e_3079880n_las	2018_683900e_3072880n_las	2018_707900e_3101880n_las
2018_726900e_3125880n_las	2018_678900e_3063880n_las	2018_681900e_3066880n_las
2018_746900e_3144880n_las	2018_787900e_3162880n_las	2018_702900e_3114880n_las
2018_676900e_3078880n_las	2018_747900e_3148880n_las	2018_679900e_3063880n_las
2018_700900e_3094880n_las	2018_673900e_3078880n_las	2018_691900e_3077880n_las

TX1803-TB-C, Hurricane Harvey Post Storm Topography/Bathymetry Project Report of Survey
December 31, 2019

2018_698900e_3092880n_las	2018_687900e_3083880n_las	2018_711900e_3115880n_las
2018_705900e_3098880n_las	2018_694900e_3084880n_las	2018_699900e_3095880n_las
2018_776900e_3157880n_las	2018_719900e_3126880n_las	2018_732900e_3139880n_las
2018_757900e_3144880n_las	2018_688900e_3093880n_las	2018_787900e_3166880n_las
2018_751900e_3138880n_las	2018_776900e_3166880n_las	2018_723900e_3124880n_las
2018_693900e_3093880n_las	2018_708900e_3113880n_las	2018_699900e_3092880n_las
2018_688900e_3083880n_las	2018_729900e_3138880n_las	2018_703900e_3106880n_las
2018_701900e_3096880n_las	2018_694900e_3093880n_las	2018_718900e_3121880n_las
2018_741900e_3134880n_las	2018_691900e_3093880n_las	2018_691900e_3081880n_las
2018_787900e_3163880n_las	2018_751900e_3147880n_las	2018_757900e_3143880n_las
2018_737900e_3132880n_las	2018_701900e_3099880n_las	2018_755900e_3141880n_las
2018_743900e_3144880n_las	2018_686900e_3075880n_las	2018_683900e_3077880n_las
2018_712900e_3113880n_las	2018_765900e_3148880n_las	2018_681900e_3085880n_las
2018_745900e_3146880n_las	2018_693900e_3079880n_las	2018_786900e_3171880n_las
2018_736900e_3128880n_las	2018_733900e_3129880n_las	2018_695900e_3113880n_las
2018_724900e_3118880n_las	2018_738900e_3135880n_las	2018_677900e_3076880n_las
2018_788900e_3168880n_las	2018_737900e_3139880n_las	2018_688900e_3077880n_las
2018_731900e_3127880n_las	2018_748900e_3148880n_las	2018_702900e_3103880n_las
2018_732900e_3134880n_las	2018_774900e_3165880n_las	2018_769900e_3152880n_las
2018_701900e_3109880n_las	2018_783900e_3164880n_las	2018_793900e_3169880n_las
2018_691900e_3099880n_las	2018_707900e_3117880n_las	2018_723900e_3121880n_las
2018_693900e_3101880n_las	2018_759900e_3144880n_las	2018_724900e_3124880n_las
2018_735900e_3129880n_las	2018_724900e_3131880n_las	2018_705900e_3110880n_las
2018_784900e_3171880n_las	2018_698900e_3107880n_las	2018_685900e_3075880n_las
2018_692900e_3111880n_las	2018_681900e_3086880n_las	2018_720900e_3119880n_las
2018_723900e_3118880n_las	2018_702900e_3107880n_las	2018_741900e_3137880n_las
2018_775900e_3159880n_las	2018_748900e_3147880n_las	2018_740900e_3137880n_las
2018_703900e_3111880n_las	2018_688900e_3099880n_las	2018_790900e_3173880n_las
2018_768900e_3166880n_las	2018_726900e_3123880n_las	2018_756900e_3144880n_las
2018_685900e_3077880n_las	2018_677900e_3084880n_las	2018_690900e_3088880n_las
2018_749900e_3142880n_las	2018_772900e_3164880n_las	2018_740900e_3134880n_las
2018_793900e_3165880n_las	2018_711900e_3109880n_las	2018_742900e_3139880n_las
2018_777900e_3171880n_las	2018_704900e_3116880n_las	2018_690900e_3104880n_las
2018_698900e_3098880n_las	2018_764900e_3150880n_las	2018_737900e_3133880n_las
2018_681900e_3077880n_las	2018_746900e_3134880n_las	2018_689900e_3099880n_las
2018_747900e_3143880n_las	2018_776900e_3159880n_las	2018_693900e_3084880n_las
2018_779900e_3171880n_las	2018_686900e_3081880n_las	2018_781900e_3167880n_las
2018_708900e_3111880n_las	2018_739900e_3138880n_las	2018_742900e_3138880n_las
2018_678900e_3066880n_las	2018_708900e_3105880n_las	2018_693900e_3100880n_las
2018_691900e_3103880n_las	2018_765900e_3149880n_las	2018_744900e_3139880n_las
2018_708900e_3102880n_las	2018_728900e_3126880n_las	2018_743900e_3131880n_las
2018_709900e_3116880n_las	2018_698900e_3106880n_las	2018_715900e_3110880n_las
2018_778900e_3167880n_las	2018_735900e_3134880n_las	2018_740900e_3143880n_las

TX1803-TB-C, Hurricane Harvey Post Storm Topography/Bathymetry Project Report of Survey
December 31, 2019

2018_679900e_3070880n_las	2018_743900e_3138880n_las	2018_682900e_3090880n_las
2018_789900e_3164880n_las	2018_715900e_3119880n_las	2018_721900e_3120880n_las
2018_687900e_3087880n_las	2018_770900e_3164880n_las	2018_747900e_3144880n_las
2018_756900e_3146880n_las	2018_697900e_3100880n_las	2018_745900e_3145880n_las
2018_744900e_3140880n_las	2018_744900e_3136880n_las	2018_713900e_3118880n_las
2018_771900e_3156880n_las	2018_692900e_3077880n_las	2018_754900e_3136880n_las
2018_698900e_3089880n_las	2018_779900e_3158880n_las	2018_712900e_3121880n_las
2018_790900e_3174880n_las	2018_715900e_3116880n_las	2018_748900e_3141880n_las
2018_715900e_3120880n_las	2018_722900e_3117880n_las	2018_752900e_3140880n_las
2018_732900e_3136880n_las	2018_750900e_3134880n_las	2018_769900e_3167880n_las
2018_714900e_3108880n_las	2018_741900e_3132880n_las	2018_703900e_3097880n_las
2018_743900e_3145880n_las	2018_756900e_3142880n_las	2018_695900e_3114880n_las
2018_676900e_3076880n_las	2018_676900e_3077880n_las	2018_711900e_3107880n_las
2018_768900e_3155880n_las	2018_684900e_3088880n_las	2018_792900e_3168880n_las
2018_715900e_3121880n_las	2018_745900e_3147880n_las	2018_707900e_3112880n_las
2018_768900e_3149880n_las	2018_763900e_3152880n_las	2018_714900e_3118880n_las
2018_689900e_3090880n_las	2018_706900e_3103880n_las	2018_726900e_3135880n_las
2018_753900e_3137880n_las	2018_772900e_3168880n_las	2018_684900e_3084880n_las
2018_719900e_3113880n_las	2018_710900e_3104880n_las	2018_769900e_3153880n_las
2018_742900e_3134880n_las	2018_752900e_3136880n_las	2018_770900e_3168880n_las
2018_789900e_3167880n_las	2018_738900e_3132880n_las	2018_743900e_3135880n_las
2018_745900e_3141880n_las	2018_746900e_3147880n_las	2018_761900e_3146880n_las
2018_694900e_3086880n_las	2018_704900e_3117880n_las	2018_738900e_3141880n_las
2018_761900e_3149880n_las	2018_679900e_3078880n_las	2018_753900e_3139880n_las
2018_687900e_3100880n_las	2018_737900e_3137880n_las	2018_676900e_3065880n_las
2018_717900e_3113880n_las	2018_684900e_3076880n_las	2018_737900e_3127880n_las
2018_705900e_3115880n_las	2018_741900e_3143880n_las	2018_683900e_3070880n_las
2018_751900e_3150880n_las	2018_760900e_3148880n_las	2018_684900e_3069880n_las
2018_754900e_3147880n_las	2018_768900e_3151880n_las	2018_758900e_3147880n_las
2018_716900e_3124880n_las	2018_752900e_3146880n_las	2018_786900e_3164880n_las
2018_717900e_3117880n_las	2018_709900e_3112880n_las	2018_692900e_3108880n_las
2018_736900e_3125880n_las	2018_760900e_3146880n_las	2018_699900e_3098880n_las
2018_696900e_3112880n_las	2018_777900e_3156880n_las	2018_686900e_3097880n_las
2018_681900e_3071880n_las	2018_706900e_3111880n_las	2018_718900e_3127880n_las
2018_684900e_3081880n_las	2018_692900e_3079880n_las	2018_734900e_3128880n_las
2018_685900e_3083880n_las	2018_691900e_3079880n_las	2018_749900e_3146880n_las
2018_742900e_3129880n_las	2018_689900e_3073880n_las	2018_684900e_3092880n_las
2018_733900e_3140880n_las	2018_727900e_3135880n_las	2018_735900e_3126880n_las
2018_778900e_3169880n_las	2018_704900e_3106880n_las	2018_692900e_3100880n_las
2018_696900e_3114880n_las	2018_697900e_3102880n_las	2018_711900e_3123880n_las
2018_769900e_3157880n_las	2018_768900e_3154880n_las	2018_720900e_3115880n_las
2018_709900e_3113880n_las	2018_686900e_3076880n_las	2018_673900e_3077880n_las
2018_685900e_3072880n_las	2018_724900e_3119880n_las	2018_713900e_3114880n_las

TX1803-TB-C, Hurricane Harvey Post Storm Topography/Bathymetry Project Report of Survey
December 31, 2019

2018_752900e_3135880n_las	2018_689900e_3094880n_las	2018_750900e_3142880n_las
2018_687900e_3095880n_las	2018_742900e_3144880n_las	2018_690900e_3079880n_las
2018_709900e_3120880n_las	2018_703900e_3113880n_las	2018_758900e_3146880n_las
2018_682900e_3081880n_las	2018_726900e_3119880n_las	2018_682900e_3086880n_las
2018_774900e_3169880n_las	2018_775900e_3170880n_las	2018_687900e_3077880n_las
2018_680900e_3081880n_las	2018_755900e_3145880n_las	2018_690900e_3076880n_las
2018_690900e_3106880n_las	2018_731900e_3139880n_las	2018_676900e_3079880n_las
2018_787900e_3170880n_las	2018_680900e_3067880n_las	2018_701900e_3101880n_las
2018_752900e_3148880n_las	2018_739900e_3128880n_las	2018_718900e_3115880n_las
2018_773900e_3165880n_las	2018_690900e_3092880n_las	2018_739900e_3129880n_las
2018_682900e_3083880n_las	2018_754900e_3143880n_las	2018_743900e_3146880n_las
2018_689900e_3095880n_las	2018_710900e_3106880n_las	2018_704900e_3100880n_las
2018_727900e_3121880n_las	2018_778900e_3160880n_las	2018_767900e_3154880n_las
2018_771900e_3152880n_las	2018_682900e_3072880n_las	2018_713900e_3108880n_las
2018_688900e_3101880n_las	2018_706900e_3108880n_las	2018_713900e_3121880n_las
2018_754900e_3141880n_las	2018_712900e_3123880n_las	2018_729900e_3122880n_las
2018_692900e_3090880n_las	2018_696900e_3097880n_las	2018_721900e_3118880n_las
2018_694900e_3096880n_las	2018_780900e_3166880n_las	2018_775900e_3169880n_las
2018_763900e_3150880n_las	2018_713900e_3117880n_las	2018_704900e_3099880n_las
2018_702900e_3115880n_las	2018_746900e_3139880n_las	2018_704900e_3104880n_las
2018_685900e_3081880n_las	2018_691900e_3109880n_las	2018_682900e_3070880n_las
2018_736900e_3139880n_las	2018_756900e_3147880n_las	2018_706900e_3099880n_las
2018_681900e_3076880n_las	2018_724900e_3121880n_las	2018_675900e_3064880n_las
2018_691900e_3097880n_las	2018_714900e_3116880n_las	2018_704900e_3098880n_las
2018_773900e_3155880n_las	2018_708900e_3115880n_las	2018_678900e_3062880n_las
2018_696900e_3088880n_las	2018_705900e_3116880n_las	2018_708900e_3104880n_las
2018_693900e_3082880n_las	2018_686900e_3088880n_las	2018_680900e_3071880n_las
2018_786900e_3162880n_las	2018_715900e_3123880n_las	2018_705900e_3117880n_las
2018_741900e_3141880n_las	2018_757900e_3139880n_las	2018_686900e_3089880n_las
2018_699900e_3106880n_las	2018_788900e_3169880n_las	2018_791900e_3167880n_las
2018_710900e_3105880n_las	2018_782900e_3161880n_las	2018_734900e_3137880n_las
2018_765900e_3147880n_las	2018_683900e_3075880n_las	2018_774900e_3168880n_las
2018_680900e_3065880n_las	2018_728900e_3127880n_las	2018_691900e_3085880n_las
2018_734900e_3130880n_las	2018_675900e_3079880n_las	2018_719900e_3130880n_las
2018_793900e_3170880n_las	2018_742900e_3142880n_las	2018_698900e_3097880n_las
2018_729900e_3128880n_las	2018_716900e_3115880n_las	2018_729900e_3126880n_las
2018_718900e_3125880n_las	2018_690900e_3090880n_las	2018_717900e_3127880n_las
2018_748900e_3143880n_las	2018_693900e_3085880n_las	2018_735900e_3132880n_las
2018_785900e_3162880n_las	2018_792900e_3175880n_las	2018_739900e_3136880n_las
2018_713900e_3120880n_las	2018_773900e_3154880n_las	2018_689900e_3083880n_las
2018_694900e_3095880n_las	2018_681900e_3079880n_las	2018_696900e_3100880n_las
2018_748900e_3138880n_las	2018_732900e_3135880n_las	2018_779900e_3161880n_las
2018_745900e_3132880n_las	2018_777900e_3169880n_las	2018_254600e_3192240n_las

TX1803-TB-C, Hurricane Harvey Post Storm Topography/Bathymetry Project Report of Survey
December 31, 2019

2018_297600e_3222240n_las	2018_308600e_3240240n_las	2018_328600e_3252240n_las
2018_319600e_3237240n_las	2018_302600e_3227240n_las	2018_232600e_3185240n_las
2018_349600e_3267240n_las	2018_287600e_3225240n_las	2018_335600e_3247240n_las
2018_208600e_3170240n_las	2018_279600e_3212240n_las	2018_322600e_3240240n_las
2018_206600e_3177240n_las	2018_314600e_3251240n_las	2018_213600e_3175240n_las
2018_352600e_3263240n_las	2018_304600e_3238240n_las	2018_334600e_3250240n_las
2018_299600e_3227240n_las	2018_240600e_3182240n_las	2018_259600e_3195240n_las
2018_326600e_3240240n_las	2018_228600e_3183240n_las	2018_307600e_3233240n_las
2018_332600e_3259240n_las	2018_269600e_3203240n_las	2018_308600e_3228240n_las
2018_330600e_3242240n_las	2018_340600e_3259240n_las	2018_358600e_3270240n_las
2018_227600e_3175240n_las	2018_209600e_3166240n_las	2018_327600e_3252240n_las
2018_354600e_3269240n_las	2018_336600e_3261240n_las	2018_315600e_3246240n_las
2018_276600e_3209240n_las	2018_232600e_3183240n_las	2018_293600e_3230240n_las
2018_225600e_3183240n_las	2018_287600e_3212240n_las	2018_252600e_3191240n_las
2018_304600e_3231240n_las	2018_238600e_3183240n_las	2018_231600e_3182240n_las
2018_306600e_3228240n_las	2018_258600e_3197240n_las	2018_211600e_3173240n_las
2018_212600e_3177240n_las	2018_284600e_3213240n_las	2018_343600e_3266240n_las
2018_347600e_3266240n_las	2018_281600e_3208240n_las	2018_299600e_3231240n_las
2018_351600e_3266240n_las	2018_310600e_3240240n_las	2018_287600e_3226240n_las
2018_338600e_3256240n_las	2018_298600e_3222240n_las	2018_230600e_3181240n_las
2018_345600e_3263240n_las	2018_217600e_3180240n_las	2018_231600e_3181240n_las
2018_210600e_3171240n_las	2018_340600e_3263240n_las	2018_321600e_3252240n_las
2018_345600e_3266240n_las	2018_283600e_3210240n_las	2018_290600e_3223240n_las
2018_318600e_3243240n_las	2018_291600e_3218240n_las	2018_352600e_3268240n_las
2018_326600e_3253240n_las	2018_224600e_3183240n_las	2018_225600e_3184240n_las
2018_297600e_3221240n_las	2018_348600e_3266240n_las	2018_212600e_3171240n_las
2018_296600e_3221240n_las	2018_231600e_3177240n_las	2018_275600e_3210240n_las
2018_315600e_3243240n_las	2018_356600e_3265240n_las	2018_248600e_3189240n_las
2018_240600e_3187240n_las	2018_314600e_3241240n_las	2018_268600e_3205240n_las
2018_313600e_3251240n_las	2018_325600e_3251240n_las	2018_312600e_3241240n_las
2018_326600e_3243240n_las	2018_247600e_3188240n_las	2018_275600e_3205240n_las
2018_242600e_3186240n_las	2018_317600e_3251240n_las	2018_221600e_3182240n_las
2018_315600e_3249240n_las	2018_316600e_3242240n_las	2018_320600e_3248240n_las
2018_351600e_3269240n_las	2018_324600e_3248240n_las	2018_312600e_3249240n_las
2018_334600e_3248240n_las	2018_328600e_3256240n_las	2018_316600e_3235240n_las
2018_307600e_3234240n_las	2018_218600e_3174240n_las	2018_300600e_3230240n_las
2018_219600e_3171240n_las	2018_342600e_3261240n_las	2018_257600e_3197240n_las
2018_268600e_3208240n_las	2018_334600e_3249240n_las	2018_314600e_3247240n_las
2018_216600e_3171240n_las	2018_214600e_3174240n_las	2018_283600e_3212240n_las
2018_212600e_3168240n_las	2018_300600e_3223240n_las	2018_332600e_3255240n_las
2018_227600e_3177240n_las	2018_256600e_3194240n_las	2018_321600e_3251240n_las
2018_295600e_3220240n_las	2018_219600e_3175240n_las	2018_296600e_3219240n_las
2018_221600e_3176240n_las	2018_263600e_3200240n_las	2018_298600e_3232240n_las

TX1803-TB-C, Hurricane Harvey Post Storm Topography/Bathymetry Project Report of Survey
December 31, 2019

2018_321600e_3237240n_las	2018_274600e_3205240n_las	2018_289600e_3225240n_las
2018_260600e_3196240n_las	2018_351600e_3263240n_las	2018_317600e_3239240n_las
2018_258600e_3194240n_las	2018_285600e_3224240n_las	2018_324600e_3243240n_las
2018_265600e_3198240n_las	2018_341600e_3262240n_las	2018_210600e_3178240n_las
2018_207600e_3172240n_las	2018_210600e_3176240n_las	2018_314600e_3252240n_las
2018_216600e_3181240n_las	2018_245600e_3188240n_las	2018_332600e_3244240n_las
2018_269600e_3201240n_las	2018_220600e_3180240n_las	2018_211600e_3174240n_las
2018_213600e_3169240n_las	2018_325600e_3244240n_las	2018_323600e_3238240n_las
2018_291600e_3219240n_las	2018_252600e_3194240n_las	2018_271600e_3206240n_las
2018_220600e_3181240n_las	2018_219600e_3174240n_las	2018_241600e_3183240n_las
2018_313600e_3240240n_las	2018_313600e_3247240n_las	2018_326600e_3252240n_las
2018_332600e_3257240n_las	2018_238600e_3186240n_las	2018_223600e_3183240n_las
2018_278600e_3207240n_las	2018_340600e_3258240n_las	2018_314600e_3246240n_las
2018_281600e_3207240n_las	2018_284600e_3220240n_las	2018_215600e_3180240n_las
2018_323600e_3246240n_las	2018_308600e_3235240n_las	2018_335600e_3250240n_las
2018_352600e_3265240n_las	2018_324600e_3242240n_las	2018_235600e_3182240n_las
2018_302600e_3231240n_las	2018_225600e_3179240n_las	2018_223600e_3177240n_las
2018_332600e_3260240n_las	2018_347600e_3264240n_las	2018_345600e_3267240n_las
2018_346600e_3268240n_las	2018_291600e_3217240n_las	2018_264600e_3199240n_las
2018_208600e_3167240n_las	2018_317600e_3248240n_las	2018_336600e_3246240n_las
2018_317600e_3245240n_las	2018_227600e_3182240n_las	2018_238600e_3184240n_las
2018_325600e_3248240n_las	2018_296600e_3224240n_las	2018_210600e_3175240n_las
2018_256600e_3191240n_las	2018_319600e_3246240n_las	2018_223600e_3180240n_las
2018_301600e_3229240n_las	2018_295600e_3231240n_las	2018_289600e_3218240n_las
2018_285600e_3214240n_las	2018_300600e_3232240n_las	2018_294600e_3225240n_las
2018_292600e_3222240n_las	2018_285600e_3221240n_las	2018_312600e_3243240n_las
2018_327600e_3251240n_las	2018_280600e_3211240n_las	2018_300600e_3236240n_las
2018_339600e_3262240n_las	2018_334600e_3262240n_las	2018_216600e_3182240n_las
2018_214600e_3172240n_las	2018_252600e_3190240n_las	2018_254600e_3194240n_las
2018_266600e_3198240n_las	2018_359600e_3267240n_las	2018_287600e_3217240n_las
2018_227600e_3179240n_las	2018_216600e_3178240n_las	2018_322600e_3241240n_las
2018_268600e_3201240n_las	2018_287600e_3223240n_las	2018_330600e_3251240n_las
2018_219600e_3173240n_las	2018_267600e_3195240n_las	2018_305600e_3229240n_las
2018_294600e_3230240n_las	2018_290600e_3225240n_las	2018_302600e_3228240n_las
2018_315600e_3248240n_las	2018_257600e_3193240n_las	2018_221600e_3183240n_las
2018_282600e_3216240n_las	2018_282600e_3217240n_las	2018_297600e_3223240n_las
2018_301600e_3235240n_las	2018_297600e_3229240n_las	2018_283600e_3218240n_las
2018_237600e_3184240n_las	2018_339600e_3263240n_las	2018_224600e_3180240n_las
2018_335600e_3249240n_las	2018_335600e_3262240n_las	2018_289600e_3222240n_las
2018_347600e_3269240n_las	2018_277600e_3212240n_las	2018_317600e_3254240n_las
2018_273600e_3201240n_las	2018_209600e_3177240n_las	2018_328600e_3241240n_las
2018_220600e_3172240n_las	2018_279600e_3211240n_las	2018_333600e_3258240n_las
2018_213600e_3168240n_las	2018_313600e_3235240n_las	2018_276600e_3208240n_las

TX1803-TB-C, Hurricane Harvey Post Storm Topography/Bathymetry Project Report of Survey
December 31, 2019

2018_236600e_3181240n_las	2018_353600e_3264240n_las	2018_288600e_3215240n_las
2018_298600e_3226240n_las	2018_289600e_3226240n_las	2018_337600e_3262240n_las
2018_271600e_3200240n_las	2018_311600e_3242240n_las	2018_320600e_3241240n_las
2018_219600e_3172240n_las	2018_267600e_3199240n_las	2018_261600e_3194240n_las
2018_346600e_3261240n_las	2018_309600e_3235240n_las	2018_270600e_3197240n_las
2018_289600e_3228240n_las	2018_253600e_3191240n_las	2018_334600e_3254240n_las
2018_318600e_3249240n_las	2018_222600e_3173240n_las	2018_300600e_3224240n_las
2018_331600e_3254240n_las	2018_274600e_3203240n_las	2018_321600e_3243240n_las
2018_325600e_3252240n_las	2018_289600e_3227240n_las	2018_213600e_3170240n_las
2018_249600e_3192240n_las	2018_297600e_3226240n_las	2018_325600e_3245240n_las
2018_239600e_3187240n_las	2018_303600e_3239240n_las	2018_337600e_3259240n_las
2018_328600e_3244240n_las	2018_316600e_3239240n_las	2018_319600e_3249240n_las
2018_332600e_3251240n_las	2018_287600e_3222240n_las	2018_325600e_3250240n_las
2018_228600e_3178240n_las	2018_312600e_3231240n_las	2018_292600e_3217240n_las
2018_260600e_3193240n_las	2018_253600e_3189240n_las	2018_290600e_3227240n_las
2018_295600e_3218240n_las	2018_312600e_3251240n_las	2018_312600e_3236240n_las
2018_315600e_3247240n_las	2018_208600e_3174240n_las	2018_315600e_3250240n_las
2018_278600e_3213240n_las	2018_213600e_3178240n_las	2018_294600e_3232240n_las
2018_274600e_3204240n_las	2018_313600e_3250240n_las	2018_295600e_3229240n_las
2018_279600e_3207240n_las	2018_336600e_3259240n_las	2018_301600e_3225240n_las
2018_345600e_3268240n_las	2018_242600e_3185240n_las	2018_261600e_3196240n_las
2018_309600e_3243240n_las	2018_253600e_3194240n_las	2018_332600e_3248240n_las
2018_210600e_3170240n_las	2018_330600e_3250240n_las	2018_264600e_3194240n_las
2018_330600e_3256240n_las	2018_280600e_3213240n_las	2018_329600e_3244240n_las
2018_284600e_3216240n_las	2018_349600e_3265240n_las	2018_287600e_3220240n_las
2018_340600e_3262240n_las	2018_323600e_3249240n_las	2018_344600e_3259240n_las
2018_353600e_3267240n_las	2018_353600e_3268240n_las	2018_344600e_3265240n_las
2018_322600e_3242240n_las	2018_276600e_3202240n_las	2018_322600e_3247240n_las
2018_327600e_3246240n_las	2018_310600e_3232240n_las	2018_294600e_3223240n_las
2018_309600e_3240240n_las	2018_298600e_3227240n_las	2018_214600e_3180240n_las
2018_266600e_3206240n_las	2018_286600e_3225240n_las	2018_311600e_3250240n_las
2018_310600e_3237240n_las	2018_272600e_3204240n_las	2018_234600e_3181240n_las
2018_342600e_3258240n_las	2018_315600e_3238240n_las	2018_268600e_3196240n_las
2018_321600e_3248240n_las	2018_300600e_3235240n_las	2018_289600e_3215240n_las
2018_217600e_3182240n_las	2018_276600e_3207240n_las	2018_219600e_3179240n_las
2018_308600e_3232240n_las	2018_294600e_3229240n_las	2018_308600e_3231240n_las
2018_254600e_3195240n_las	2018_270600e_3198240n_las	2018_242600e_3187240n_las
2018_290600e_3228240n_las	2018_221600e_3179240n_las	2018_312600e_3240240n_las
2018_277600e_3207240n_las	2018_334600e_3252240n_las	2018_323600e_3251240n_las
2018_303600e_3236240n_las	2018_263600e_3198240n_las	2018_233600e_3183240n_las
2018_287600e_3218240n_las	2018_268600e_3206240n_las	2018_213600e_3179240n_las
2018_288600e_3214240n_las	2018_280600e_3210240n_las	2018_323600e_3239240n_las
2018_247600e_3189240n_las	2018_289600e_3217240n_las	2018_336600e_3257240n_las

TX1803-TB-C, Hurricane Harvey Post Storm Topography/Bathymetry Project Report of Survey
December 31, 2019

2018_230600e_3184240n_las	2018_326600e_3251240n_las	2018_214600e_3176240n_las
2018_271600e_3198240n_las	2018_213600e_3176240n_las	2018_225600e_3182240n_las
2018_320600e_3247240n_las	2018_334600e_3257240n_las	2018_232600e_3180240n_las
2018_305600e_3236240n_las	2018_285600e_3222240n_las	2018_249600e_3188240n_las
2018_255600e_3193240n_las	2018_329600e_3254240n_las	2018_321600e_3244240n_las
2018_318600e_3238240n_las	2018_312600e_3244240n_las	2018_236600e_3185240n_las
2018_352600e_3269240n_las	2018_267600e_3198240n_las	2018_323600e_3242240n_las
2018_291600e_3228240n_las	2018_206600e_3169240n_las	2018_354600e_3268240n_las
2018_267600e_3205240n_las	2018_208600e_3180240n_las	2018_288600e_3220240n_las
2018_278600e_3211240n_las	2018_333600e_3252240n_las	2018_267600e_3207240n_las
2018_284600e_3219240n_las	2018_330600e_3257240n_las	2018_209600e_3169240n_las
2018_304600e_3225240n_las	2018_222600e_3182240n_las	2018_288600e_3216240n_las
2018_212600e_3180240n_las	2018_320600e_3249240n_las	2018_207600e_3169240n_las
2018_269600e_3197240n_las	2018_222600e_3175240n_las	2018_303600e_3229240n_las
2018_253600e_3193240n_las	2018_212600e_3179240n_las	2018_271600e_3202240n_las
2018_309600e_3237240n_las	2018_273600e_3205240n_las	2018_335600e_3251240n_las
2018_322600e_3246240n_las	2018_246600e_3191240n_las	2018_289600e_3216240n_las
2018_260600e_3194240n_las	2018_269600e_3208240n_las	2018_311600e_3244240n_las
2018_335600e_3245240n_las	2018_335600e_3254240n_las	2018_221600e_3173240n_las
2018_226600e_3175240n_las	2018_263600e_3199240n_las	2018_283600e_3220240n_las
2018_303600e_3228240n_las	2018_263600e_3197240n_las	2018_210600e_3177240n_las
2018_220600e_3173240n_las	2018_311600e_3243240n_las	2018_212600e_3175240n_las
2018_292600e_3219240n_las	2018_248600e_3188240n_las	2018_213600e_3180240n_las
2018_301600e_3226240n_las	2018_227600e_3180240n_las	2018_302600e_3230240n_las
2018_290600e_3221240n_las	2018_331600e_3246240n_las	2018_332600e_3249240n_las
2018_325600e_3253240n_las	2018_313600e_3237240n_las	2018_226600e_3179240n_las
2018_279600e_3213240n_las	2018_293600e_3222240n_las	2018_331600e_3248240n_las
2018_213600e_3172240n_las	2018_229600e_3179240n_las	2018_290600e_3214240n_las
2018_317600e_3241240n_las	2018_321600e_3239240n_las	2018_279600e_3206240n_las
2018_305600e_3234240n_las	2018_305600e_3241240n_las	2018_286600e_3222240n_las
2018_343600e_3259240n_las	2018_327600e_3245240n_las	2018_321600e_3250240n_las
2018_231600e_3180240n_las	2018_220600e_3174240n_las	2018_225600e_3176240n_las
2018_322600e_3245240n_las	2018_285600e_3216240n_las	2018_225600e_3181240n_las
2018_285600e_3220240n_las	2018_330600e_3255240n_las	2018_275600e_3207240n_las
2018_318600e_3237240n_las	2018_306600e_3237240n_las	2018_317600e_3242240n_las
2018_330600e_3249240n_las	2018_268600e_3204240n_las	2018_269600e_3199240n_las
2018_306600e_3230240n_las	2018_332600e_3252240n_las	2018_358600e_3271240n_las
2018_296600e_3230240n_las	2018_239600e_3184240n_las	2018_318600e_3253240n_las
2018_339600e_3256240n_las	2018_209600e_3178240n_las	2018_291600e_3227240n_las
2018_355600e_3264240n_las	2018_215600e_3179240n_las	2018_217600e_3179240n_las
2018_339600e_3257240n_las	2018_270600e_3207240n_las	2018_251600e_3188240n_las
2018_342600e_3260240n_las	2018_305600e_3228240n_las	2018_229600e_3184240n_las
2018_330600e_3246240n_las	2018_239600e_3185240n_las	2018_246600e_3190240n_las

TX1803-TB-C, Hurricane Harvey Post Storm Topography/Bathymetry Project Report of Survey
December 31, 2019

2018_243600e_3189240n_las	2018_209600e_3170240n_las	2018_305600e_3237240n_las
2018_287600e_3224240n_las	2018_310600e_3236240n_las	2018_290600e_3224240n_las
2018_288600e_3224240n_las	2018_283600e_3211240n_las	2018_300600e_3237240n_las
2018_318600e_3240240n_las	2018_308600e_3229240n_las	2018_342600e_3265240n_las
2018_302600e_3233240n_las	2018_311600e_3237240n_las	2018_264600e_3198240n_las
2018_316600e_3254240n_las	2018_286600e_3224240n_las	2018_326600e_3245240n_las
2018_331600e_3255240n_las	2018_353600e_3265240n_las	2018_318600e_3241240n_las
2018_292600e_3229240n_las	2018_278600e_3212240n_las	2018_324600e_3244240n_las
2018_216600e_3179240n_las	2018_299600e_3225240n_las	2018_288600e_3219240n_las
2018_280600e_3208240n_las	2018_322600e_3251240n_las	2018_319600e_3245240n_las
2018_245600e_3190240n_las	2018_281600e_3211240n_las	2018_315600e_3234240n_las
2018_307600e_3230240n_las	2018_281600e_3210240n_las	2018_303600e_3235240n_las
2018_287600e_3214240n_las	2018_226600e_3180240n_las	2018_291600e_3226240n_las
2018_316600e_3248240n_las	2018_280600e_3209240n_las	2018_302600e_3235240n_las
2018_343600e_3265240n_las	2018_353600e_3270240n_las	2018_359600e_3271240n_las
2018_306600e_3229240n_las	2018_298600e_3220240n_las	2018_208600e_3178240n_las
2018_251600e_3191240n_las	2018_208600e_3179240n_las	2018_276600e_3210240n_las
2018_246600e_3187240n_las	2018_258600e_3193240n_las	2018_279600e_3205240n_las
2018_312600e_3237240n_las	2018_311600e_3236240n_las	2018_336600e_3250240n_las
2018_212600e_3174240n_las	2018_337600e_3255240n_las	2018_302600e_3238240n_las
2018_318600e_3244240n_las	2018_258600e_3195240n_las	2018_356600e_3269240n_las
2018_292600e_3216240n_las	2018_336600e_3256240n_las	2018_258600e_3192240n_las
2018_302600e_3237240n_las	2018_211600e_3175240n_las	2018_344600e_3266240n_las
2018_321600e_3247240n_las	2018_326600e_3254240n_las	2018_330600e_3244240n_las
2018_266600e_3201240n_las	2018_285600e_3212240n_las	2018_275600e_3203240n_las
2018_227600e_3185240n_las	2018_315600e_3241240n_las	2018_296600e_3225240n_las
2018_330600e_3245240n_las	2018_344600e_3264240n_las	2018_216600e_3170240n_las
2018_263600e_3196240n_las	2018_305600e_3240240n_las	2018_333600e_3256240n_las
2018_310600e_3234240n_las	2018_292600e_3215240n_las	2018_286600e_3211240n_las
2018_236600e_3182240n_las	2018_357600e_3271240n_las	2018_250600e_3188240n_las
2018_323600e_3250240n_las	2018_292600e_3228240n_las	2018_239600e_3183240n_las
2018_314600e_3236240n_las	2018_251600e_3190240n_las	2018_341600e_3259240n_las
2018_329600e_3253240n_las	2018_237600e_3182240n_las	2018_312600e_3242240n_las
2018_295600e_3221240n_las	2018_329600e_3243240n_las	2018_308600e_3230240n_las
2018_313600e_3239240n_las	2018_212600e_3178240n_las	2018_240600e_3186240n_las
2018_269600e_3196240n_las	2018_213600e_3171240n_las	2018_210600e_3174240n_las
2018_261600e_3197240n_las	2018_299600e_3226240n_las	2018_306600e_3231240n_las
2018_318600e_3246240n_las	2018_351600e_3264240n_las	2018_333600e_3244240n_las
2018_319600e_3238240n_las	2018_291600e_3222240n_las	2018_305600e_3232240n_las
2018_337600e_3257240n_las	2018_296600e_3222240n_las	2018_313600e_3248240n_las
2018_343600e_3262240n_las	2018_336600e_3247240n_las	2018_294600e_3231240n_las
2018_337600e_3263240n_las	2018_213600e_3177240n_las	2018_301600e_3233240n_las
2018_333600e_3250240n_las	2018_286600e_3214240n_las	2018_258600e_3196240n_las

TX1803-TB-C, Hurricane Harvey Post Storm Topography/Bathymetry Project Report of Survey
December 31, 2019

2018_338600e_3260240n_las	2018_302600e_3226240n_las	2018_351600e_3268240n_las
2018_209600e_3180240n_las	2018_288600e_3223240n_las	2018_235600e_3180240n_las
2018_340600e_3260240n_las	2018_291600e_3216240n_las	2018_328600e_3254240n_las
2018_214600e_3175240n_las	2018_316600e_3252240n_las	2018_345600e_3262240n_las
2018_295600e_3224240n_las	2018_342600e_3259240n_las	2018_271600e_3204240n_las
2018_274600e_3201240n_las	2018_225600e_3178240n_las	2018_334600e_3253240n_las
2018_290600e_3217240n_las	2018_355600e_3270240n_las	2018_305600e_3226240n_las
2018_272600e_3200240n_las	2018_266600e_3197240n_las	2018_270600e_3202240n_las
2018_281600e_3214240n_las	2018_242600e_3183240n_las	2018_206600e_3172240n_las
2018_294600e_3217240n_las	2018_349600e_3268240n_las	2018_282600e_3219240n_las
2018_332600e_3253240n_las	2018_309600e_3229240n_las	2018_290600e_3226240n_las
2018_325600e_3243240n_las	2018_308600e_3243240n_las	2018_281600e_3213240n_las
2018_308600e_3239240n_las	2018_294600e_3219240n_las	2018_215600e_3176240n_las
2018_296600e_3229240n_las	2018_349600e_3263240n_las	2018_354600e_3266240n_las
2018_309600e_3244240n_las	2018_317600e_3250240n_las	2018_220600e_3171240n_las
2018_283600e_3221240n_las	2018_291600e_3224240n_las	2018_259600e_3194240n_las
2018_211600e_3169240n_las	2018_289600e_3219240n_las	2018_269600e_3204240n_las
2018_349600e_3262240n_las	2018_208600e_3166240n_las	2018_335600e_3258240n_las
2018_310600e_3243240n_las	2018_245600e_3189240n_las	2018_283600e_3213240n_las
2018_218600e_3177240n_las	2018_234600e_3184240n_las	2018_249600e_3187240n_las
2018_210600e_3180240n_las	2018_334600e_3260240n_las	2018_223600e_3176240n_las
2018_311600e_3239240n_las	2018_252600e_3189240n_las	2018_325600e_3240240n_las
2018_302600e_3229240n_las	2018_282600e_3214240n_las	2018_284600e_3211240n_las
2018_224600e_3178240n_las	2018_298600e_3231240n_las	2018_320600e_3246240n_las
2018_347600e_3261240n_las	2018_234600e_3179240n_las	2018_222600e_3174240n_las
2018_278600e_3210240n_las	2018_291600e_3220240n_las	2018_220600e_3178240n_las
2018_222600e_3177240n_las	2018_341600e_3263240n_las	2018_250600e_3191240n_las
2018_208600e_3173240n_las	2018_318600e_3242240n_las	2018_337600e_3256240n_las
2018_302600e_3236240n_las	2018_208600e_3169240n_las	2018_303600e_3231240n_las
2018_290600e_3216240n_las	2018_262600e_3196240n_las	2018_211600e_3172240n_las
2018_304600e_3237240n_las	2018_214600e_3181240n_las	2018_338600e_3257240n_las
2018_312600e_3245240n_las	2018_223600e_3173240n_las	2018_270600e_3206240n_las
2018_215600e_3174240n_las	2018_353600e_3269240n_las	2018_285600e_3215240n_las
2018_295600e_3222240n_las	2018_259600e_3193240n_las	2018_282600e_3213240n_las
2018_214600e_3178240n_las	2018_299600e_3232240n_las	2018_245600e_3186240n_las
2018_327600e_3249240n_las	2018_274600e_3207240n_las	2018_293600e_3218240n_las
2018_346600e_3263240n_las	2018_296600e_3227240n_las	2018_210600e_3179240n_las
2018_222600e_3179240n_las	2018_220600e_3182240n_las	2018_348600e_3268240n_las
2018_299600e_3234240n_las	2018_314600e_3233240n_las	2018_275600e_3202240n_las
2018_246600e_3189240n_las	2018_282600e_3212240n_las	2018_298600e_3224240n_las
2018_313600e_3249240n_las	2018_301600e_3234240n_las	2018_222600e_3183240n_las
2018_212600e_3172240n_las	2018_206600e_3174240n_las	2018_207600e_3171240n_las
2018_282600e_3211240n_las	2018_226600e_3183240n_las	2018_343600e_3261240n_las

TX1803-TB-C, Hurricane Harvey Post Storm Topography/Bathymetry Project Report of Survey
December 31, 2019

2018_216600e_3175240n_las	2018_242600e_3184240n_las	2018_315600e_3239240n_las
2018_285600e_3223240n_las	2018_248600e_3187240n_las	2018_319600e_3243240n_las
2018_281600e_3215240n_las	2018_320600e_3244240n_las	2018_316600e_3241240n_las
2018_265600e_3199240n_las	2018_301600e_3230240n_las	2018_287600e_3219240n_las
2018_209600e_3168240n_las	2018_350600e_3266240n_las	2018_312600e_3233240n_las
2018_256600e_3192240n_las	2018_292600e_3227240n_las	2018_234600e_3183240n_las
2018_281600e_3209240n_las	2018_246600e_3188240n_las	2018_327600e_3248240n_las
2018_335600e_3259240n_las	2018_306600e_3241240n_las	2018_244600e_3189240n_las
2018_360600e_3267240n_las	2018_268600e_3197240n_las	2018_300600e_3233240n_las
2018_311600e_3235240n_las	2018_271600e_3203240n_las	2018_209600e_3172240n_las
2018_272600e_3202240n_las	2018_229600e_3176240n_las	2018_255600e_3195240n_las
2018_329600e_3250240n_las	2018_289600e_3221240n_las	2018_321600e_3241240n_las
2018_270600e_3199240n_las	2018_272600e_3206240n_las	2018_244600e_3188240n_las
2018_286600e_3216240n_las	2018_229600e_3178240n_las	2018_319600e_3250240n_las
2018_261600e_3198240n_las	2018_280600e_3206240n_las	2018_286600e_3212240n_las
2018_341600e_3257240n_las	2018_332600e_3256240n_las	2018_207600e_3174240n_las
2018_313600e_3236240n_las	2018_289600e_3224240n_las	2018_253600e_3192240n_las
2018_272600e_3205240n_las	2018_328600e_3255240n_las	2018_211600e_3178240n_las
2018_309600e_3231240n_las	2018_311600e_3241240n_las	2018_304600e_3240240n_las
2018_301600e_3223240n_las	2018_206600e_3167240n_las	2018_328600e_3251240n_las
2018_237600e_3181240n_las	2018_310600e_3231240n_las	2018_313600e_3245240n_las
2018_304600e_3232240n_las	2018_260600e_3195240n_las	2018_295600e_3228240n_las
2018_215600e_3175240n_las	2018_319600e_3251240n_las	2018_298600e_3228240n_las
2018_326600e_3244240n_las	2018_301600e_3224240n_las	2018_308600e_3241240n_las
2018_317600e_3246240n_las	2018_221600e_3174240n_las	2018_321600e_3242240n_las
2018_327600e_3241240n_las	2018_267600e_3200240n_las	2018_356600e_3268240n_las
2018_238600e_3181240n_las	2018_314600e_3253240n_las	2018_264600e_3196240n_las
2018_247600e_3190240n_las	2018_304600e_3230240n_las	2018_279600e_3209240n_las
2018_304600e_3239240n_las	2018_327600e_3247240n_las	2018_337600e_3258240n_las
2018_314600e_3238240n_las	2018_206600e_3165240n_las	2018_330600e_3254240n_las
2018_319600e_3252240n_las	2018_333600e_3257240n_las	2018_287600e_3213240n_las
2018_320600e_3250240n_las	2018_230600e_3185240n_las	2018_208600e_3176240n_las
2018_254600e_3190240n_las	2018_335600e_3260240n_las	2018_244600e_3185240n_las
2018_307600e_3242240n_las	2018_283600e_3217240n_las	2018_339600e_3259240n_las
2018_319600e_3253240n_las	2018_320600e_3240240n_las	2018_261600e_3195240n_las
2018_232600e_3181240n_las	2018_256600e_3196240n_las	2018_320600e_3252240n_las
2018_297600e_3233240n_las	2018_298600e_3235240n_las	2018_310600e_3238240n_las
2018_317600e_3252240n_las	2018_332600e_3245240n_las	2018_260600e_3198240n_las
2018_336600e_3248240n_las	2018_211600e_3177240n_las	2018_348600e_3269240n_las
2018_299600e_3222240n_las	2018_221600e_3180240n_las	2018_278600e_3205240n_las
2018_285600e_3210240n_las	2018_257600e_3192240n_las	2018_250600e_3193240n_las
2018_324600e_3251240n_las	2018_235600e_3181240n_las	2018_299600e_3236240n_las
2018_300600e_3225240n_las	2018_319600e_3239240n_las	2018_339600e_3260240n_las

TX1803-TB-C, Hurricane Harvey Post Storm Topography/Bathymetry Project Report of Survey
December 31, 2019

2018_358600e_3272240n_las	2018_353600e_3263240n_las	2018_336600e_3258240n_las
2018_310600e_3241240n_las	2018_334600e_3247240n_las	2018_276600e_3205240n_las
2018_283600e_3214240n_las	2018_269600e_3206240n_las	2018_351600e_3265240n_las
2018_211600e_3179240n_las	2018_304600e_3228240n_las	2018_220600e_3183240n_las
2018_214600e_3169240n_las	2018_343600e_3260240n_las	2018_209600e_3179240n_las
2018_277600e_3210240n_las	2018_226600e_3184240n_las	2018_299600e_3221240n_las
2018_307600e_3229240n_las	2018_227600e_3181240n_las	2018_335600e_3252240n_las
2018_206600e_3176240n_las	2018_333600e_3254240n_las	2018_317600e_3236240n_las
2018_349600e_3269240n_las	2018_313600e_3234240n_las	2018_300600e_3229240n_las
2018_328600e_3249240n_las	2018_282600e_3210240n_las	2018_209600e_3173240n_las
2018_219600e_3178240n_las	2018_233600e_3179240n_las	2018_243600e_3185240n_las
2018_291600e_3225240n_las	2018_292600e_3220240n_las	2018_280600e_3214240n_las
2018_285600e_3219240n_las	2018_351600e_3267240n_las	2018_316600e_3234240n_las
2018_301600e_3227240n_las	2018_302600e_3234240n_las	2018_349600e_3266240n_las
2018_241600e_3185240n_las	2018_312600e_3238240n_las	2018_348600e_3264240n_las
2018_211600e_3180240n_las	2018_238600e_3185240n_las	2018_292600e_3225240n_las
2018_323600e_3241240n_las	2018_307600e_3238240n_las	2018_296600e_3233240n_las
2018_254600e_3191240n_las	2018_322600e_3250240n_las	2018_318600e_3236240n_las
2018_257600e_3191240n_las	2018_301600e_3232240n_las	2018_320600e_3238240n_las
2018_217600e_3173240n_las	2018_223600e_3182240n_las	2018_224600e_3182240n_las
2018_235600e_3183240n_las	2018_267600e_3206240n_las	2018_347600e_3268240n_las
2018_230600e_3179240n_las	2018_266600e_3200240n_las	2018_311600e_3232240n_las
2018_295600e_3223240n_las	2018_295600e_3225240n_las	2018_261600e_3199240n_las
2018_350600e_3267240n_las	2018_236600e_3183240n_las	2018_327600e_3255240n_las
2018_301600e_3236240n_las	2018_330600e_3253240n_las	2018_336600e_3263240n_las
2018_321600e_3246240n_las	2018_228600e_3184240n_las	2018_308600e_3234240n_las
2018_213600e_3174240n_las	2018_308600e_3236240n_las	2018_210600e_3172240n_las
2018_231600e_3178240n_las	2018_316600e_3249240n_las	2018_304600e_3235240n_las
2018_237600e_3186240n_las	2018_346600e_3264240n_las	2018_224600e_3176240n_las
2018_334600e_3245240n_las	2018_313600e_3243240n_las	2018_329600e_3257240n_las
2018_286600e_3220240n_las	2018_215600e_3173240n_las	2018_327600e_3253240n_las
2018_209600e_3174240n_las	2018_300600e_3222240n_las	2018_350600e_3265240n_las
2018_329600e_3252240n_las	2018_295600e_3232240n_las	2018_271600e_3205240n_las
2018_354600e_3267240n_las	2018_220600e_3179240n_las	2018_308600e_3233240n_las
2018_307600e_3241240n_las	2018_268600e_3202240n_las	2018_326600e_3242240n_las
2018_300600e_3234240n_las	2018_228600e_3185240n_las	2018_221600e_3181240n_las
2018_333600e_3260240n_las	2018_357600e_3269240n_las	2018_355600e_3265240n_las
2018_303600e_3224240n_las	2018_250600e_3190240n_las	2018_291600e_3229240n_las
2018_276600e_3206240n_las	2018_207600e_3166240n_las	2018_299600e_3229240n_las
2018_229600e_3177240n_las	2018_243600e_3188240n_las	2018_255600e_3190240n_las
2018_206600e_3166240n_las	2018_329600e_3245240n_las	2018_288600e_3221240n_las
2018_318600e_3252240n_las	2018_317600e_3244240n_las	2018_334600e_3258240n_las
2018_311600e_3238240n_las	2018_306600e_3232240n_las	2018_293600e_3216240n_las

TX1803-TB-C, Hurricane Harvey Post Storm Topography/Bathymetry Project Report of Survey
December 31, 2019

2018_277600e_3204240n_las	2018_299600e_3228240n_las	2018_218600e_3175240n_las
2018_305600e_3233240n_las	2018_304600e_3236240n_las	2018_297600e_3225240n_las
2018_309600e_3241240n_las	2018_208600e_3175240n_las	2018_284600e_3222240n_las
2018_217600e_3181240n_las	2018_323600e_3247240n_las	2018_273600e_3202240n_las
2018_321600e_3238240n_las	2018_333600e_3249240n_las	2018_316600e_3244240n_las
2018_357600e_3267240n_las	2018_322600e_3238240n_las	2018_329600e_3247240n_las
2018_336600e_3260240n_las	2018_272600e_3203240n_las	2018_294600e_3224240n_las
2018_349600e_3261240n_las	2018_320600e_3251240n_las	2018_269600e_3205240n_las
2018_308600e_3242240n_las	2018_242600e_3189240n_las	2018_331600e_3247240n_las
2018_211600e_3170240n_las	2018_330600e_3248240n_las	2018_267600e_3197240n_las
2018_237600e_3185240n_las	2018_345600e_3259240n_las	2018_251600e_3189240n_las
2018_280600e_3207240n_las	2018_217600e_3170240n_las	2018_316600e_3247240n_las
2018_233600e_3184240n_las	2018_329600e_3256240n_las	2018_214600e_3177240n_las
2018_322600e_3244240n_las	2018_241600e_3186240n_las	2018_288600e_3217240n_las
2018_355600e_3271240n_las	2018_345600e_3264240n_las	2018_349600e_3264240n_las
2018_302600e_3225240n_las	2018_264600e_3195240n_las	2018_316600e_3237240n_las
2018_229600e_3185240n_las	2018_231600e_3184240n_las	2018_293600e_3227240n_las
2018_359600e_3266240n_las	2018_356600e_3271240n_las	2018_315600e_3236240n_las
2018_289600e_3214240n_las	2018_303600e_3230240n_las	2018_319600e_3247240n_las
2018_346600e_3265240n_las	2018_299600e_3224240n_las	2018_266600e_3195240n_las
2018_251600e_3192240n_las	2018_209600e_3167240n_las	2018_338600e_3262240n_las
2018_288600e_3227240n_las	2018_223600e_3174240n_las	2018_314600e_3235240n_las
2018_355600e_3267240n_las	2018_332600e_3254240n_las	2018_328600e_3243240n_las
2018_260600e_3197240n_las	2018_303600e_3227240n_las	2018_263600e_3195240n_las
2018_207600e_3177240n_las	2018_291600e_3223240n_las	2018_318600e_3248240n_las
2018_235600e_3184240n_las	2018_273600e_3200240n_las	2018_339600e_3264240n_las
2018_327600e_3243240n_las	2018_252600e_3193240n_las	2018_341600e_3261240n_las
2018_321600e_3245240n_las	2018_208600e_3172240n_las	2018_281600e_3216240n_las
2018_316600e_3250240n_las	2018_219600e_3183240n_las	2018_235600e_3185240n_las
2018_317600e_3243240n_las	2018_333600e_3253240n_las	2018_218600e_3171240n_las
2018_294600e_3220240n_las	2018_341600e_3260240n_las	2018_262600e_3194240n_las
2018_266600e_3207240n_las	2018_356600e_3267240n_las	2018_330600e_3252240n_las
2018_289600e_3223240n_las	2018_338600e_3264240n_las	2018_309600e_3233240n_las
2018_214600e_3179240n_las	2018_244600e_3187240n_las	2018_325600e_3241240n_las
2018_315600e_3253240n_las	2018_332600e_3258240n_las	2018_295600e_3230240n_las
2018_317600e_3255240n_las	2018_310600e_3233240n_las	2018_301600e_3237240n_las
2018_293600e_3224240n_las	2018_316600e_3245240n_las	2018_286600e_3221240n_las
2018_314600e_3245240n_las	2018_236600e_3180240n_las	2018_217600e_3177240n_las
2018_232600e_3184240n_las	2018_227600e_3178240n_las	2018_243600e_3187240n_las
2018_206600e_3171240n_las	2018_288600e_3226240n_las	2018_324600e_3240240n_las
2018_296600e_3226240n_las	2018_324600e_3239240n_las	2018_225600e_3174240n_las
2018_307600e_3228240n_las	2018_216600e_3173240n_las	2018_317600e_3240240n_las
2018_319600e_3236240n_las	2018_206600e_3170240n_las	2018_226600e_3181240n_las

TX1803-TB-C, Hurricane Harvey Post Storm Topography/Bathymetry Project Report of Survey
December 31, 2019

2018_307600e_3231240n_las	2018_219600e_3177240n_las	2018_307600e_3240240n_las
2018_309600e_3236240n_las	2018_212600e_3170240n_las	2018_335600e_3257240n_las
2018_316600e_3246240n_las	2018_360600e_3268240n_las	2018_280600e_3212240n_las
2018_296600e_3231240n_las	2018_228600e_3177240n_las	2018_268600e_3199240n_las
2018_311600e_3240240n_las	2018_256600e_3193240n_las	2018_244600e_3190240n_las
2018_328600e_3245240n_las	2018_327600e_3256240n_las	2018_238600e_3182240n_las
2018_324600e_3250240n_las	2018_288600e_3225240n_las	2018_286600e_3215240n_las
2018_243600e_3184240n_las	2018_347600e_3262240n_las	2018_311600e_3234240n_las
2018_343600e_3263240n_las	2018_219600e_3182240n_las	2018_351600e_3262240n_las
2018_218600e_3173240n_las	2018_356600e_3270240n_las	2018_328600e_3242240n_las
2018_226600e_3177240n_las	2018_322600e_3239240n_las	2018_294600e_3222240n_las
2018_315600e_3242240n_las	2018_230600e_3183240n_las	2018_331600e_3250240n_las
2018_334600e_3256240n_las	2018_339600e_3261240n_las	2018_355600e_3268240n_las
2018_358600e_3266240n_las	2018_215600e_3169240n_las	2018_337600e_3260240n_las
2018_297600e_3220240n_las	2018_296600e_3232240n_las	2018_261600e_3193240n_las
2018_290600e_3222240n_las	2018_267600e_3202240n_las	2018_224600e_3174240n_las
2018_241600e_3187240n_las	2018_321600e_3240240n_las	2018_293600e_3219240n_las
2018_350600e_3263240n_las	2018_283600e_3219240n_las	2018_214600e_3173240n_las
2018_345600e_3261240n_las	2018_216600e_3174240n_las	2018_275600e_3206240n_las
2018_248600e_3192240n_las	2018_208600e_3171240n_las	2018_268600e_3198240n_las
2018_286600e_3218240n_las	2018_263600e_3194240n_las	2018_309600e_3242240n_las
2018_270600e_3205240n_las	2018_271600e_3199240n_las	2018_209600e_3175240n_las
2018_326600e_3255240n_las	2018_318600e_3239240n_las	2018_329600e_3242240n_las
2018_342600e_3262240n_las	2018_273600e_3203240n_las	2018_335600e_3255240n_las
2018_210600e_3173240n_las	2018_218600e_3178240n_las	2018_328600e_3250240n_las
2018_334600e_3259240n_las	2018_307600e_3239240n_las	2018_322600e_3243240n_las
2018_313600e_3246240n_las	2018_346600e_3262240n_las	2018_316600e_3243240n_las
2018_304600e_3227240n_las	2018_272600e_3207240n_las	2018_259600e_3198240n_las
2018_303600e_3232240n_las	2018_347600e_3263240n_las	2018_275600e_3204240n_las
2018_350600e_3262240n_las	2018_296600e_3228240n_las	2018_247600e_3187240n_las
2018_259600e_3196240n_las	2018_287600e_3216240n_las	2018_334600e_3251240n_las
2018_214600e_3171240n_las	2018_266600e_3196240n_las	2018_210600e_3168240n_las
2018_259600e_3192240n_las	2018_326600e_3246240n_las	2018_279600e_3214240n_las
2018_359600e_3269240n_las	2018_285600e_3217240n_las	2018_355600e_3269240n_las
2018_293600e_3228240n_las	2018_314600e_3244240n_las	2018_280600e_3216240n_las
2018_279600e_3215240n_las	2018_207600e_3168240n_las	2018_298600e_3233240n_las
2018_276600e_3203240n_las	2018_293600e_3217240n_las	2018_325600e_3242240n_las
2018_274600e_3209240n_las	2018_267600e_3201240n_las	2018_284600e_3218240n_las
2018_206600e_3175240n_las	2018_329600e_3248240n_las	2018_239600e_3186240n_las
2018_233600e_3181240n_las	2018_274600e_3208240n_las	2018_322600e_3249240n_las
2018_207600e_3179240n_las	2018_316600e_3253240n_las	2018_228600e_3176240n_las
2018_216600e_3172240n_las	2018_233600e_3180240n_las	2018_297600e_3231240n_las
2018_273600e_3207240n_las	2018_332600e_3246240n_las	2018_248600e_3191240n_las

TX1803-TB-C, Hurricane Harvey Post Storm Topography/Bathymetry Project Report of Survey
December 31, 2019

2018_313600e_3242240n_las	2018_265600e_3195240n_las	2018_352600e_3266240n_las
2018_259600e_3197240n_las	2018_316600e_3236240n_las	2018_282600e_3209240n_las
2018_348600e_3262240n_las	2018_278600e_3209240n_las	2018_212600e_3169240n_las
2018_254600e_3193240n_las	2018_289600e_3220240n_las	2018_298600e_3234240n_las
2018_325600e_3246240n_las	2018_306600e_3240240n_las	2018_286600e_3213240n_las
2018_318600e_3247240n_las	2018_324600e_3245240n_las	2018_342600e_3263240n_las
2018_265600e_3197240n_las	2018_335600e_3246240n_las	2018_228600e_3182240n_las
2018_278600e_3206240n_las	2018_248600e_3190240n_las	2018_284600e_3215240n_las
2018_270600e_3208240n_las	2018_265600e_3200240n_las	2018_267600e_3196240n_las
2018_298600e_3225240n_las	2018_356600e_3266240n_las	2018_288600e_3222240n_las
2018_214600e_3170240n_las	2018_358600e_3269240n_las	2018_357600e_3268240n_las
2018_327600e_3254240n_las	2018_272600e_3201240n_las	2018_335600e_3256240n_las
2018_333600e_3245240n_las	2018_354600e_3265240n_las	2018_224600e_3175240n_las
2018_218600e_3179240n_las	2018_303600e_3238240n_las	2018_336600e_3249240n_las
2018_340600e_3265240n_las	2018_320600e_3243240n_las	2018_304600e_3229240n_las
2018_287600e_3215240n_las	2018_207600e_3175240n_las	2018_326600e_3250240n_las
2018_338600e_3263240n_las	2018_236600e_3184240n_las	2018_319600e_3240240n_las
2018_206600e_3173240n_las	2018_222600e_3180240n_las	2018_269600e_3202240n_las
2018_274600e_3206240n_las	2018_270600e_3204240n_las	2018_313600e_3244240n_las
2018_357600e_3270240n_las	2018_286600e_3219240n_las	2018_336600e_3262240n_las
2018_306600e_3233240n_las	2018_331600e_3245240n_las	2018_348600e_3261240n_las
2018_341600e_3264240n_las	2018_312600e_3250240n_las	2018_318600e_3251240n_las
2018_208600e_3177240n_las	2018_314600e_3243240n_las	2018_283600e_3209240n_las
2018_281600e_3217240n_las	2018_226600e_3176240n_las	2018_319600e_3242240n_las
2018_331600e_3249240n_las	2018_292600e_3223240n_las	2018_313600e_3238240n_las
2018_224600e_3177240n_las	2018_288600e_3213240n_las	2018_265600e_3196240n_las
2018_334600e_3246240n_las	2018_233600e_3182240n_las	2018_239600e_3182240n_las
2018_298600e_3221240n_las	2018_314600e_3248240n_las	2018_346600e_3260240n_las
2018_297600e_3227240n_las	2018_294600e_3221240n_las	2018_211600e_3176240n_las
2018_304600e_3226240n_las	2018_321600e_3249240n_las	2018_355600e_3266240n_las
2018_218600e_3176240n_las	2018_221600e_3178240n_las	2018_315600e_3237240n_las
2018_223600e_3184240n_las	2018_348600e_3263240n_las	2018_322600e_3248240n_las
2018_230600e_3178240n_las	2018_240600e_3183240n_las	2018_303600e_3225240n_las
2018_215600e_3170240n_las	2018_284600e_3221240n_las	2018_334600e_3261240n_las
2018_290600e_3220240n_las	2018_323600e_3244240n_las	2018_221600e_3172240n_las
2018_268600e_3200240n_las	2018_290600e_3218240n_las	2018_218600e_3181240n_las
2018_270600e_3201240n_las	2018_284600e_3214240n_las	2018_246600e_3186240n_las
2018_249600e_3190240n_las	2018_207600e_3167240n_las	2018_347600e_3260240n_las
2018_219600e_3180240n_las	2018_306600e_3234240n_las	2018_325600e_3249240n_las
2018_207600e_3176240n_las	2018_251600e_3193240n_las	2018_225600e_3175240n_las
2018_243600e_3186240n_las	2018_275600e_3201240n_las	2018_275600e_3209240n_las
2018_352600e_3264240n_las	2018_299600e_3233240n_las	2018_315600e_3245240n_las
2018_269600e_3198240n_las	2018_313600e_3232240n_las	2018_215600e_3181240n_las

TX1803-TB-C, Hurricane Harvey Post Storm Topography/Bathymetry Project Report of Survey
December 31, 2019

2018_305600e_3227240n_las	2018_314600e_3234240n_las	2018_336600e_3254240n_las
2018_323600e_3243240n_las	2018_339600e_3258240n_las	2018_319600e_3241240n_las
2018_230600e_3177240n_las	2018_313600e_3252240n_las	2018_271600e_3207240n_las
2018_293600e_3223240n_las	2018_311600e_3245240n_las	2018_312600e_3232240n_las
2018_250600e_3192240n_las	2018_273600e_3204240n_las	2018_310600e_3230240n_las
2018_352600e_3267240n_las	2018_333600e_3247240n_las	2018_284600e_3210240n_las
2018_357600e_3265240n_las	2018_230600e_3182240n_las	2018_219600e_3181240n_las
2018_333600e_3255240n_las	2018_265600e_3201240n_las	2018_216600e_3177240n_las
2018_291600e_3221240n_las	2018_276600e_3211240n_las	2018_319600e_3244240n_las
2018_226600e_3178240n_las	2018_297600e_3230240n_las	2018_329600e_3255240n_las
2018_241600e_3184240n_las	2018_249600e_3191240n_las	2018_227600e_3184240n_las
2018_358600e_3267240n_las	2018_314600e_3237240n_las	2018_328600e_3248240n_las
2018_226600e_3182240n_las	2018_218600e_3180240n_las	2018_277600e_3208240n_las
2018_295600e_3226240n_las	2018_320600e_3237240n_las	2018_211600e_3171240n_las
2018_287600e_3221240n_las	2018_323600e_3245240n_las	2018_271600e_3208240n_las
2018_331600e_3253240n_las	2018_345600e_3265240n_las	2018_341600e_3265240n_las
2018_245600e_3185240n_las	2018_347600e_3265240n_las	2018_229600e_3180240n_las
2018_292600e_3218240n_las	2018_262600e_3199240n_las	2018_347600e_3267240n_las
2018_280600e_3215240n_las	2018_310600e_3244240n_las	2018_314600e_3242240n_las
2018_237600e_3183240n_las	2018_334600e_3255240n_las	2018_309600e_3232240n_las
2018_282600e_3218240n_las	2018_253600e_3190240n_las	2018_276600e_3204240n_las
2018_327600e_3244240n_las	2018_317600e_3237240n_las	2018_358600e_3268240n_las
2018_312600e_3239240n_las	2018_320600e_3245240n_las	2018_310600e_3245240n_las
2018_220600e_3175240n_las	2018_333600e_3261240n_las	2018_228600e_3179240n_las
2018_303600e_3237240n_las	2018_264600e_3197240n_las	2018_264600e_3200240n_las
2018_277600e_3209240n_las	2018_234600e_3180240n_las	2018_232600e_3179240n_las
2018_218600e_3182240n_las	2018_301600e_3228240n_las	2018_312600e_3235240n_las
2018_285600e_3213240n_las	2018_210600e_3167240n_las	2018_211600e_3167240n_las
2018_333600e_3251240n_las	2018_282600e_3220240n_las	2018_217600e_3178240n_las
2018_215600e_3177240n_las	2018_257600e_3194240n_las	2018_221600e_3175240n_las
2018_329600e_3249240n_las	2018_317600e_3235240n_las	2018_316600e_3255240n_las
2018_294600e_3227240n_las	2018_331600e_3244240n_las	2018_325600e_3247240n_las
2018_293600e_3221240n_las	2018_324600e_3249240n_las	2018_329600e_3251240n_las
2018_300600e_3227240n_las	2018_346600e_3266240n_las	2018_211600e_3168240n_las
2018_314600e_3240240n_las	2018_297600e_3224240n_las	2018_270600e_3203240n_las
2018_274600e_3202240n_las	2018_297600e_3232240n_las	2018_338600e_3259240n_las
2018_293600e_3229240n_las	2018_262600e_3193240n_las	2018_353600e_3266240n_las
2018_216600e_3176240n_las	2018_244600e_3186240n_las	2018_216600e_3180240n_las
2018_299600e_3235240n_las	2018_342600e_3264240n_las	2018_333600e_3246240n_las
2018_320600e_3239240n_las	2018_256600e_3195240n_las	2018_341600e_3258240n_las
2018_283600e_3216240n_las	2018_208600e_3168240n_las	2018_278600e_3204240n_las
2018_223600e_3181240n_las	2018_337600e_3248240n_las	2018_338600e_3261240n_las
2018_318600e_3250240n_las	2018_217600e_3174240n_las	2018_357600e_3272240n_las

TX1803-TB-C, Hurricane Harvey Post Storm Topography/Bathymetry Project Report of Survey
December 31, 2019

2018_340600e_3264240n_las	2018_215600e_3178240n_las	2018_305600e_3231240n_las
2018_265600e_3194240n_las	2018_344600e_3267240n_las	2018_315600e_3244240n_las
2018_242600e_3188240n_las	2018_231600e_3179240n_las	2018_255600e_3194240n_las
2018_250600e_3189240n_las	2018_317600e_3249240n_las	2018_346600e_3267240n_las
2018_252600e_3192240n_las	2018_350600e_3264240n_las	2018_296600e_3223240n_las
2018_269600e_3207240n_las	2018_312600e_3246240n_las	2018_300600e_3226240n_las
2018_298600e_3223240n_las	2018_286600e_3217240n_las	2018_338600e_3258240n_las
2018_297600e_3234240n_las	2018_345600e_3260240n_las	2018_288600e_3218240n_las
2018_340600e_3257240n_las	2018_317600e_3238240n_las	2018_232600e_3182240n_las
2018_314600e_3239240n_las	2018_285600e_3218240n_las	2018_294600e_3228240n_las
2018_316600e_3251240n_las	2018_284600e_3217240n_las	2018_304600e_3233240n_las
2018_212600e_3173240n_las	2018_228600e_3181240n_las	2018_323600e_3240240n_las
2018_311600e_3246240n_las	2018_227600e_3183240n_las	2018_262600e_3197240n_las
2018_207600e_3170240n_las	2018_330600e_3243240n_las	2018_333600e_3259240n_las
2018_302600e_3224240n_las	2018_217600e_3172240n_las	2018_344600e_3261240n_las
2018_299600e_3223240n_las	2018_303600e_3226240n_las	2018_319600e_3248240n_las
2018_293600e_3231240n_las	2018_222600e_3181240n_las	2018_240600e_3185240n_las
2018_309600e_3234240n_las	2018_294600e_3218240n_las	2018_333600e_3248240n_las
2018_348600e_3267240n_las	2018_327600e_3250240n_las	2018_215600e_3172240n_las
2018_209600e_3171240n_las	2018_215600e_3171240n_las	2018_285600e_3211240n_las
2018_268600e_3207240n_las	2018_357600e_3266240n_las	2018_245600e_3187240n_las
2018_344600e_3263240n_las	2018_331600e_3257240n_las	2018_309600e_3230240n_las
2018_272600e_3199240n_las	2018_328600e_3247240n_las	2018_212600e_3176240n_las
2018_228600e_3180240n_las	2018_332600e_3247240n_las	2018_231600e_3185240n_las
2018_344600e_3260240n_las	2018_291600e_3215240n_las	2018_279600e_3210240n_las
2018_293600e_3226240n_las	2018_314600e_3250240n_las	2018_346600e_3269240n_las
2018_292600e_3226240n_las	2018_315600e_3251240n_las	2018_343600e_3258240n_las
2018_306600e_3238240n_las	2018_344600e_3262240n_las	2018_311600e_3233240n_las
2018_305600e_3238240n_las	2018_296600e_3220240n_las	2018_283600e_3215240n_las
2018_282600e_3208240n_las	2018_354600e_3270240n_las	2018_266600e_3199240n_las
2018_209600e_3176240n_las	2018_232600e_3178240n_las	2018_284600e_3212240n_las
2018_310600e_3242240n_las	2018_277600e_3206240n_las	2018_206600e_3168240n_las
2018_255600e_3192240n_las	2018_337600e_3261240n_las	2018_305600e_3230240n_las
2018_292600e_3221240n_las	2018_281600e_3212240n_las	2018_305600e_3239240n_las
2018_230600e_3180240n_las	2018_231600e_3183240n_las	2018_310600e_3235240n_las
2018_330600e_3247240n_las	2018_279600e_3208240n_las	2018_229600e_3181240n_las
2018_207600e_3173240n_las	2018_229600e_3183240n_las	2018_320600e_3242240n_las
2018_255600e_3191240n_las	2018_207600e_3178240n_las	2018_240600e_3184240n_las
2018_316600e_3240240n_las	2018_335600e_3261240n_las	2018_326600e_3247240n_las
2018_306600e_3239240n_las	2018_312600e_3234240n_las	2018_290600e_3219240n_las
2018_277600e_3203240n_las	2018_337600e_3247240n_las	2018_257600e_3195240n_las
2018_359600e_3268240n_las	2018_229600e_3182240n_las	2018_317600e_3247240n_las
2018_271600e_3201240n_las	2018_313600e_3233240n_las	2018_315600e_3235240n_las

TX1803-TB-C, Hurricane Harvey Post Storm Topography/Bathymetry Project Report of Survey
December 31, 2019

2018_247600e_3186240n_las
2018_348600e_3265240n_las
2018_311600e_3231240n_las
2018_210600e_3169240n_las
2018_277600e_3211240n_las
2018_217600e_3171240n_las
2018_331600e_3256240n_las
2018_269600e_3200240n_las
2018_286600e_3223240n_las
2018_324600e_3241240n_las
2018_313600e_3241240n_las
2018_331600e_3243240n_las
2018_224600e_3184240n_las
2018_315600e_3254240n_las
2018_315600e_3240240n_las
2018_324600e_3246240n_las
2018_331600e_3252240n_las
2018_307600e_3232240n_las
2018_323600e_3248240n_las
2018_233600e_3185240n_las
2018_222600e_3176240n_las
2018_273600e_3206240n_las
2018_326600e_3241240n_las
2018_354600e_3264240n_las

2018_218600e_3172240n_las
2018_328600e_3253240n_las
2018_316600e_3238240n_las
2018_234600e_3182240n_las
2018_315600e_3252240n_las
2018_278600e_3208240n_las
2018_318600e_3245240n_las
2018_307600e_3235240n_las
2018_257600e_3196240n_las
2018_300600e_3228240n_las
2018_326600e_3248240n_las
2018_327600e_3242240n_las
2018_227600e_3176240n_las
2018_282600e_3215240n_las
2018_350600e_3268240n_las
2018_324600e_3247240n_las
2018_335600e_3248240n_las
2018_290600e_3215240n_las
2018_340600e_3261240n_las
2018_262600e_3195240n_las
2018_225600e_3177240n_las
2018_306600e_3227240n_las
2018_331600e_3258240n_las
2018_247600e_3191240n_las

2018_331600e_3251240n_las
2018_224600e_3181240n_las
2018_270600e_3200240n_las
2018_275600e_3208240n_las
2018_314600e_3249240n_las
2018_213600e_3173240n_las
2018_329600e_3246240n_las
2018_298600e_3230240n_las
2018_262600e_3198240n_las
2018_249600e_3189240n_las
2018_317600e_3253240n_las
2018_332600e_3250240n_las
2018_217600e_3176240n_las
2018_241600e_3188240n_las
2018_328600e_3246240n_las
2018_326600e_3249240n_las
2018_293600e_3220240n_las
2018_342600e_3266240n_las
2018_336600e_3255240n_las
2018_277600e_3205240n_las
2018_295600e_3219240n_las
2018_292600e_3230240n_las
2018_223600e_3175240n_las
2018_343600e_3264240n_las

Appendix D

GPS Processing Reports